THE ROLE OF ASSEMBLY FACTORS IN 30S SUBUNIT BIOGENESIS

UNDERSTANDING THE ROLE OF ASSEMBLY FACTORS IN 30S SUBUNIT BIOGENESIS

By BRETT THOMAS THURLOW, BMSc, MSc

A Thesis Submitted to the School of Graduate Studies in Partial Fulfilment of the

Requirements for the Degree Doctor of Philosophy

McMaster University

DOCTOR OF PHILOSOPHY (2016) McMaster University

(Biochemistry and Biomedical Sciences) Hamilton, Ontario

TITLE: Understanding the Role of Assembly Factors in 30S Subunit Biogenesis

AUTHOR: Brett T. Thurlow, BMSc (Honours) (Western University), MSc (Western University)

SUPERVISOR: Dr. Joaquin Ortega

NUMBER OF PAGES: xvi, 151

LAY ABSTRACT

One of the most fundamental processes in all living cells is the synthesis of proteins by the ribosome. The ribosome is a massive macromolecular complex that consists of both proteins and RNA, which must be manufactured from its individual components before it can perform its function. There is a myriad of protein factors that assist in the assembly of ribosomes to ensure that biogenesis proceeds rapidly and efficiently. The purpose of this thesis was to gain a better understanding of how the assembly factors YjeQ, Era, RbfA and RimM work by studying the intermediates that accumulate when they are removed or depleted from the cell. Specifically, the fate, binding interactions and structure of the immature particles that accumulate in the assembly factor knockout or depletion strains were investigated. The work here brings new insights into the nature of these immature ribosomal particles and the maturation reactions catalyzed by these factors.

ABSTRACT

Our understanding regarding the function of YjeQ, RbfA, RimM and Era in ribosome biogenesis has been derived in part from the study of immature 30S particles that accumulate in bacteria strains lacking one of these factors. However, their mechanistic details are still unknown. Here, we demonstrate that the $30S_{\Delta yjeQ}$ and $30S_{\Delta rimM}$ immature particles are not dead-end products of assembly, but progress into mature 30S subunits. Mass spectrometry analysis revealed that *in vivo* the occupancy level of these factors in these immature 30S particles is below 10% and that the concentration of factors does not increase when immature particles accumulate in cells. Analysis of the binding interactions of these assembly factors with mature 30S subunits and the immature particles demonstrated that YjeQ and Era bind to the mature 30S subunit with high affinity, however binding of these factors to the immature particles and of RimM and RbfA to mature or immature particles is weak. This indicates that binding of the assembly factors to the immature particles is not occurring at physiological concentrations. These results suggest that in the absence of these factors, the immature particles evolve into a thermodynamically stable intermediate that exhibits low affinity for the assembly factors and that the true substrates of YjeQ, RbfA, RimM and Era are immature particles that precede the ribosomal particles accumulating in the knockouts strains. We also developed an Era-depletion and Δ*rbfA* strain, which exhibited slow-growth, cold-sensitivity and an aberrant ribosome profile, which are all characteristic of ribosome assembly defects. Cryo-EM structural analysis of the $30S_{\text{Era-depleted}}$ particles revealed that multiple classes at various stages in the assembly process accumulate upon

depletion of Era, suggesting that Era may have a global effect on biogenesis. Ultimately, this thesis provides new insights into the nature of 30S particles that accumulate during assembly factor perturbation and advances our understanding of ribosome biogenesis as a whole.

AKNOWLEDGMENTS

I would like to extend my sincere gratitude to my supervisor, Dr. Joaquin Ortega, for his support, encouragement and patience throughout my PhD studies. His guidance was instrumental in helping me to complete my degree and develop as a scientist.

I would like to thank my committee members, Drs. Russell Bishop and Nathan Magarvey, for their advice and valuable opinions throughout my project.

I am pleased to acknowledge our collaborators, Drs. Joseph Davis, James Williamson, Trevor Moraes, Eric Brown, Jean-Philippe Cote and John Rubinstein. Their technical and theoretical contributions to my PhD project were very much appreciated. Thanks to Dr. Alba Guarnè for sharing her lab equipment.

I thank the entire Ortega Lab, both past and present, for stimulating discussions about ribosome assembly and science as a whole. Particular thanks to Bilal Ahsan and Aida Razi for all of our insightful conversations over coffee. Thanks to Vivian Leong and Dr. Ahmad Jomaa for teaching me invaluable laboratory techniques. Thanks to Dr. Dinorah Leyva and Christine Lai for technical assistance with the microscale thermophoresis experiments.

Lastly, I offer my sincerest appreciation to my family and friends for their constant love and support throughout my education. Most importantly, I thank my parents, Dr. Paul and Holly Thurlow, for making all of this possible. I could not have completed this milestone without them. Special thanks to Nicole Hitzroth for her love and devotion during the pursuit of my degree.

TABLE OF CONTENTS

LIST OF FIGURES

CHAPTER FIVE

CHAPTER SIX

LIST OF TABLES

LIST OF ABBREVIATIONS

16S	mature 30S subunit rRNA molecule
17S	immature 30S subunit rRNA molecule
21S	precursor ribosomal particle
23S	mature 50S subunit rRNA molecule
2D	two-dimensional
30S	prokaryotic small ribosome subunit
$30S_{Era\text{-}depleted}$	30S particle that accumulates in Era-depleted strain
$30S_{\Delta rbfA}$	immature 30S particles that accumulates in Δ*rbfA* strain
$30S_{\Delta rimM}$	immature 30S particles that accumulates in Δ*rimM* strain
$30S_{\Delta yjeQ}$	immature 30S particle that accumulates in Δ*yjeQ* strain
3D	three-dimensional
40S	eukaryotic small subunit
50S	prokaryotic large ribosome subunit
5S	mature 50S subunit rRNA molecule
60S	eukaryotic large ribosome subunit
70S	prokaryotic ribosome
80S	eukaryotic ribosome
A	adenine
AS	ammonium sulfate
A-site	aminoacyl site
BSA	bovine serum albumin
C	cytosine
Cryo-EM	cryo-electron microscopy
C-terminal	carboxyl terminal
DNA	deoxyribonucleic acid
DTT	dithiothreitol
E. coli	Escherichia *coli*
EDTA	ethylenediaminetetraacettic acid
EM	electron-microscopy
EMDB	electron microscopy databank
Enp1	essential nuclear protein
Era	*E.coli* ras-like protein
E-site	exit site
FT	flow-through
g	gravitational force
G	guanosine
GDP	guanosine diphosphate
GMP-PNP	guanylyl imidophosphate
GTP	guanosine triphosphate
GTPase	guanosine triphosphate hydrolase
h44	helix-44
HSP 70	heat shock protein 70

IPTG	isopropyl β-D-1-thiogalactopyranoside
k_{cat}	catalysis rate
K_d	disassociation constant
kDa	kilodalton
KH domain	RNA-binding K homology domain
K_M	Michaelis-Menten constant
LB	luria-bertani
l-protein	large ribosomal subunit protein
Ltv1	low temperature viability
MDa	megadalton
mRNA	messenger ribonucleic acid
MS	mass spectrometry
MRM	multiple reaction monitoring
MST	microscale thermophoresis
MWCO	molecular weight cut-off
N-terminal	amino terminal
OB binding fold	oligonucleotide/oligosaccharide binding
OD	optical density
$_{p1}$30S	30S precursor particle 1
$_{p2}$30S	30S precursor particle 2
PBS	phosphate buffer saline
PC-QMS	pulse-chase quantified by mass spectrometry
PDB	protein data bank
PEI	polyethyleneimine
P-loop	phosphate binding loop
PRC	photosynthetic reaction centre
P-site	peptidyl site
PTC	peptidyl transferase centre
qMS	quantitative mass spectrometry
RbfA	ribosome binding factor A
RbgA	ribosome binding GTPase A
RI	reconstitution intermediate
RimM	ribosome maturation factor
RNA	ribonucleic acid
RNase	ribonuclease
rpm	revolutions per minute
r-protein	ribosomal protein
rrn	ribosomal RNA operon
rRNA	ribosomal ribonucleic acid
RsgA	ribosomal small subunit GTPase A
S.typimurium	Salmonella *typhimurium*
SDS-PAGE	sodium dodecyl sulfate polyacrylamide gel electrophoresis
SSU	small subunit particles
s-protein	small subunit protein

T	thymine
TBE	tris/borate/EDTA buffer
TEV	tobacco etch virus
tRNA	transfer RNA
Tsr1	twenty S rRNA accumulation
U	uracil
UTR	untranslated region
UV	ultraviolet
wt	wild type

DECLARATION OF ACADEMIC ACHIEVEMENT

Experiments discussed in this thesis were designed and executed by me in consultation with Dr. Joaquin Ortega, unless stated otherwise in the chapter preface. Pulse-chase experiments discussed in chapter 3 were performed by Vivian Leong. Mass spectrometry analysis discussed in chapter 4 was performed by Dr. Joseph Davis.

CHAPTER ONE

INTRODUCTION

1.1 The Prokaryotic Ribosome

The translation of genetic material into functional proteins is central to all life and is orchestrated by a 2.5 MDa ribonucleoprotein complex known as the ribosome. In bacteria, this macromolecular assembly consists of two subunits designated as the 30S (or small) and 50S (or large) subunits that associate to form the 70S ribosome (Fig. 1.1). These subunits are described in terms of their rates of sedimentation in an ultracentrifuge, which roughly correlates to their size (Voet et al., 2006). The importance of the ribosome in performing the essential task of protein translation in all cells is exemplified by the facts that ribosomes constitute ~30% of the dry mass of cells and ~40% of energy turnover is dedicated to protein synthesis (Wilson and Nierhaus, 2007). Accordingly, numerous antibiotics specifically target the ribosome, demonstrating its critical importance to cellular homeostasis (Wilson, 2014). Ribosome biogenesis also serves as a fundamental model system for understanding ribonucleic acid (RNA) and protein folding, protein-RNA interactions and assembly of complex multi-component biological systems (Shajani et al., 2011) and dysfunctional ribosome biogenesis has been associated with a number of human diseases (Danilova and Gazda, 2015) (Freed et al., 2010) (Donati et al., 2012) (Montanaro et al., 2012). Therefore, gaining a comprehensive understanding of ribosome assembly will provide insights into these diseases and help us to better appreciate fundamental principles governing the biochemistry of all cells.

Since the ribosome's discovery in 1955 by George Palade (Palade, 1955), a tremendous amount of biochemical and structural research has been dedicated to learning about how this macromolecular machine efficiently translates the genetic code into protein. Despite the wealth of information about ribosome structure and function, how this extraordinary machine assembles within cells remains largely elusive. The focus of this thesis has been on the assembly of the 30S subunit, so specific attention will be given to its structure, function and assembly.

1.1.1 Structure of the Prokaryotic Ribosome

After the ribosome's discovery in the 1950s, it took over 20 years for the first low resolution electron microscopy (EM) images of the ribosome to be obtained (Lake, 1976) and the subsequent determination of the primary structure of 16S (Brosius et al., 1978) and 23S ribosomal RNA (rRNA) (Brosius et al., 1980) from *E.coli*. Following this, the secondary structure map of 16S rRNA (Noller and Woese, 1981) and 23S rRNA (Noller et al., 1981), as well as the placement of various s-proteins on the rRNA scaffold (Engelman et al., 1975) were solved. Rigorous investigations then ensued to try and elucidate a three-dimensional (3D) model of the ribosome in high resolution.

Some of these most ambitious efforts came from structural biologist that aspired to seek out high-resolution x-ray crystallography structures of the ribosome and its subunits at the dawn of the new millennium. In 2000, high-resolution crystal structures of the 30S subunit were independently solved by the groups of Ada Yonath (Schluenzen et al., 2000) and Venkatraman Ramakrishnan (Wimberly et al., 2000) and of the 50S

subunit by Thomas Steitz's group (Ban et al., 2000), followed by atomic resolution structures of the 70S ribosome (Yusupov et al., 2001). These atomic structures provided unprecedented details regarding the architecture of the ribosome with a contribution of such magnificence that the principal investigators were awarded the Nobel Prize in Chemistry in 2009. In more recent years there have been numerous published structures of the ribosome and ribosome complexes that have provided tremendous advances in the field including a detailed mechanistic understanding of translation, the conformation of essential functional sites, antibiotic interactions, ribosome assembly and many others.

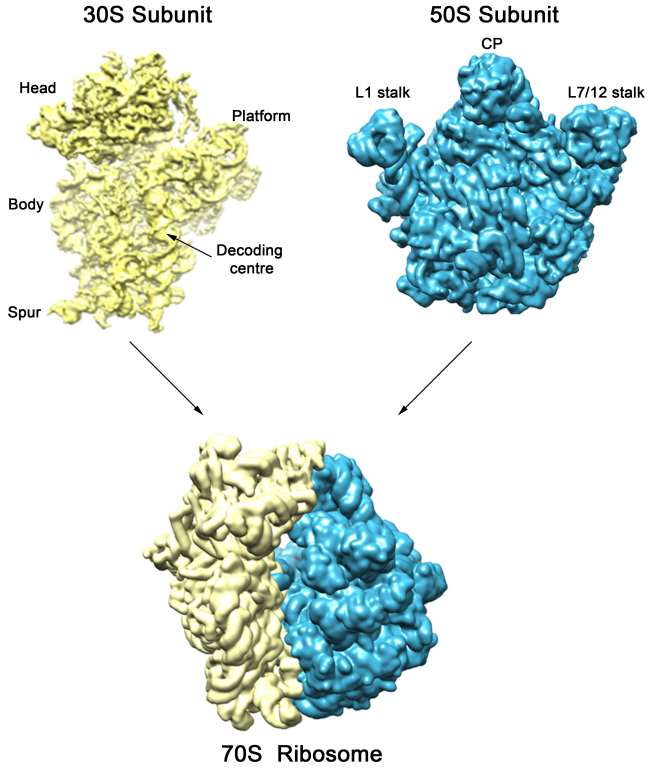

Figure 1.1. Structure of the prokaryotic ribosome.
Structure of the bacterial 30S (yellow) and 50S subunits (blue) and 70S ribosome. Subunits are being displayed from the canonical interface side. The 30S and 50S subunit assemble independently within the cell and then associate to form the 70S ribosome.

Major 30S landmarks including the head, body, spur, platform and decoding centre are shown. Labelled 50S features are the L1 stalk, central protuberance (CP) and L7/12 stalk. Figure was prepared in USCF chimera with EMDB 6306.

It is now well established that the 30S subunit is comprised of a 16S ribosomal RNA molecule and 21 ribosomal proteins (Shajani et al., 2011) (s-proteins, designated bS1 – bS21 (Ban et al., 2014)). The 30S subunit has a molecular weight of approximately 0.85 MDa and the 16S rRNA molecule is comprised of 1542 nucleotides (Culver, 2003). The overall shape of the 30S subunit is largely determined by the rRNA scaffold, as none of the gross morphological features contain all protein (Wimberly et al., 2000). There are several landmark morphological features used to describe the 30S subunit using the canonical subunit interface view including the head with a beak pointing leftwards, the platform at the top right, the body with the shoulder at the top left and spur at the bottom left (Wimberly et al., 2000) (Fig. 1.1). These morphological features are comprised of four individual 16S rRNA secondary structural domains that can fold independently (Samaha et al., 1994) (Agalarov et al., 1998) (Weitzmann et al., 1993), which include the 5’ domain, central domain, 3’ major domain and 3’ minor domain. The 5’ and 3’ minor domains constitute the majority of the body, the central domain the bulk of the platform and the 3’ major domain the majority of the head (Wimberly et al., 2000). The protein distribution surrounding the 16S rRNA domains is asymmetric with the majority of proteins being located on the solvent exposed side and near the top and sides (Wimberly et al., 2000). These four domains extend from a central position in the neck, where they are especially tightly associated and which is functionally the most important region of the 30S subunit (Wimberly et al., 2000). The

functional core of the 30S subunit, responsible for decoding the messenger RNA (mRNA) message during protein translation, is located in the 3' minor domain in helix 44 (h44), also known as the penultimate stem.

The 50S subunit contains two rRNA molecules (23S and 5S) and up to 34 ribosomal proteins (l-proteins, designated uL1 – bL36 (Ban et al., 2014)). It is composed of a compact structure containing seven secondary structure domains, six that stem from the 23S rRNA and one from the 5S rRNA (Ban et al., 2000). There are three extensions protruding from the 50S subunit interface: the L1 stalk, the central protuberance and the L7/L12 stalk (Ban et al., 2000) (Fig. 1.1). The 50S subunit interface is also largely absent of l-proteins with the majority being positioned on the solvent exposed interface. The functional core, known as the peptidyltransferase centre (PTC), catalyzes peptide bond formation during translation and is situated in the interface region.

1.1.2 Function of the Ribosome

A fundamental process in all living cells is the biosynthesis of proteins during translation, which is orchestrated on the ribosome spanning three major sites: aminoacyl (A)-site, peptidyl(P)-site and exit(E)-site (reviewed in (Ogle and Ramakrishnan, 2005) (Ramakrishnan, 2002) (Frank, 2003) (Noller, 1991) (Steitz, 2008)). In addition to the ribosome, there are several other molecules that are essential to the process of translation at various stages including: messenger RNA, transfer RNA (tRNA), initiation factors, elongation factors, release factors and recycling factors (Voet et al., 2006). Translation initiation begins with the recruitment of mRNA to the 30S subunit by base pairing

between the Shine-Dalgorno sequence in the 5' untranslated region (UTR) of mRNA and the anti-Shine-Dalgorno sequence found in the 3'major domain of the 30S subunit (Shine and Dalgarno, 1974). Subsequently, aminoacylated "charged" initiator tRNA is recruited to the P-site followed by the association of the 30S and 50S subunits and the commencement of translation. This process is facilitated by initiation factors 1-3 and requires energy from guanosine triphosphate (GTP) hydrolysis for subsequent removal.

Elongation of the polypeptide chain commences after the initiation complex has formed, which is mediated by the decoding and peptidyl transferase centre. The anticodon of the tRNA and codon of the mRNA interact at the A-site and the decoding centre monitors the geometry of the canonical codon/anticodon base pairing using the universally conserved nucleotides A1492, A1493 and G530 in a proofreading step (Ogle et al., 2001) (Yoshizawa et al., 1999). If non-cognate base pairing occurs, then the incorrect aminoacylated – tRNA (aa-tRNA) is ejected from the A-site so that the correct aa-tRNA can be recruited to the A-site to continue chain elongation. Once proper base pairing between the cognate aa-tRNA and mRNA have occurred, the amino acid will be accommodated into the PTC for subsequent nucleophilic attack of the α-amino group on the A-site amino acid to the carbonyl group of the nascent polypeptide chain in the P-site, thus facilitating catalysis (Nissen et al., 2000) (Hansen et al., 2002). The ribosome then translocates along the mRNA by one codon using a ratcheting motion, moving the deacylated P-site tRNA into the E-site and the nascent polypeptide chain A-site tRNA and attached mRNA into the P-site. The uncharged E-site tRNA is then ejected from the complex and the growing polypeptide chain is now situated in the P-site ready for another

cycle of chain elongation. Once synthesis of the protein is complete, signified by a STOP codon in the mRNA, a series of recycling factors facilitate the termination of the translation apparatus, release of polypeptide chain and disassociation of the 30S and 50S subunits.

1.2 30S Subunit Assembly

Despite the detailed biochemical and structural knowledge of the ribosome and the specific mechanisms involved in protein synthesis, there still remains much to learn about how these macromolecular machines assemble within cells and the specific factors involved. A testament to the disproportionate amount of information we have about mature ribosome structures and translation compared to the assembly process is that antimicrobial efforts have often exploited bacterial translation; however there remains to be any approved drugs specific to ribosome biogenesis (Maguire, 2009) (Comartin and Brown, 2006) (Poehlsgaard and Douthwaite, 2005) (Stokes and Brown, 2015). Over the past 50 years there has been a detailed analysis of ribosome structure and assembly using a combination of techniques including equilibrium binding assays (Traub and Nomura, 1969a) (Traub and Nomura, 1969b) (Nomura et al., 1969a) (Held et al., 1973) (Held et al., 1974) (Mizushima and Nomura, 1970) (Jeganathan et al., 2015), x-ray crystallography (Clemons Jr. et al., 1999) (Wimberly et al., 2000) (Tocilj et al., 1999) (Schluenzen et al., 2000) (Harms et al., 2001) (Ban et al., 2000) (Nissen et al., 2000), electron microscopy (Mulder et al., 2010) (Jomaa et al., 2011a) (Jomaa et al., 2011b) (Jomaa et al., 2014) (Leong et al., 2013) (Yang et al., 2014) (Guo et al., 2013) (Guo et al.,

2011), chemical footprinting (Adilakshmi et al., 2008) (Clatterbuck Soper et al., 2013), mass spectrometry (Talkington et al., 2005) (Bunner et al., 2010a) (Bunner et al., 2010b) and computer simulations (Earnest et al., 2015). Together, these studies have advanced our understanding of ribosome assembly by demonstrating that it is an immensely complex process characterized by multiple events occurring simultaneously with extreme precision and efficiency. Overall, ribosome biogenesis occurs in a series of overlapping steps including rRNA transcription, ribosomal protein translation, rRNA processing, rRNA folding, protein binding and protein and rRNA modification (Fig. 1.2) (reviewed in (Shajani et al., 2011) (Sykes and Williamson, 2009) (Connolly and Culver, 2009) (Culver, 2003) (Kaczanowska and Ryden-Aulin, 2007) (Strunk and Karbstein, 2009)).

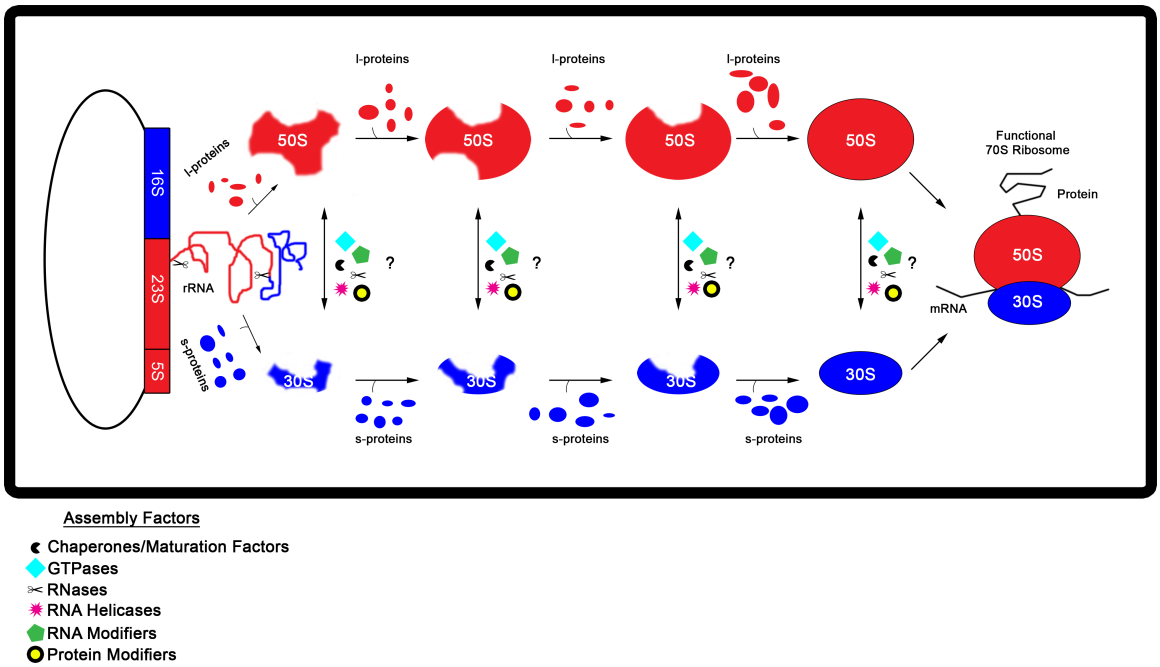

Figure 1.2. Overview of ribosome assembly.
Prokaryotic ribosome biogenesis initiates with the transcription of rRNA from a polycistronic operon containing 17S, 23S and 5S rRNA. Immediately upon transcription the rRNA is processed and begins to fold into its secondary and tertiary structures. While

the rRNA is folding, r-proteins bind to the rRNA scaffold in a hierarchical and dependent fashion. Once the rRNA has been completely processed and all r-proteins have bound, mature 30S and 50S subunits can associate to form 70S ribosomes. Despite the complexities and numerous components involved in the assembly of this massive 2.5 MDa macromolecule, the process is extremely efficient in cells and only takes several minutes for completion. There are numerous putative auxiliary factors such as RNases, helicases, GTPases, chaperones and protein and RNA modifying enzymes that help facilitate ribosome assembly. Although numerous factors have been implicated in this process, their specific functions and temporal placement are not well understood (?).

1.2.1 R-protein Binding

In the late 1960S, pioneering studies from the Nomura lab sought to gain a better understanding of the assembly process by determining that 30S subunits can be reconstituted *in vitro* in the presence of s-proteins and 16S rRNA under non-physiological conditions (Traub and Nomura, 1968) (Traub and Nomura, 1969b) (Traub and Nomura, 1969a) (Nomura et al., 1969b). Remarkably, these *in vitro* reconstitution studies revealed that all of the information needed to assemble an active 30S subunit was encoded within the rRNA and r-proteins themselves. Furthermore, by varying the order in which the s-proteins were added during *in vitro* reconstitution, the Nomura group also demonstrated that s-proteins bind to the rRNA scaffold in a hierarchal manner with binding events being thermodynamically interdependent (Mizushima and Nomura, 1970) (Held et al., 1974). The binding of s-proteins to rRNA has been categorized into three classes: primary s-proteins bind directly the rRNA, secondary s-proteins require the presence of primary s-proteins and tertiary s-proteins require the presence of secondary s-proteins. Generally, due to the 5' to 3' directionality of rRNA transcription, the early-binding proteins interact with the 5' domain (body) of the rRNA, mid-binding proteins

with the central domain (platform) and late-binding proteins with the 3'domain (head). This hierarchy of s-protein binding as been termed the "Nomura Assembly Map" and has amazingly remained largely unchanged since its discovery over 45 years ago, with only minor additions amended to the map (Powers et al., 1993) (Grondek and Culver, 2004) (Culver and Noller, 1999) (Holmes and Culver, 2005) (Chen and Williamson, 2013) (Fig. 1.3). Current evidence suggests that the binding of s-proteins to the 16S rRNA stabilizes local rRNA secondary structure allowing for conformations that facilitate the subsequent binding of additional s-proteins (Kim et al., 2014) (Culver, 2003) (Shajani et al., 2011) (Sykes and Williamson, 2009). Furthermore, many s-proteins control their own expression to help ensure that ribosome assembly is regulated according to the cells' needs (Zengel and Lindahl, 1994). Post-translation modifications can occur on five s-proteins and their exact roles remain largely enigmatic (Arnold and Reilly, 1999) (Kaczanowska and Ryden-Aulin, 2007) (Kowalak and Walsh, 1996). Following the elucidation of the 30S assembly map, a more complex assembly map was established for the 50S subunit, termed the "Nierhaus Assembly Map" (Dohme and Nierhaus, 1976) (Herold and Nierhaus, 1987) (Rohl and Nierhaus, 1982).

1.2.2 rRNA Processing

A critical component to 30S subunit biogenesis *in vivo* is the transcription and processing of rRNA. Initially, the premature 16S rRNA, termed 17S rRNA, is transcribed as a single transcript from the *rrn* operon along with 23S rRNA, 5S rRNA and one or two tRNA molecules (Lund et al., 1976) (Ginsburg and Steitz, 1975) (Brosius

et al., 1981) (Fig. 1.4). Transcription of rRNA has previously been described as the rate-limiting step of ribosome biogenesis *in vivo* and is regulated by multiple factors spanning two tandem promoter and terminator sequences (Paul et al., 2004) (Kaczanowska and Ryden-Aulin, 2007) (Sarmientos et al., 1983) (Glaser et al., 1983). There are seven *rrn* operons in *E.coli*, which are believed to accommodate the high demand for protein synthesis during exponential growth of cells (Kenerley et al., 1977) (Kiss et al., 1977). The rRNA transcript begins to immediately fold before transcription is complete (Kaczanowska and Ryden-Aulin, 2007). Subsequently, 17S rRNA is processed by the endonuclease RNAse III, causing removal and separation of the precursor molecules from the transcript (Young and Steitz, 1978) (Fig. 1.4).

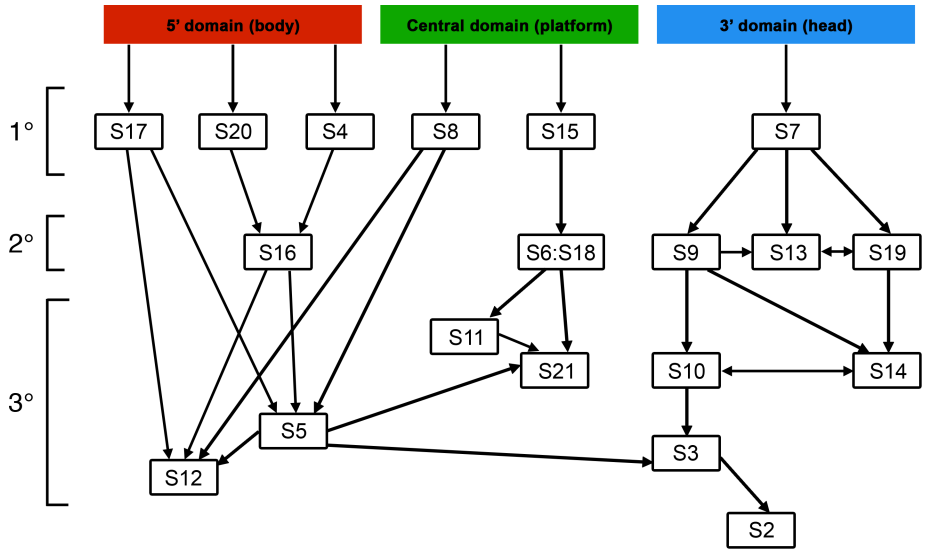

Figure 1.3. Nomura assembly map.
This figure shows the order, location and dependencies of s-proteins binding to the rRNA scaffold during 30S biogenesis as determined by the Nomura group. This assembly map has remained largely unchanged since its discovery over 45 years ago. Arrows represent thermodynamic protein binding dependencies. The rRNA is divided into the 5' (red), central (green) and 3' domains (blue). Primary (1°) s-proteins require only the presence of rRNA for binding. Secondary proteins (2°) require the presence of primary proteins to

bind. Tertiary (3°) proteins require the presence of primary and secondary proteins for binding to occur. Binding of proteins follows a 5' to 3' directionality in a cooperative and hierarchal manner.

The precursor 17S rRNA contains an additional 115 and 33 nucleotides at the 5' and 3' ends respectively, requiring further trimming by multiple endonucleases and exonucleases (Shajani et al., 2011). RNase E cleaves the first 49 nucleotides and RNase G removes the remaining 66 nucleotides (Li et al., 1999) (Wachi et al., 1999) (Fig 1.4). Processing of the 3' end is less well characterized, however recent studies have implicated at least four exonucleases (RNase II, RNase R, RNase PH and PNPase) (Sulthana and Deutscher, 2013), as well as YbeY (Davies et al., 2010) (Jacob et al., 2013) in the removal and processing of the additional 33 nucleotides (Fig 1.4). Impairment of 3' end processing prevents the removal of the additional nucleotides on the 5' end, indicating that the two processes are linked. Interestingly, YbeY, a UPF0054 protein family member, is involved in processing of all three premature rRNA transcripts (16S, 23S and 5S) and impairment of its function leads to defects in ribosome assembly, activity and fidelity: suggesting it plays a role in rRNA quality control (Davies et al., 2010) (Jacob et al., 2013). Finally, there up to eleven nucleotides on 16S rRNA that can be exposed to post-transcriptional modifications, which are believed to stabilize ribosome structure, regulate translation and alter antibiotic resistance (Milanowska et al., 2013) (Popova and Williamson, 2014) (Decatur and Fournier, 2002). Upon completion of the rRNA processing steps and the coordinated binding of all s-proteins, functional 30S subunits are ready to engage in translation.

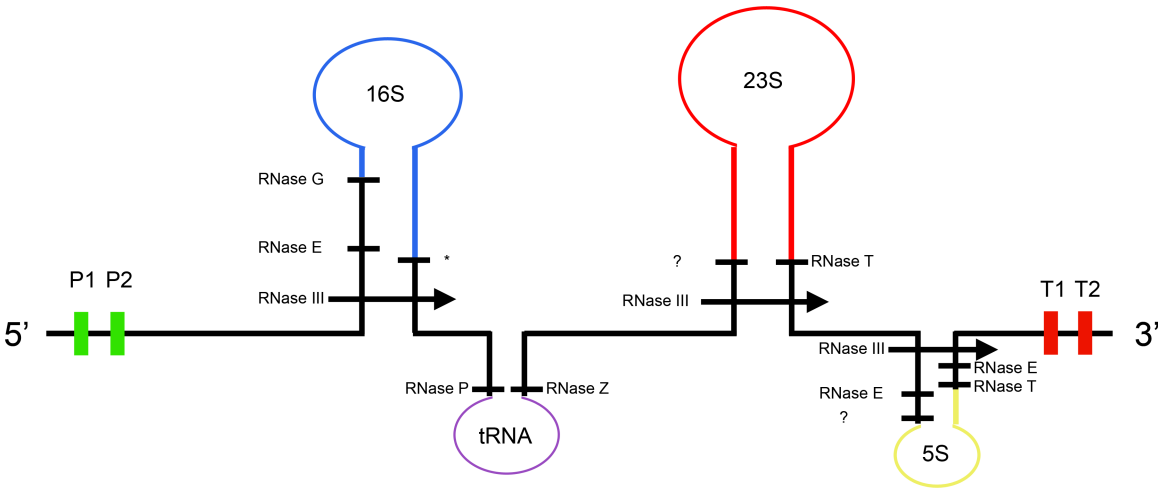

Figure 1.4. rRNA processing.
rRNA is transcribed from a polycistronic operon containing 17S rRNA, 23 rRNA, 5S rRNA and one or two tRNA molecules. Shown here is the rRNA transcript in 5' to 3' orientation with known cleavage sites and their respective nucleases indicated. The promoter (P1 and P2) and terminator (T1 and T2) sequences are labelled. There are numerous endo and exo ribonucleases that facilitate rRNA processing during 30S biogenesis. The site marked with an asterisk (*) has been suggested to be processed by several enzymes (RNase II, RNase R, RNase PH, PNPase). The sites marked with a question mark (?) are cleaved by currently unknown nucleases.

1.2.3 Assembly Landscape of 30S Subunit

Early ribosome assembly studies focused on *in vitro* investigations to gain a better understanding of the general concepts behind rRNA folding and hierarchical protein binding. Initially, *in vitro* reconstitution experiments performed at different temperatures identified two 30S intermediates that were stable for isolation (Traub and Nomura, 1969a) (Nomura et al., 1969b) (Traub and Nomura, 1969a) (Traub and Nomura, 1969b) (Held et al., 1973). At low temperatures (0 – 15 °C), a 21S reconstitution intermediate (RI) with 15 s-proteins bound to the 16S rRNA accumulates. Upon shift to a higher temperature (40 °C), a conformational rearrangement occurs forming a 25S reconstitution

intermediate (RI*) that can form functional 30S subunits (Fig. 1.5A). Similarly, pulse labelling and polyacrylamide gel electrophoresis were used to identify two *in vivo* 30S assembly intermediates that sediment at 21S and 30S termed $_{p1}$30S and $_{p2}$30S, respectively (Hayes and Hayes, 1971) (Lindahl, 1973) (Fig. 1.5A). Due to the extreme efficiency and robustness of ribosome biogenesis *in vivo*, these intermediates comprised of only 2-5% of the total rRNA population in exponentially growing cells (Lindahl, 1975). Together, these foundational studies led researchers to speculate that 30S subunit assembly proceeds down a linear pathway with one or two rate limiting steps.

Over the past decade there has been a tremendous effort by numerous labs to better elucidate the mechanisms, kinetics and energetics involved in 30S biogenesis. A groundbreaking study by the Williamson lab used an elegant pulse-chase quantified by mass spectrometry (PC-QMS) technique to determine the rates of association of all s-proteins binding to 16S rRNA molecules *in vitro* (Talkington et al., 2005). Additionally, this study assessed the kinetic parameters at various temperatures and then used Arrhenius plots to determine the activation energies for each s-protein. By using this approach, the authors were able to demonstrate that local transformations throughout biogenesis have similar but distinct activation energies, indicating that there is not one global rate-limiting step (Talkington et al., 2005). Rather, assembly proceeds down a landscape with numerous local conformation transitions, similar to the folding landscape of a protein (Talkington et al., 2005) (Fig. 1.5B). This PC-QMS method was further adapted to determine how assembly factors affect the kinetics of s-protein binding *in vitro* (Bunner et al., 2010b), assess s-protein kinetic cooperativity (Bunner et al., 2010a),

determine the rates of s-protein incorporation *in vivo* (Chen and Williamson, 2013) and identify rRNA post-transcriptional modifications (Popova and Williamson, 2014), ultimately making great strides in the field.

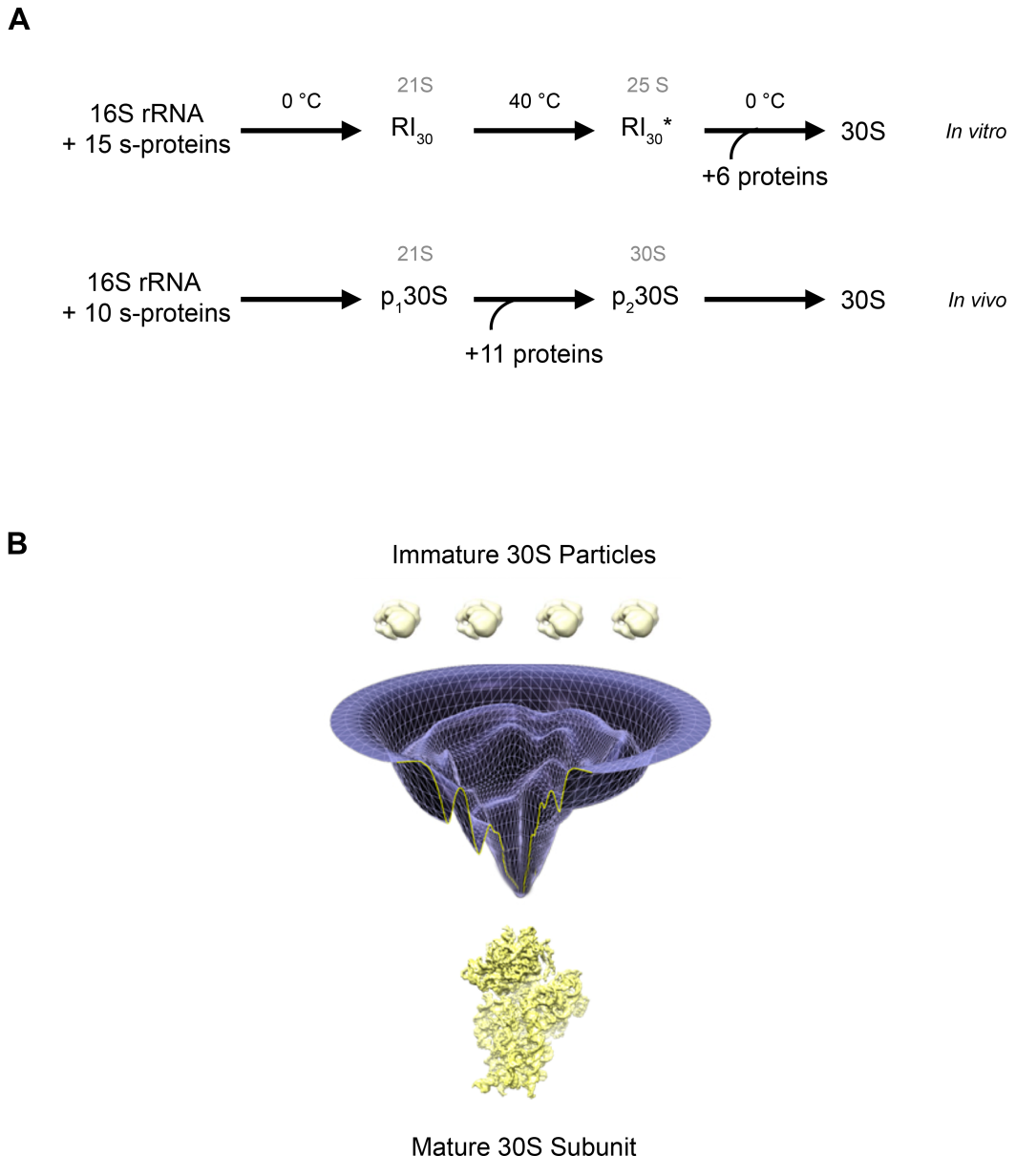

Figure 1.5. An assembly landscape for 30S subunit biogenesis.
(A) 30S assembly was originally believed to follow a linear pathway with one or two rate limiting steps. Shown here are *in vitro* and *in vivo* assembly mechanisms for the 30S

subunit. (B) Recent evidence has indicated that 30S biogenesis involves multiple parallel folding pathways and can be viewed as an assembly landscape. The vertical axis represents free energy and the horizontal axis represents conformational space. Local rRNA folding creates s-protein binding sites and large changes in the landscape are accompanied by protein binding events. Ultimately, sequential stages of rRNA folding and protein binding leads to the formation of mature 30S subunits that converge at the final structure indicated by the bottom of the funnel.

Supporting the notion of multiple parallel 30S subunit assembly pathways, the Woodson lab used an innovative time-resolved hydroxyl radical footprinting method (Adilakshmi et al., 2006) to demonstrate that 16S rRNA nucleates concurrently along different points of the molecule during s-protein binding (Adilakshmi et al., 2008). Impressively, this technique was able to monitor structural changes in the rRNA with single nucleotide resolution mere milliseconds after the addition of s-proteins *in vitro* (Adilakshmi et al., 2008). These studies revealed that helical junctions within each domain form extremely rapidly (<100 milliseconds), whereas regions between each domain and surrounding the decoding centre take several minutes to fold (Adilakshmi et al., 2008). The time-resolved hydroxyl footprinting method was also used to identify protein independent folding pathways (Adilakshmi et al., 2005), specific protein-RNA interactions (Bellur and Woodson, 2009) and assess the effects of assembly factors on 30S biogenesis (Clatterbuck Soper et al., 2013). Multiple parallel 30S assembly pathways have also been visualized *in vitro* by using time-resolved single particle electron microscopy to take millions of snapshots of maturing particles, thus enabling the identification of multiple intermediates and the change in these populations over time (Mulder et al., 2010). It is believed these multiple pathways introduce the necessary flexibility and redundancy to make 30S biogenesis an extremely robust and efficient

process. Together, these studies have provided great advancements to our understanding of 30S assembly and a further appreciation of the immense complexity involved in this process.

1.3 Assembly Factors Mediate 30S Biogenesis

Despite the ability of 30S subunits to assemble *in vitro* by incubating 16S rRNA with s-proteins (Nomura et al., 1969b) (Culver and Noller, 1999), the reaction conditions required are far from physiological (Shajani et al., 2011). These *in vitro* reactions used temperatures, salt concentrations and incubation times that would not sustain the requirements necessary for the rapid proliferation of bacterial cells (Held et al., 1973) (Culver, 2003). Indeed, a testament to the efficiency of ribosome assembly is that exponentially growing *E.coli* cells can produce functional ribosomes within mere minutes (Lindahl, 1975) (Michaels, 1972) (Chen and Williamson, 2013). The ability of cells to assemble such a large and complex macromolecule with the high precision needed to ensure accurate protein translation is truly a magnificent feat. These differences between *in vivo* and *in vitro* ribosome assembly led researchers to speculate early on that there likely existed auxiliary factors within the cell that helped to expedite ribosome biogenesis (Mangiarotti et al., 1975). Furthermore, errors during RNA folding can causes molecules to become stuck in local "kinetic traps" that can impede the progress of ribosome assembly (Treiber and Williamson, 1999) (Uhlenbeck, 1995). In fact, it has been suggested that the $_{p1}$30S and $_{p2}$30S *in vivo* assembly intermediates accumulate as a result of aberrant rRNA folding leading to the kinetically trapped particles (Traub et al., 1967).

Ultimately, these observations fortified the notion that ribosome assembly within the cell is much more complex than *in vitro* and that non-ribosomal factors could help facilitate the process by guiding rRNA folding and lowering the activation energy needed for assembly (Culver, 2003).

Indeed, there have now been upwards of 60 prokaryotic and 200 eukaryotic ribosome auxiliary factors identified to have a role in the ribosome assembly process. These factors have been classified into several main categories in bacteria: RNA processing enzymes, protein and RNA modifying enzymes, RNA helicases, chaperones, maturation factors and GTPases (Shajani et al., 2011) (Woodson, 2011). Protein and RNA modifying enzymes catalyze the post-translation and post-transcriptional modifications that occur, respectively. Specifically, *E.coli* 16S rRNA nucleotides can be subjected to post-transcriptional methylations or pseudo-uridinlyations (Popova and Williamson, 2014) (Machnicka et al., 2013) and s-proteins can be exposed to post-translational methylations, acetylations and amino acid additions (Nesterchuk et al., 2011). The specific roles of these modifications remain elusive, however they are not vital and are believed to have regulatory functions (Nesterchuk et al., 2011). RNA helicases involved in ribosome assembly are mostly from a large family known as the DEAD box proteins, which possess a core of ~350 amino acids that contains at least 9 conserved motifs, one of which is a D-E-A-D box (Tanner et al., 2003) (Linder et al., 1989). These helicases generally contain RNA dependent ATPase activity and are involved in unwinding of local RNA secondary structure, assisting in RNA folding and altering RNA – protein interactions (Mohr et al., 2002) (Jankowsky et al., 2001) (Linder,

2006). Protein chaperones are also involved in ribosome assembly and deletion of genes involved in the heat shock protein 70 (HSP 70) molecular machinery results in an accumulation of immature 30S subunits that can slowly progress to the mature state (El Hage et al., 2001) (Alix and Guérin, 1993). Lastly, maturation factors and GTPases have diverse functions in ribosome assembly and have been implicated in altering RNA – protein interactions, RNA folding, domain organization and acting as a regulatory checkpoint (Shajani et al., 2011) (Britton, 2009) (Caldon et al., 2001). Ultimately, these assembly factors contribute to the extreme robustness of ribosome biogenesis that permits the manufacturing of one of the most complex cellular machines with the precision and speed needed to sustain life.

The final steps in the maturation of the 30S subunit are critical for the production of functional ribosomes. It is at that stage when the functional core of the subunit, the decoding centre, completes its maturation (Jomaa et al., 2011b) (Leong et al., 2013) (Guo et al., 2013) (Yang et al., 2014) (Clatterbuck Soper et al., 2013). There are at least four protein factors, YjeQ (also known as RsgA), RbfA, RimM and Era that bind at or near this site and ensure this motif folds properly into the functional conformation observed in the mature 30S subunit (Clatterbuck Soper et al., 2013) (Bunner et al., 2010b) (Jomaa et al., 2011a) (Guo et al., 2011) (Bylund et al., 1998) (Sharma et al., 2005). The specific roles implemented by each of these factors during maturation of the 30S decoding centre are still largely unknown. Proposed functions include altering the rRNA folding landscape and limiting the number of unproductive conformations by facilitating proper rRNA folding and mediating RNA-protein and protein–protein interactions (Clatterbuck

Soper et al., 2013) (Bunner et al., 2010b) (Shajani et al., 2011) (Wilson and Nierhaus, 2007) (Connolly and Culver, 2009) (Brown, 2005).

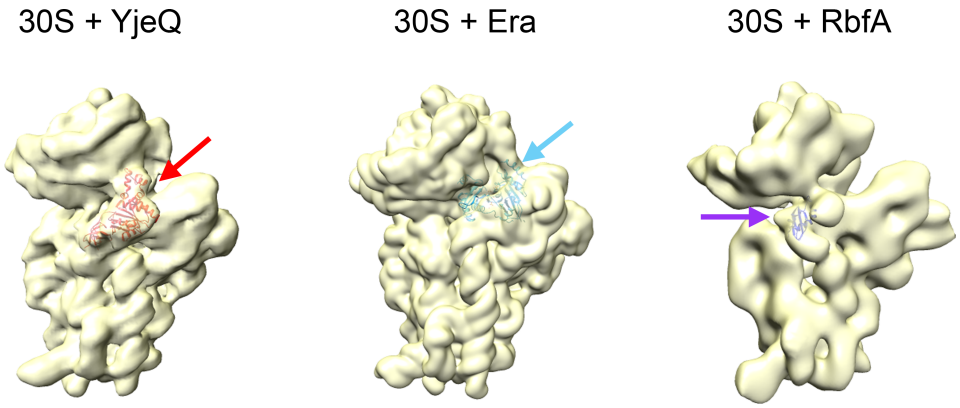

Figure 1.6. 30S subunit and assembly factor complexes.
The co-structures of the 30S complex bound to YjeQ (red), Era (light blue) or RbfA (purple) are shown. The binding sites for each assembly factor are indicated by coloured arrows. All three assembly factors have non-overlapping binding sites near the functional core of the 30S subunit. YjeQ binds near the central part of the 30S subunit, close to the decoding centre. The YjeQ + 30S co-structure was generated by fitting PDB 2YKR into the cryo-EM density corresponding to EMDB 1884. Era binds to the cleft between the head and platform near the solvent facing interface. The Era + 30S co-structure was generated by producing a cryo-EM density map of EMDB 1775 fitted with PDB 1X1L. The resulting cryo-EM density map was then fit with PDB 1EGA. RbfA binds to the 30S subunit in a position overlapping the A and P sites. The RbfA + 30S co-structure was generated by fitting PDB 2R1C and 2R1G with EMDB 1413. All structures were produced in UCSF Chimera.

1.3.1 YjeQ

Genome sequencing initially revealed YjeQ as a putative ATPase with unknown function that is broadly conserved amongst bacterial species (Arigoni et al., 1998). Subsequent analysis revealed that YjeQ is in fact a GTPase (Daigle et al., 2002) that can interact with the 30S subunit (Daigle and Brown, 2004) (Himeno et al., 2004) and is required for virulence in bacteria (Campbell et al., 2006). It is now known that YjeQ is a

39 kDa protein that can be divided into three domains: the N-terminal domain containing an oligonucleotide/oligosaccharide binding (OB) fold, the central domain containing a unique circularly permuted GTPase motif and the C-terminal zinc binding domain (Levdikov et al., 2004) (Shin et al., 2004) (Nichols et al., 2007). Structural investigations of YjeQ in complex with the small subunit by cryo-electron microscopy (cryo-EM) have revealed that it interacts with the decoding centre, head, platform and three essential inter-subunit bridges that are important for interactions between the 30S and 50S subunits (Jomaa et al., 2011a) (Guo et al., 2011) (Fig. 1.6). Furthermore, both the N-terminal (Guo et al., 2011) and C-terminal (Jomaa et al., 2011a) (Jeganathan et al., 2015) domains have been shown to be crucial for interactions of YjeQ with h44 in the small subunit. These interactions with the 30S subunit are dependent on YjeQ's nucleotide bound state with it stably bound in the presence of GMP-PNP, but not GTP or GDP (Himeno et al., 2004). Enzyme kinetic analysis have revealed that YjeQ has weak intrinsic GTPase activity, which is greatly enhanced in the presence of the small ribosomal subunit by two orders of magnitude (Daigle and Brown, 2004). Although YjeQ is dispensable in *E. coli*, deletion of YjeQ leads to an abnormal accumulation of free 30S and 50S subunits, a decrease in 70S ribosome formation, an accumulation of unprocessed 17S rRNA, resistance to salt stress and a slow growth phenotype, suggesting aberrant ribosome biogenesis and emphasizing its importance to the overall health of the cell (Himeno et al., 2004) (Daigle and Brown, 2004) (Jomaa et al., 2011b) (Guo et al., 2011) (Hase et al., 2009) (Table 1.1). Despite several studies now implicating YjeQ as a putative GTPase

involved in the maturation of the 30S subunit, its specific substrate in the assembly pathway and mechanism of action remains elusive.

1.3.2 Era

Era (*E.coli* ras like protein) is a widely conserved essential 33 kDa GTPase found in both prokaryotes and eukaryotes that contains a phosphate binding loop (P-loop) motif and RNA-binding K homology (KH) domain (Britton et al., 2000) (Comartin and Brown, 2006). It is considered to be a pleotropic protein that has been implicated in cell division (Britton et al., 1997) (Britton et al., 1998) (Gollop and March, 1991a) (Lerner et al., 1992), carbon metabolism (Powell et al., 1995) (Lerner and Inouye, 1991), cell membrane homeostasis (Gollop and March, 1991b) (Hang et al., 2001) (Hang and Zhao, 2003) and ribosome assembly (Sayed et al., 1999) (Sharma et al., 2005) (Tu et al., 2009) (Tu et al., 2011) (Inoue et al., 2006) (Inoue et al., 2003). Era can interact with various 16S rRNA oligonucleotides (Tu et al., 2009) (Tu et al., 2011), as well as the complete 30S subunit (Sharma et al., 2005), and facilitates the entry of late binding s-proteins across all three domains (Bunner et al., 2010b). A cryo-EM structure of the *T. Thermophilus* 30S – Era complex has shown that it binds near the decoding centre on the cleft formed by the platform and head and induces a conformational change that inhibits association of the 30S subunit with the 50S subunit (Sharma et al., 2005) (Fig. 1.6). Furthermore, Era depletion leads to an abnormal ribosome profile with a decrease in 70S ribosome formation, an accumulation of unprocessed precursor rRNA and substantially impaired cellular growth (Sayed et al., 1999) (Sharma et al., 2005) (Table 1.1).

1.3.3 RbfA

RbfA (ribosome binding factor A) is a 15 kDa protein that contains an RNA binding type II KH domain (Huang et al., 2003). It was originally classified as a cold shock protein capable of aiding in the continuous synthesis of ribosomal proteins and optimal growth at low temperatures (Dammel and Noller, 1995) (Jones and Inouye, 1996). RbfA is a multicopy suppressor of a 16S rRNA C23U cold-sensitivity mutation (Dammel and Noller, 1995), is important for the processing of 16S rRNA (Bylund et al., 1998), interacts directly with free 30S subunits (Xia et al., 2003) (Datta et al., 2007) and facilitates conformational changes in the 5' domain that are essential for proper pseudoknot formation (Clatterbuck Soper et al., 2013). A cryo-EM co-structure of the 30S-RbfA complex in *Thermus thermophilus* revealed that RbfA binds to a position overlapping the binding sites of the A and P site tRNAs and that there is a displacement of h44 (Datta et al., 2007) (Fig. 1.6). Furthermore, deletion of *rbfA* in *E.coli* leads to perturbed ribosome assembly characterized by an accumulation of precursor 17S RNA, an increase in free 30S and 50S subunits and an associated decrease in 70S ribosomes and polysomes (Inoue et al., 2003) (Bylund et al., 1998) (Table 1.1). Together, these studies strongly suggest that RbfA has an important role in 30S maturation and it has been categorized as a putative maturation factor.

1.3.4 RimM

RimM (ribosome maturation factor M) is a 21 kDa protein conserved amongst most eubacteria that contains an N-terminal RNA-binding KH domain and a C-terminal

photosynthetic reaction centre (PRC) domain (Bylund et al., 1997) (Lovgren et al., 2004). RimM was originally implicated in ribosome assembly because it associates directly with free 30S subunits and mutations that suppress a Δ*rimM* phenotype are present in the small subunit proteins, S13 (Bylund et al., 1997). Deletion of *rimM* in *E.coli* leads to a substantially reduced growth rate, decreased protein synthesis, defects in 16S rRNA processing and a perturbed ribosome profile (Bylund et al., 1997) (Bylund et al., 1998) (Leong et al., 2013) (Guo et al., 2013) (Table 1.1). Furthermore, RimM has been shown to interact with S19 through genetic (Lovgren et al., 2004), x-ray crystallography (PDB ID 3A1P) and nuclear magnetic resonance (NMR) (Suzuki et al., 2007) approaches, thus highlighting its possible interactions with the 3' head domain of the 30S subunit. Accordingly, RimM increases the rates of association of late-binding head domain s-proteins (Bunner et al., 2010b) and reduces 3' domain rRNA misfolding during 30S subunit maturation (Clatterbuck Soper et al., 2013).

Table 1.1. Description of Maturation Factors Involved in 30S Subunit Biogenesis.

Protein	Function	Dispensability Phenotypes			Interacts with	Cold Sensitivity
		Growth	RNA	Ribosome Profile		
YjeQ	GTPase	Slow	↑ 17S	↑ 30S ↑50S ↓70S	30S	✓
Era	GTPase	Essential	↑ 17S	↑ 30S ↑50S ↓70S	30S	✓
RbfA	Unknown	Slow	↑ 17S	↑ 30S ↑50S ↓70S	30S	✓
RimM	Unknown	Slow	↑ 17S	↑ 30S ↑50S ↓70S	30S	✓

1.3.5 Functional Interplay between Factors

Extensive genetic and biochemical studies suggest that these factors assist in the maturation of structurally important regions of the 30S subunit by acting in conjunction or in steps that are immediately linked (Campbell and Brown, 2008) (Bylund et al., 1998) (Bylund et al., 2001) (Goto et al., 2011) (Inoue et al., 2003) (Inoue et al., 2006) (Fig. 1.7). Genetic studies have demonstrated that slow growth and impaired ribosome biogenesis caused by the deletion of *rbfA* (Inoue et al., 2003) or *yjeQ* (Campbell and Brown, 2008) can be suppressed by overexpression of Era. Additionally, the slow growth and defective translation in Δ*rimM* cells can be suppressed by overexpression of *rbfA* (Bylund et al., 1998) and deletion of *rimM* enhances the slow growth in Δ*yjeQ* cells (Campbell and Brown, 2008). The most rigorous biochemical analysis of functional interplays has shown that YjeQ facilitates the release of RbfA during the late stages of 30S maturation (Goto et al., 2011) (Jeganathan et al., 2015). Ultimately, these investigations suggest that these factors have coordinated roles during ribosome assembly and may be functionally linked, however a model describing how these factors work together is still lacking. Specifically, it is has not been established exactly when these factors perform their function during 30S assembly or what intermediates they interact with. Furthermore, it remains to be determined whether each factor can recognize only a single or multiple intermediates and whether the binding of these assembly factors to the immature particles follows a specific hierarchy.

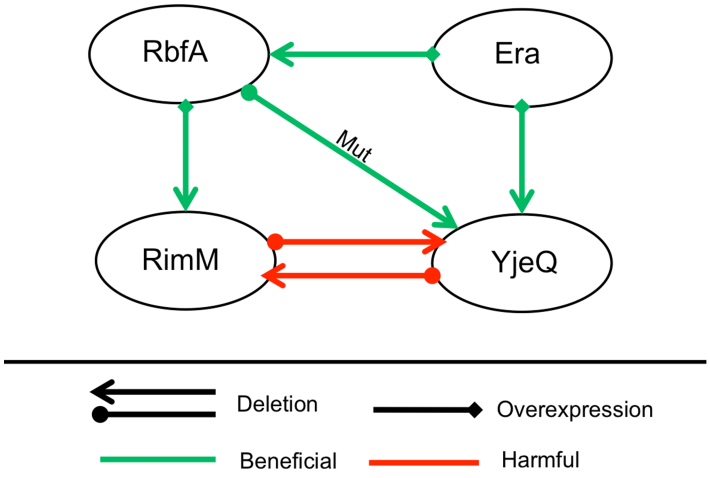

Figure 1.7. Functional interplay amongst assembly factors.
Interaction network showing that overexpression or mutation of assembly factors can compensate for deletion of other factors and that double assembly factor knockouts can have suppressing effects in cells. A square indicates overexpression and circles indicate deletion. A mutation is indicated by mut. Green arrows indicate the effects are beneficial (suppress deletion phenotype) and red arrows indicate negative effects (enhance deletion phenotype) to the cells. YjeQ and Era are GTPases and RbfA and RimM are maturation factors. All four factors have non-overlapping binding sites and have been shown to interact directly with 30S subunits. Figure adapted from (Shajani et al., 2011).

1.4 Assembly Factor Knockout Strains Provide a Powerful Tool for Investigating Maturation

The experimental approach most extensively used by multiple groups to gain new insights about the ribosome assembly process has been the use of knockout or depletion strains that lack one of the protein factors assisting in the process (Leong et al., 2013) (Jomaa et al., 2011b) (Clatterbuck Soper et al., 2013) (Yang et al., 2014) (Guo et al., 2013) (Goto et al., 2011) (Inoue et al., 2006) (Inoue et al., 2003) (Campbell and Brown, 2008) (Lovgren et al., 2004) (Bylund et al., 2001). These investigations have been extremely informative for identifying proteins, cellular phenotypes, functional interplays

and structural information associated with the ribosome assembly process. Furthermore, these studies have demonstrated that the deletion or depletion of 30S assembly factors leads to several common phenotypes that represent hallmarks of defective ribosome assembly (Table 1.1).

Studying ribosome assembly *in vivo* is a formidable challenge because the process is extremely efficient, resulting in little accumulation of precursor intermediates (Lindahl, 1973) (Lindahl, 1975) (Sykes et al., 2010). Researchers have been able to circumvent this problem by utilizing assembly factor deletion or depletion strains that perturb ribosome biogenesis leading to an accumulation of immature ribosomal particles that can be isolated and investigated (Jomaa et al., 2011b) (Leong et al., 2013) (Yang et al., 2014) (Guo et al., 2013) (Clatterbuck Soper et al., 2013). Structural and biochemical characterizations of the intermediates that accumulate in these strains have revealed that they have a structure and protein complement that is reminiscent of a late stage intermediate with unprocessed 17S rRNA. Most of the structural motifs of these immature ribosomal particles resemble those of the mature 30S subunit, however they all have a depletion of tertiary binding s-proteins and contain severe distortions at the decoding centre and essential intersubunit bridges that renders them unable to associate with 50S subunits or engage in translation. Furthermore, the particles that accumulate in the Δ*yjeQ* (Jomaa et al., 2011b), Δ*rimM* (Leong et al., 2013) (Guo et al., 2013) and Δ*yjeQ*Δ*rbfA* (Yang et al., 2014) strains have a similar structure and protein composition, suggesting that the multiple parallel pathways of assembly may converge to a few common intermediates near the final stages of maturation (Fig. 1.8).

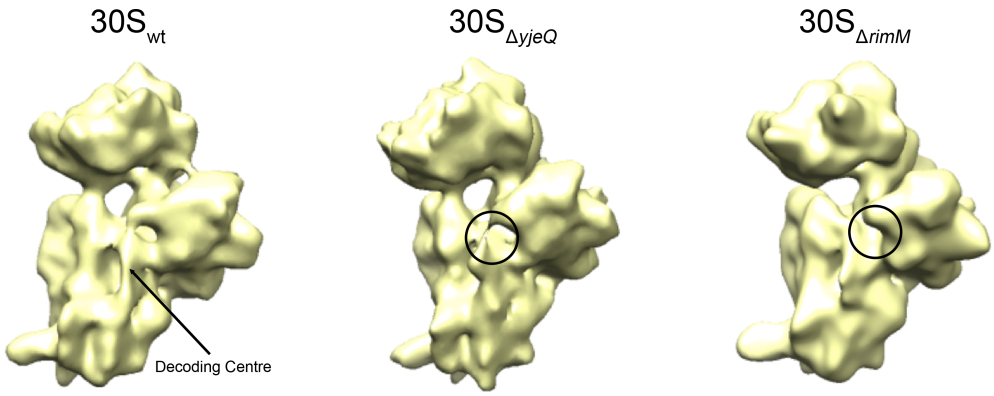

Figure 1.8. Cryo-EM density maps of immature 30S particles harvested from assembly factor knockout strains.
Cryo-EM density maps of 30S particles purified from wild type, Δ*yjeQ* and Δ*rimM E.coli* strains. The immature particles that accumulate in these strains have a distortion in the 3' minor domain containing the decoding center and an underrepresentation of tertiary s-proteins relative to the mature subunit. Similarities between the 30S$_{\Delta yjeQ}$ and 30S$_{\Delta rimM}$ particles have been suggested to be consistent with an early convergence model, in which the multiple parallel pathways of 30S subunit assembly converge into common intermediates prior to the final stages of maturation (Leong et al., 2013). The decoding centre in the mature 30S subunit and distorted decoding centre (circle) in the immature 30S particles are labelled. Figure was prepared in USCF Chimera with EMDB 1775 (wt), 1774 (30S$_{\Delta yjeQ}$) and 5595 (30S$_{\Delta rimM}$).

1.5 Thesis Objective

Despite the wealth of information that has been provided by these studies, it still remains to be shown whether the immature 30S particles that accumulate in these assembly factor null strains represent bona fide intermediates of the biogenesis pathway that are the actual substrates of the removed factors. Furthermore, although there has been structural analysis of immature 30S particles that accumulate upon deletion of the non-essential factors YjeQ (Jomaa et al., 2011b), RimM (Leong et al., 2013) (Guo et al.,

2013) and RbfA (Guo et al., 2011), there remains to be any structural studies of the particles that accumulate upon depletion of the essential factor, Era.

Therefore, the focus of this thesis project was to gain insights into the roles of 30S assembly factors by advancing our understanding about the particles that accumulate upon their deletion or depletion in bacterial strains. In particular, we aimed to determine whether the immature 30S particles that accumulate in these strains represent bona fide intermediates of the assembly pathway by establishing whether they are competent for maturation and rigorously assessing their interactions with assembly factors. Furthermore, we initiated the first structural investigation of immature 30S particles that accumulate upon depletion of an essential gene involved in 30S maturation, thus providing "snapshots" of assembling particles. Ultimately, this project provides new information about the nature of the immature ribosomal particles that assembly factor knockout or depletion strains accumulate by addressing three major questions:

1. Are the immature particles that accumulate in the Δ*yjeQ* and Δ*rimM E.coli* strains competent for maturation?
2. How do the assembly factors YjeQ, Era, RbfA and RimM interact with these accumulated particles?
3. What is the structure of immature 30S particles that accumulate upon depletion of Era?

1.6 Thesis Organization

This thesis is divided into three research chapters with additional chapters for general introduction, materials and methods and concluding remarks. Chapter 1 provides a general overview of the background information surrounding the 30S ribosome subunit and its assembly. Chapter 2 contains the detailed methods and materials that were used throughout this project for the experiments described in the research chapters. Chapters 3 and 4 contain research from two published manuscripts in the journals of *RNA* and *Nucleic Acids Research*. Chapter 3 aims to determine the ability of accumulated immature 30S particles from assembly factor single knockout strains to be competent for maturation. Chapter 4 assesses the interactions of numerous assembly factors with immature 30S particles. Chapter 5 discusses the development of an essential gene depletion strain for the 30S assembly factor *era* and a preliminary structural investigation of the 30S particles that accumulate. Chapter 6 contains concluding statements linking the findings in each chapter and providing a broader context to the relevance of this research to the field of ribosome assembly.

CHAPTER TWO

METHODS AND MATERIALS

2.1 Author's Preface

This chapter contains methods and materials that were conducted for two published manuscripts in the journals *RNA* and *Nucleic Acids Research*, as well as additional unpublished data. All of these protocols were conducted by me as a graduate student in Dr. Joaquin Ortega's lab unless otherwise noted in the respective results chapters (chapter 3-5). This thesis chapter has been modified and adapted from the two original published manuscripts. The full citations are listed below:

Jeganathan, Ajitha., Razi, Aida., Thurlow, Brett., Ortega, Joaquin. (2015). *The C-terminal helix in the YjeQ zing-finger domain catalyzes the releases of RbfA during 30S ribosome subunit assembly*. RNA. 21(6):1203-1216.

Thurlow, Brett., Davis, Joseph., Leong, Vivian., Moraes, Trevor., Williamson, James., Ortega, Joaquin. (2016). *Binding properties of YjeQ (RsgA), RbfA, RimM and Era to assembly intermediates of the 30S subunit*. Nucleic Acids Research. Epub ahead of print.

2.2 Cell Strains and Protein Overexpression Clones

Parental *E. coli* K-12 (BW25113), Δ*yjeQ* and Δ*rimM* strains were obtained from the Keio collection, a set of *E. coli* K-12 in-frame, single gene knockout mutants (Baba et al., 2006).

The high copy plasmids pCA24N, pCA24N-*rimM* and pCA24N-*yjeQ* were obtained from the ASKA collection, which contains a complete set of open reading frame clones of *E. coli* (Kitagawa et al., 2005). These vectors express N-terminal histidine-

tagged RimM and YjeQ respectively, under the control of isopropyl-beta-D-thiogalactopyranoside (IPTG)-inducible promoter $P_{T5\text{-}lac}$. The pDEST17-*yjeQ* plasmid used to overexpress YjeQ protein with an N-terminal His_6 tag cleavable by tobacco etch virus (TEV) protease was generated as previously described (Jomaa et al., 2011a).

The pET15b-*rbfA*, pET15b-*rimM* and pET15b-*era* plasmids used for overexpression of RbfA, RimM and Era, respectively were produced as follows. The sequence of the *rbfA* (NCBI reference: NC_007779.1), *rimM* gene (NCBI reference sequence: NC_010473.1) and *era* gene (GenBank reference: AP009048.1) were optimized for overexpression in *E. coli* cells using the GeneOptimizer software® and subsequently synthesized (Life Technologies; Thermo Fisher Scientific) with an *NdeI* and a *BamHI* site in the 5' and 3' ends of the gene, respectively. The genes were cloned into the carrier pMA-T plasmid using the *SfiI* and *SfiI* cloning sites and subsequently subcloned into the final expression vector pET15b using the *NdeI* and a *BamHI* restriction sites. The resulting pET15b-*rbfA*, pET15b-*rimM* and pET15b-*era* plasmids produce the RbfA, RimM and Era proteins with an N-terminal His_6 tag cleavable by thrombin. Sequencing (MOBIX, McMaster University) was used to validate all overexpression clones.

2.3 Generation of Era-depleted and Δ*rbfA E.coli* Strains

Table 2.1. Oligonucleotide sequences used for creation and screening of Era-depleted and Δ*rbfA E.coli* strains.

Oligonucleotide	Sequence
Era_up -R	5′-CATATGAGCATCGATAAAAGCTAC-3′
Era_down-F	5′-GGATCCTTACAGATCATCCACATAACC-3′
Era_Apra-F	5′-GAGCAGGCTGCCGCCGAACAGGCGTTGAAAAAACTGGAGCTGGAATGAGCAGCAAAAGGGGATGATAAGTTTATC-3′

Era_Apra-R	5′-GCGCTGCCAGCCTTCCATCGGAGTTACTCTTAAAGATCGTCAACGTAACCTCAGCCAATCGACTGGCGAGCGG-3′
Ara_up-R	5′-CGTTGGCCTCAATCGGC-3′
Ara_int-F	5′-CGATGCAGTACAGCTCACCG-3′
Kan_int-R	5′-GCCATCCTATGGAACTGCCTC-3′
EraKO_confirm-R	5`-CCTTTGGCAACCAGACGC-3′
EraKO_confirm-F	5′-CGCTGCCGACTTATCTGGTAG-3′
Apra_int-F	5′-CAGGCAGAGCAGATCATCTCTG-3′
Apra_int-R	5′-CAGAGATGATCTGCTCTGCCTG-3′
Rbfa_Apr-F	5′-ATTTTAAAAAGGGGCTAACAGCCCCTTTTTTGTCAGGAGAATTTATTATGAGCAAAAGGGGATGATAAGTTTATC-3′
Rbfa_Apr-R	5′-GACGACGAGGACGACTCATTAGTCCTCCTTGCTGTCGTCCGGGTTAACACTCAGCCAATCGACTGGCGAGCGG-3′
RbfaKO_confirm-F	5′-GTTCCATGCGGGATAAGGC-3′
RbfaKO_confirm -R	5′-GCGCACCGGTATGCC-3′

To generate the essential *era* gene depletion strain in the BW25113 *E.coli* background, the pBS-*araBAD*flank*kan* plasmid previously described in Campbell & Brown (Campbell and Brown, 2002) (Fig. 5.1A) and the temperature sensitive pSim6 plasmid previously described in Datta et al. (Datta et al., 2006) were used for insertion of *era* at the *araBAD* locus and recombination into the chromosome, respectively. PCR amplification of the *era* gene was performed with the Era_up-R and Era_down-F oligonucleotides (Table 2.1) using the previously described pET15b-*era* plasmid (see 2.2) as a template for amplification. The amplified product was cloned into the *PmeI* site of the pBS-*araBAD*flank*kan* and the resulting plasmid with *era* in the forward orientation with respect to the *araBAD* promoter was sequenced (Mobix, McMaster University) and named "pBS-*araBAD*flank*erakan"*. The *era* knockout cassette was generated by PCR amplification of pSET152 with the Era_Apra-F and Era_Apra-R oligonucleotides (Table 2.1). This generated an approximately 1100 bp product that contained the apramycin^r cassette flanked by 50 bp of the upstream and downstream sequences of the native *era* gene.

The precise deletion of *era* was carried out as described by Datsenko et al (Datsenko and Wanner, 2000) and Link et al (Link et al., 1997). pBS-*araBAD*flank*erakan* was double digested with *NotI* and *PsiI* resulting in an approximately 3,200–bp and 2,600-bp product. The digestion reaction was resolved in a 1% agarose gel and the 3.2 kb product containing the *era* gene flanked by homologous regions to the *araBAD* promoter was excised and gel purified using the QIAquick gel extraction kit (Qiagen) (Fig. 2.1A). Approximately 100 ng of this product was used to transform BW25113-pSim6 competent cells using electroporation and cells were plated on LB-agar containing 50 µg/ml kanamycin at 37 °C overnight to select for integrants at *araBAD* and facilitate curing of the temperature-sensitive pSim6 plasmid. To screen for strains in which the *araBAD* genes had been replaced by *era*, genomic DNA was isolated from the clones and used as a template for PCR amplification with the Era_down-F and Ara_up-R oligonucleotides (Table 2.1) (positive for chromosomal integrants) (Fig. 5.1C – top panel). A second round of PCR screening was performed using the Ara_int-F and Kan_int-R oligonucelotides (Table 2.1) (positive for chromosomal integrants) (Fig 5.1C – bottom panel). A strain positive for chromosomal integration was selected and named "*araBAD-era*". The *era* gene deletion protocol was conducted by transforming approximately 100 ng of the *era* knockout cassette using electroporation into *araBAD-era*-pSim6 cells followed by plating onto LB-agar containing 50 µg/ml kanamycin and 100 µg/ml apramycin and overnight incubation at 37 °C to select for integrants at the *era* locus and enable curing of the pSim6 plasmid (Fig. 2.1A). Genomic DNA was isolated from clones and used a template for PCR amplification using the EraKO_confirm-R and

Apra_int-F oligonucleotides (Table 2.1) (Fig. 5.1D – top panel) and the Apra_int-R and EraKO_confirm-F oligonucleotides (Table 2.1) (Fig. 5.1D – bottom panel) were used to confirm the deletion of *era*. The resulting strain with genotype *araBAD*::*era-kan*^{r}, *era*::*apr*^{r} was called "Era-depleted".

The precise deletion of *rbfA* in the BW25112 *E.coli* strain was performed according to the methods previously described by Datsenko et al (Datsenko and Wanner, 2000) and Link et al (Link et al., 1997) using the pSim6 plasmid described by Datta et al (Datta et al., 2006). The *rbfA* knockout cassette was generated by PCR amplification of pSET152 with RbfA_Apr-F and RbfA_Apr-R oligonucleotides (Table 2.1). This generated an approximately 1100 bp product that contained the apramycin^r cassette flanked by 50 bp of the upstream and downstream sequences of the native *rbfA* gene. Deletion of *rbfA* was accomplished by transforming approximately 100 ng of the *rbfA* knockout cassette into BW25113-pSim6 cells and plating cells onto LB-agar containing 100 μg/ml apramycin followed by overnight incubation at 37 °C to select for integrants at the *rbfA* locus and facilitate curing of the pSim6 plasmid (Fig. 2.1B). Genomic DNA was isolated from overnight colonies and used as a template for PCR amplification with the RbfaKO_confirm-R and Apra_int-F oligonucleotides (Table 2.1) (Fig. 5.1E – top panel) and RbfaKO_confirm-F and Apr_int-R oligonucleotides (Table 2.1) (Fig. 5.1E – bottom panel) to confirm the deletion of *rbfa.* The resulting strain with genotype *rbfA*::*apr*^{r} was called "Δ*rbfA*".

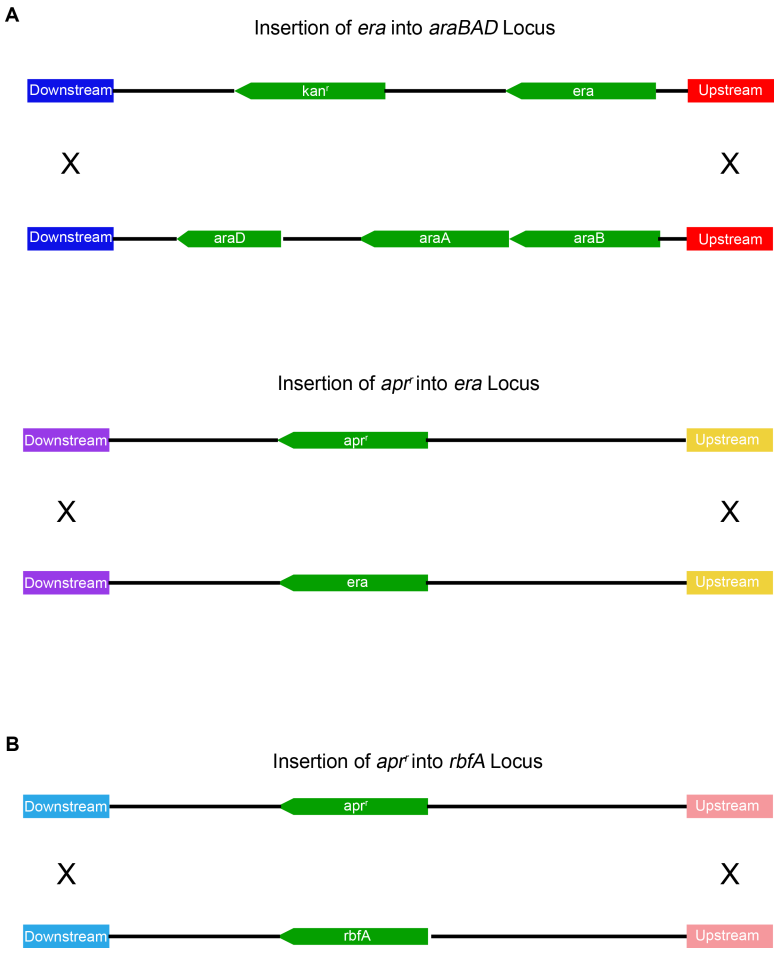

Figure 2.1. Diagram showing the creation of the Era-depleted and Δ*rbfA E.coli* strains in the parental BW25113 background.
(A) *era* was PCR amplified using the pET15b-*era* plasmid, cloned into the pBS-*araBAD*flank*kan* plasmid using the *PmeI* restriction enzyme site and integrated into the *E.coli* chromosome at the *araBAD* locus by recombination with the homologous upstream (red) and (dark blue) downstream sequences. The resulting strain was termed *araBAD-era*. The knockout of the native *era* gene was then facilitated by recombination of the apramycin^r *era* knockout cassette into the *E.coli* chromosome facilitated by the homologous upstream (yellow) and downstream sequences (purple). The genotype of the resulting strain was *araBAD*::*era-kan*^{r}, *era*::*apr*^{r} and was named Era-depleted. (B) The *rbfA* knockout strain was generated by inserting the apramycin^r *rbfA* knockout cassette into the *E.coli* chromosome facilitated by the homologous upstream (pink) and downstream (light blue) sequences. The genotype of the resulting strain was *rbfA*::*apr*^{r} and was named Δ*rbfA*.

2.4 Culture Growth Conditions

To obtain the growth curves for the wild type, Era-depleted and Δ*rbfA E.coli* strains, the cultures were grown overnight in LB media at 37 °C with shaking at 225 rpm in an Excella E24 incubator (New Brunswick). In the case of the Era-depleted strain, the LB media was supplemented with 1% arabinose. The overnight cultures were diluted 1/10,000 with LB media to a final volume of 100 µl in a 96-well plate with fresh LB media and the Era-depleted strain was grown in either the presence or absence of 1% arabinose. Cultures were incubated at either 37 °C or 15 °C with shaking in a Tecan Sunrise^{TM} Plate Reader for either 24 or 72 hours, respectively. Culture density was monitored by measuring the optical density at 600 nm (OD_{600}) every ten minutes during the time course of the experiment. Optical density was plotted over time (minutes) to show the growth curve for each strain at both 37 °C and 15 °C. The experiment was performed with five replicates.

2.5 Protein Overexpression and Purification

The purification procedure for YjeQ used in this study was established in a previous publication (Jomaa et al., 2011a), however at the onset of this thesis there were no purifications protocols for Era, RimM or RbfA. YjeQ was overexpressed as an N-terminal His_6-tag protein by transforming *E. coli* BL21-A1 with the pDEST17-*yjeQ* plasmid described above. Era, RimM and RbfA were overexpressed as N-terminal His_6-tag proteins by transforming *E. coli* BL21-DE3 with pET15b-*Era,* pET15b-*rimM* or pET15b-*rbfA* plasmids, respectively.

To determine the optimal purification conditions for Era, RbfA and RimM, solubility and expression for each protein was assessed at various temperature and induction times. Briefly, Bl21-DE3 cells transformed with pET15b-*era*, pET15b-*rimM* and pET15b-*rbfA* were grown in LB media at either 15 °C, 25 °C or 37 °C and expression of each protein was induced with IPTG. Prior to IPTG induction, and at multiple time points post-induction, a sample of culture was removed, lysed and centrifuged. Aliquots of both the supernatant and pellet were collected and analyzed using SDS-PAGE to determine the distribution of protein in the soluble (supernatant) and insoluble (pellet) fractions. It was determined that at 37 °C there was optimal expression and solubility for Era, RbfA and RimM, thus those conditions were chosen as the starting point for determining the purification procedure for each protein.

The overexpression protocol, as well as the harvesting and lysis of the cells prior to protein purification, was performed for the four proteins in the same manner. Typically, one liter of LB medium was inoculated with 10 ml of saturated overnight culture and cells were grown to OD_{600} = 0.6 by incubation at 37 °C and shaking at 225 rpm in an Excella E24 incubator (New Brunswick). Expression was induced with 0.2% L-arabinose for YjeQ or 1 mM IPTG for Era, RimM and RbfA. Cells were then induced for 3 hours at 37 °C and harvested by centrifugation at 3,700*g* for 15 min. Cell pellets were washed with 1 X PBS buffer (137 mM NaCl, 2.7 mM KCl, 8.1 mM Na_2HPO_4 at pH 7.4) and resuspended in 20 ml of lysis buffer (50 mM Tris-HCl at pH 8.0, 10% [w/v] sucrose, 100 mM NaCl) containing a protease inhibitor cocktail (cOmplete™ Mini Protease Inhibitor Cocktail Tablets, Roche). The cell suspension was passed through a

French pressure cell at 1400 kg/cm^2 three consecutive times to lyse the cells. The lysate was spun at 39,200*g* for 45 min to clear cell debris and the supernatant was collected. All of the following steps were performed at 4 °C.

In the case of the Era protein, the purification process started with drop-wise addition of a 5% polyethyleneimine (PEI) solution to the lysate with shaking to a final concentration of 0.0175% [v/v]. After centrifugation at 1,200*g* for ten minutes in an Eppendorf Mini-spin centrifuge, the soluble portion was recovered. Saturated ammonium sulfate (AS) (4.1 M) solution was then added drop-wise while the solution was shaking until a concentration of 45% AS [v/v] was reached. The precipitate that formed was collected and dissolved in ~10 ml of buffer containing 50 mM Tris-HCl at pH 8.0, 0.5 M NaCl and 5% [v/v] glycerol. The purification of Era then proceeded using a combination of metal chelating and anion exchange chromatography (see below). In the case of YjeQ, RimM and RbfA the purification was performed in the same manner but without the initial polyethyleneimine and AS precipitation steps.

To this end, NaCl was added to the supernatant of the YjeQ, RimM and RbfA overexpressing cells to a concentration of 0.5 M. Clarified cell lysates of all four assembly factors were passed through a 0.45-µm syringe filter (Millipore) and loaded to a HiTrap Metal Chelating Column (GE Healthcare Life Sciences) previously equilibrated with 50 mM Tris-HCl at pH 8.0, 0.5 M NaCl and 5% [v/v] glycerol. Nonspecifically bound proteins were washed with incremental step-wise increases in the concentration of imidazole from 45 mM to 90 mM for YjeQ, Era and RimM and 30 mM and 75 mM for RbfA. YjeQ, RimM and RbfA were eluted with 240 mM imidazole and Era with 255

mM imidazole. Purity of the fractions was monitored by SDS-PAGE and fractions containing each respective protein were collected and pooled together.

For YjeQ, the N-terminal His_6-tag was removed by digestion with TEV protease at a ratio of 10:1 (YjeQ:TEV) during overnight dialysis against buffer containing 50 mM Tris-HCl at pH 8.0, 60 mM imidazole and 0.2 M NaCl. Any overnight precipitate was removed by spinning at 12,000*g* for 10 min and the supernatant was collected and loaded onto a HiTrap Metal Chelating Column previously equilibrated with 50 mM Tris-HCl at pH 8.0, 0.2 M NaCl and 60 mM imidazole. Fractions were collected and their purity evaluated by SDS-PAGE and Coomassie Brilliant Blue staining. Fractions containing pure untagged YjeQ were pooled and dialyzed against 50 mM Tris-HCl at pH 8.0, 5% [v/v] glycerol overnight. A 10 kDa-cutoff filter (Amicon) was used to concentrate the protein and the purified YjeQ was frozen in liquid nitrogen and stored at -80 °C.

For Era and RimM, the N-terminal His_6-tag was removed by digestion with thrombin (Sigma) at a concentration of 10 U/mg during overnight dialysis against 50 mM Tris-HCl at pH 8.0, 5% [v/v] glycerol. In the case of RbfA, the pooled fractions were dialyzed overnight against 50 mM Tris-HCl at pH 8.0, 5% [v/v] glycerol, but the N-terminal His_6-tag in RbfA was not removed for easier visualization of the protein in the binding assays with the 30S ribosomal subunits. Dialyzed protein preparations were spun at 12,000*g* for ten minutes in an Eppendorf Mini-spin centrifuge to remove any precipitated protein. Supernatant was collected and loaded onto a Hi-Trap QHP anion exchange column (GE Healthcare Life Sciences) previously equilibrated with 50 mM Tris-HCl at pH 8.0, 5% [v/v] glycerol. RimM was washed with a linear NaCl gradient

and was eluted between 350-500 mM NaCl. RbfA was washed with 50 mM NaCl and eluted with 100 mM NaCl. An incremental step-wise increase in NaCl concentration at 50 mM and 150 mM was used to wash Era and this protein was eluted with 450 mM NaCl. SDS-PAGE followed by staining with Coomassie Brilliant Blue was used to evaluate the purity of the eluted fractions containing Era, RimM or RbfA. Fractions containing pure protein were pooled, dialyzed against 50 mM Tris-HCl at pH 8.0, 5% [v/v] glycerol overnight and concentrated using a 10 kDa-cutoff filter (Amicon). Pure proteins were frozen in liquid nitrogen and stored at -80 °C.

To obtain ^{15}N-labelled proteins for mass spectrometry analysis, the assembly factors were purified as described above with the following modifications to the growth conditions. A mixture containing 2.5 ml of LB media and 2.5 ml of M9 minimal media containing 18.7 mM $^{15}NH_4Cl$ was inoculated with *E.coli* cells transformed with the overexpression plasmids pDEST17-*yjeQ*, pET15b-*Era*, pET15b-*rbfA* or pET15b-*rimM*. The cells were grown for 8 hours at 37 °C with shaking at 225 rpm until cultures reached turbidity. Saturated cultures were then inoculated into 100 ml of M9 minimal media containing 18.7 mM $^{15}NH_4Cl$ and grown overnight at 37 °C with shaking at 225 rpm. A volume of 900 ml of fresh M9 minimal media containing 18.7 mM $^{15}NH_4Cl$ was then inoculated with 100 ml of the saturated overnight culture and cells were grown at 37 °C with shaking at 225 rpm until they reached to OD_{600} = 0.6. All subsequent steps for the protein over-expression, lysing and harvesting of cells and purification of the N15 labelled assembly factors were performed as described above. For mass spectrometry analysis, the N-terminal His_6-tag was removed in all four proteins, including RbfA. In

the case of RbfA, the N-terminal His_6-tag was removed by digestion with thrombin at a concentration of 10 U/mg during overnight dialysis against 50 mM Tris HCl at pH 8.0, 5% [v/v] glycerol.

2.6 Purification of 30S Ribosomal Subunits

Purified 30S subunits from wild type (BW25113), Δ*yjeQ*, Δ*rimM*, Δ*rbfA* and Era-depleted *E. coli* strains were prepared using ultracentrifugations over sucrose cushions and gradients as previously described (Leong et al., 2013). For the Δ*yjeQ*, Δ*rimM* and Δ*rbfA* strains, 4 liters of LB media were inoculated with 40 ml of saturated overnight culture and cells were grown at 37 °C with 225 rpm of shaking in an Excella E24 incubator (New Brunswick) to an OD_{600} of 0.2. For the wild type strain, 1 liter of LB media was grown in a similar manner to an OD_{600} of 0.6. Cells were cooled down to 4 °C and all subsequent steps were conducted at this temperature as described in (Leong et al., 2013).

For the $30S_{Era\text{-}depleted}$ particles, overnight cultures were grown in LB media containing 1% arabinose, 100 μg/ml apramycin and 50 μg/ml kanamycin at 37 °C with 225 rpm of shaking. To initiate depletion, cells from saturated overnight cultures were pelleted by centrifugation at 12000*g* in a microcentrifuge and all arabinose containing media was removed. Cells were then diluted to OD_{600} = 0.02 in LB media containing 100 μg/ml apramycin and 50 μg/ml kanamycin and grown at 37 °C with agitation until they reached a doubling time of ~150 minutes. Cells were not allowed to grow beyond an OD_{600} of 0.2, thus if at this point cells were still exhibiting doubling times <150 min, then

the culture was diluted again to OD_{600} = 0.02 into pre-warmed LB media without arabinose. Typically, two cycles of growth dilution were required before the cells reached ~150 min doubling time and then cultures were used to inoculate 4 liters of pre-warmed media to an OD_{600} of 0.02 and cells were grown with agitation until they reached OD_{600} = 0.2. Full depletion of the Era protein was obtained in cells with a doubling time of 225 - 275 min. At that point, cells were harvested and $30S_{Era\text{-}depleted}$ subunits were prepared as previously described.

In the case of the 30S subunits purified under "low salt conditions" for mass spectrometry analysis, a similar protocol as described in (Leong et al., 2013) was used, however all buffers A to F contained only 60 mM NH_4Cl. In addition, the high salt wash performed in buffer C was omitted.

2.7 rRNA Analysis

In the experiment where the rRNA content in fractions of the sucrose gradients was analyzed (Fig. 3.3), fractions containing the free 30S, free 50S and 70S ribosomes were collected independently. Fractions for each subunit were pooled together and the ribosomal particles pelleted overnight at 120,000*g*. Pellets were resuspended in 80 µl of water, and the concentration was determined. Volume was adjusted to 100 µl and the total amount of rRNA did not exceed 100 µg. Proteinase K was added to a final concentration of 100 µg/ml and the mixture was incubated at room temperature for 30 min. 350 µl of RLT buffer from Qiagen RNeasy mini isolation kit and 250 µl of 100% ethanol was then added to the samples. The reaction was mixed and loaded onto the

column provided by the Qiagen RNeasy mini isolation kit. Subsequent washes of the column were done according to the manufacture's protocol. RNA Loading Dye 2X (ThermoScientific) was added to 2 μg of purified rRNA samples, heated at 70 ºC for 10 min and put on ice for 5 min before loading into a modified agarose gel containing 0.7% agarose and 0.9% Synergel (Diversified Biotech) in 0.5X TBE buffer. RNA was separated by electrophoresis and visualized under ultraviolet (UV) light.

2.8 Pulse-Chase Labelling Experiments

Cultures of wild type (BW25113), Δ*yjeQ* and Δ*rimM E. coli* strains were grown overnight at 37 °C with shaking at 225 rpm to saturation in modified AB minimal media without uracil. 0.5 ml of each overnight culture was used to inoculate 50 ml of fresh AB media without uracil and these cultures were grown to mid-log phase. IPTG was added where indicated at the beginning of the "chase" phase of the experiment at the concentrations shown in Fig. 3.4. Cells were harvested by centrifuging at 5,300*g* for 10 min in a conical tube and resuspended with 1 ml of modified AB media without uracil. Cells were incubated at 37 °C with shaking at 225 rpm for 5 min to equilibrate and then 125 μCi of ^{3}H (tritium) uracil was added to the conical tube for a 2 min pulse at 37 ºC. Subsequently, to perform the chase, 200 μl samples of the culture were removed and added to multiple conical tubes each containing 4 ml of AB media with 8.9 mM uracil. At each time point of the chase, 420 μl of phenol-ethanol solution (5% water-saturated phenol, 95% ethanol) was added to the conical tubes to stop rRNA processing. To harvest the cells, samples collected from all time points were spun at 5,300*g* for 5 min,

flash frozen in liquid nitrogen and stored at -20 °C for subsequent rRNA analysis. Total RNA was extracted using the RNeasy Mini Kit (Qiagen) according to the manufacture's protocol. Isolated total RNA was loaded onto an 8% urea + 4% polyacrylamide gel and subjected to electrophoresis. The gel was washed in 0.5X Tris-buffered saline (TBS) and transferred to an Immobilon-Ny+ nylon membrane (Millipore) using electrophoresis. The nylon membrane was cross-linked by baking at 80 °C for 2 hours, sprayed with En^{3}hance Spray (PerkinElmer) and placed in a BioMax TranScreen-LE intensifying screen (Kodak) with BioMax MS film (Kodak). The BioMax Cassette (Kodak) was placed at -80 °C for ~96 hours and the film was developed.

2.9 *In Vitro* Ribosome Subunit Maturation Assay

In vitro maturation of 30S subunits was observed by monitoring the association of 30S subunits with 50S subunits to form 70S ribosomes. Crude ribosomes were prepared from wild type, Δ*yjeQ* and Δ*rimM E.coli* strains by inoculating 1 liter of LB media with 10 ml of saturated overnight culture. Cells were grown at 37 °C with 225 rpm of shaking to an OD_{600} of 0.2 for the null strains and 0.6 for the parental strain. Cells were cooled down to 4 °C and all subsequent steps were performed at this temperature unless otherwise noted. Cultures were harvested by centrifugation at 3,300*g* for 15 min and the cell pellet was washed in buffer QPA (10 mM Tris-HCl, pH 7.5, 10.5 mM $MgCl_2$, 60 mM KCl). Cells were centrifuged at 3,400*g* for 15 min and resuspended in 6 ml lysis buffer (10 mM Tris-HCl, pH 7.5, 10.5 mM $MgCl_2$, 60 mM KCl, 0.5% Tween 20 (v/v) and 1 mM dithiothreitol (DTT)) with the addition of cOmplete^{TM} Mini protease inhibitor

cocktail and DNaseI (Roche). Cell lysis was performed by passing the suspension through a French pressure cell at 1400 kg/cm^2 three consecutive times. Cellular debris was clarified by spinning the lysate at 27,700*g* for 20 min. Recovered supernatant was loaded into an Amicon Ultra 10 kDa MWCO filter (Millipore) and spun at 3,400*g* for 25 min to concentrate the volume to ~ 1 ml. The concentrated cell lysate was then divided into equal volumes for subsequent treatments and incubated at 37 °C or 4 °C for 1 or 2 hours, as indicated. After the treatment, cell lysates were subjected to ultracentrifugation at 386,400*g* for 45 min and the pellet gently washed by rinsing in 500 µl of buffer QPB (20 mM Tris-HCl, pH 7.5, 6 mM $MgCl_2$, 30 mM NH_4Cl, 1mM DTT). Subsequently, the pellet containing the crude ribosomes was resuspended in 250 µl of buffer QPB. Then, an equal volume of buffer QPC (20 mM Tris-HCl, pH 7.5, 6 mM $MgCl_2$, 800 mM NH_4Cl, 1mM DTT) was added for a stringent high salt wash and the mixture was incubated at 4 °C for 1 hr. The mixture was clarified by spinning at 31,900*g* for ten min and the supernatant was collected. Crude ribosomes were pelleted by spinning at 386,400*g* for 45 min and the pellet was gently washed by rinsing it and then resuspending it in 500 µl of buffer QPD (20 mM Tris-HCl at pH 7.5, 10 mM $MgCl_2$, 30 mM NH_4Cl, 1mM DTT) for 1 hour. The crude ribosomes were clarified by spinning at 31,900*g* for 10 min and the supernatant was collected.

A portion of the crude ribosome suspension (10 A_{260} units) was layered onto a 10 ml 10%-30% (w/v) sucrose gradient made in buffer QPE (20 mM Tris-HCl at pH 7.5, 10 mM $MgCl_2$, 50 mM NH_4Cl, 1mM DTT) and centrifuged at 48,400*g* for 16.5 hours. Gradients were fractionated using an AKTA prime purification system (GE healthcare)

and the elution peaks corresponding to 30S, 50S and 70S particles were monitored by absorbance at A_{260}. The areas under each respective peak were integrated using PrimeView Evaluation software and the total area for all three peaks was normalized for each data set. The proportions of free subunits and absolute value of 70S ribosomes were calculated. The area of the 30S peak plus one-third the area of the 70S peak corresponds to the total 30S population. The area of the 50S peak plus two-thirds the area of the 70S peak corresponds to the total 50S population. The standard deviations calculated for the different maturation assays were obtained from three replicas of the experiment.

2.10 Filtration Binding Assays

Initially, 100 kDa Nanosep Omega centrifugal devices (PALL) were prepared by blocking for non-specific binding of proteins by incubating the filter membrane with 500 µl of 1% [w/v] bovine serum albumin (BSA) for 90 min. Filters were then washed by rinsing with 500 µl of RNase free water and then removing any residual blocking solution by adding 500 µl of RNase free water and spinning at 12000*g* for 10 min. Binding reactions were prepared by incubating 200 pmoles of each assembly factor (YjeQ, Era, RimM and/or RbfA) with 40 pmoles of mature or immature 30S subunit in a 100 µl reaction in Binding Buffer (10 mM Tris-HCl at pH 8.0, 7 mM magnesium acetate, 300 mM NH_4Cl, 1 mM DTT). Nucleotide (GMP-PNP or GDP) was added where indicated to a final concentration of 0.4 mM. Reactions were incubated at 37 °C for 30 min followed by centrifugation in the blocked 100 kDa Nanosep Omega centrifugal devices (PALL) at 12000*g* for 10 min to separate 30S particles and 30S-bound proteins that were retained by

the filter from unbound proteins in the flow-through (FT) fraction. The flow-through was collected and the filter was gently washed twice with 100 µl of Binding Buffer followed by a 5 min spin at 12,000*g*. Finally, the 30S particles and 30S-bound proteins retained by the filter were vigorously resuspended in 100 µl of Binding Buffer and collected as the bound fraction (B). To resolve the flow-through and bound fractions, 30 µl of sample were mixed with 6X SDS-PAGE loading buffer and loaded into a 4-12% Criterion™ XT Bis-tris gel (Bio-Rad). Samples were run in XT MOPS buffer (Bio-Rad). Gels were stained with Coomassie Brilliant Blue and visualized using a ChemiDoc MP system (Bio-Rad). All filtration-binding experiments shown and discussed in this thesis were performed as described above unless otherwise noted in the figure description.

To assess the functional interplay between YjeQ and RbfA (Chapter 4) Image Lab (V5) software (Biorad) was used to perform densitometry analysis on the Coomassie stained gels for relative quantification of RbfA binding to the 30S particles. Specifically, the lanes were automatically detected using a background subtraction with a disc size of 5 mm. Bands were then automatically detected using high sensitivity settings (sensitivity: 5, size scale: 7, noise filter: 4, shoulder: 1) followed by manual adjustment of both lanes and bands to ensure accurate measurements. The quantity tools implemented with the Image Lab software package were used to determine the relative amounts of RbfA in the bound portion to the uS4 protein within the same lane. Binding of RbfA to the immature $30S_{\Delta yjeQ}$ particles subunit was considered as 1 and all other binding interactions were quantified with respect to this value.

2.11 Pelleting Binding Assays

Reactions were prepared by mixing 350 pmoles (7 μM) of YjeQ or Era with 50 pmoles (1 μM) of 30S particle in a 50 μl reaction in Binding Buffer (10 mM Tris-HCl at pH 8.0, 7 mM magnesium chloride, 300 mM NH_4Cl, 1 mM DTT) with 1 mM GMPNP. Reactions were incubated at 37 °C for 30 min. Following incubation, reactions were laid over a 150 μl 1.1 M sucrose cushion in Binding Buffer and ultracentrifuged at 436,000*g* for 3.5 hr. The supernatant (S) containing free protein that did not pellet with the 30S subunits was collected. The pellet (P) containing the 30S particles and 30S-bound proteins was resuspended in 200 μl of Binding Buffer. To resolve the supernatant and pellet fractions, 30 μl of sample was mixed with 6X SDS-PAGE loading buffer and loaded into a 4-12% Criterion™ XT Bis-tris gel (Bio-Rad). Samples were run in XT MOPS buffer (Bio-Rad). Gels were stained with Coomassie Brilliant Blue.

2.12 GTPase Assays

The intrinsic GTPase hydrolysis activity of YjeQ and Era was determined by incubating a constant concentration of 4 μM or 2μM of each protein respectively, with a range of GTP concentrations from 2 μM to 250 μM. The background of the assay itself was measured by running control reactions with no YjeQ or Era at each GTP concentration. These background values were subtracted from the total GTPase activity exhibited by the reactions containing the assembly factor at each GTP concentration. Reactions to test the stimulation of YjeQ and Era GTPase activity by ribosomal particles contained 50 nM concentration of YjeQ or Era and an equal concentration of either

mature 30S subunits or one of the immature particles. All assays were performed by first calculating the background GTPase stimulation from the ribosomal particles at 50 nM incubated with 2 to 250 uM of GTP. This background subtraction was performed for each ribosomal particle to ensure accuracy in the calculations by removing all background phosphate production not due to the assembly factors themselves. All reactions were incubated at 37 °C for 30 min before measuring the released free phosphate by the malachite green reagent (BioAssays Systems). The assay showed a linear behaviour for this incubation time. The reactions were performed in buffer (50 mM Tris-HCl (pH 7.5), 200 mM KCl, 10 mM $MgCl_2$ and 1 mM DTT) and terminated by the addition of malachite green reagent. Released phosphate was detected by monitoring the color formation at 620nm using a 96-well plate reader (Tecan Sunrise). The values of K_m and k_{cat} were calculated by fitting the data to the Michaelis-Menten equation using non-linear regression in GraphPad Prism. The assays were performed with three replicates of the experiment.

2.13 Microscale Thermophoresis

Microscale thermophoresis is an immobilization free biomolecular interaction technique that exploits how any change in the hydration shell, size or charge of a molecule due to an association with another molecule affects its ability to move along a temperature gradient. This change in the thermophoretic mobility can then be used to determine a disassociation constant, K_d. Initially, a 2 – 7 uM solution of mature 30S subunits ($30S_{wt}$) or immature 30S particles ($30S_{\Delta yjeQ}$ or $30S_{\Delta rimM}$) was fluorescently

labelled with maleimide red on cysteine residues using the Monolith NT^{TM} Protein Labelling Kit with the addition of 10 mM Mg acetate added to the supplied labelling buffer. Labelling efficiency was ~0.5:1 (fluorescent label: ribosome particle). This value was obtained by measuring the molar concentrations of the ribosomal particle at A_{260} and the fluorescent label at A_{650}.

For a typical MST experiment, a titration series with 16 dilutions was prepared in 0.5 ml Protein LoBind eppendorf tubes. The concentration of fluorescently labelled 30S subunit was kept constant between 10 – 40 nM and the concentration of titrant was varied. Prior to the preparation of the titration series all samples were centrifuged at 14000*g* for ten minutes to remove any aggregates. A 1:1 serial dilution of non-labelled titrant was then prepared in MST buffer (20 mM Tris-HCl pH=7.5, 150 mM NaCl, 10 mM $MgCl_2$, 1 mM DTT, 0.05% Tween-20, 0.4 mg/ml BSA) at the concentrations specified. For the experiments involving the addition of nucleotide, a concentration of either 1mM GMP-PNP or GDP was used where indicated. Ten microliters of the serial dilution of the non-labelled assembly factor was mixed with 10 microliters of the fluorescently labelled 30S subunit and reactions were incubated for ten minutes. Mixed samples were then loaded into hydrophobic capillaries (NanoTemper Technologies) and MST analysis was performed using the Monolith NT.115 at ambient temperature. Typically, an LED power of 60-80% was used and all trials were performed with both 60% and 80% MST power. The resulting binding curves were obtained by plotting the normalized fluorescence (F_{Norm} (‰)=F_1/F_0) versus the logarithm of different assembly factor concentrations. K_ds were calculated using the K_d Fit Function derived from the law

of mass action in the NanoTemper Analysis software (version 1.5.41). All experiments were performed in triplicate or greater.

2.14 Quantitative Mass Spectrometry

Subunit r-protein and assembly factor occupancy were measured in duplicate using either 6 pmol (replicate 1) or 12 pmol (replicate 2) of the subunit. Each ^{14}N-labelled subunit (wild-type 30S, wild-type 70S, $30S_{\Delta rimM,}$ or $30S_{\Delta yjeQ}$) was mixed with 6 pmol of ^{15}N-labelled 70S particles as well as 6 pmols of ^{15}N-labelled RimM, YjeQ, Era, and RbfA proteins. These 'spiked' samples were then precipitated by addition of 13% TCA, pellets were sequentially washed with 10% TCA and acetone as described previously (Jomaa et al., 2014). Pellets were then resuspended in 55 µL buffer DB [100 mM NH_4CO_3, 5% acetonitrile, 5 mM dithiotreitol] and incubated for 10 minutes at 65 °C. Iodoacetamide was added to a final concentration of 10 mM and samples were incubated at 30 °C for 30 minutes before addition of 0.5 µg trypsin and overnight incubation at 37 °C. Tryptic peptides were then purified on C-18 PepClean columns (Pierce).

Tryptic peptides were analyzed on an AB/Sciex Triple-TOF 5600+ mass spectrometer coupled to an Eksigent nano-HPLC. Briefly, peptides were loaded onto a 200 µm x 0.5 mm ChromXP C18-CL 3 µm 120 Å trap column using 95 % mobile phase A [0.1% v/v formic acid in water], 5 % mobile phase B [0.1% v/v formic acid in acetonitrile]. A 2 hour concave gradient ranging 5% - 45% mobile phase B was then run over the aforementioned trap column and a subsequent 75 µm x 15 mm ChromXP C18-CL 3 µm 120 Å analytic column.

A custom MRM-HR mass spectrometry method targeting multiple peptides for each ribosomal protein and the assembly factors was developed using Skyline software (University of Washington) (MacLean et al., 2010), as well as spectral data from prior "discovery" mass spectrometry analyses of ribosomal proteins (Stokes et al., 2014) and purified assembly factors. Peptides were chosen that gave strong MS^1 and MS^2 signals, generally lacked spectral interference, and spanned the elution gradient, allowing for efficient retention time-based scheduling. After filtering on these criteria, 286 precursor ions were selected for analysis. A single method using 7.5 minute scheduling windows, which included a 200 ms MS^1 scan (400-1,250 m/z) with up to 40 successive 100 ms MS^2 scans (100-1800 m/z) was then used to analyze each sample.

Precursor and product ion chromatograms were extracted using Skyline, filtered for spectral interference and the final peptide measurements were plotted using a series of custom Python scripts (Gulati et al., 2014).

2.15 Negative Staining Electron Microscopy

Purified $30S_{\text{Era-depleted}}$ and $30S_{\Delta rbfA}$ samples were diluted to 47 nM in ribosome storage buffer (10 mM Tris pH=7.5, 10 mM Mg acetate, 60 mM NH_4Cl, 3 mM β-mercaptoethanol). Electron microscopy grids (Electron Microscopy Sciences, G400-Cu) freshly coated with a continuous layer of carbon were glow discharged (5 mA for 15 s) and then floated on 5 µl drops of sample. Grids were then blotted and floated for 1 min on a 5 µl drop of 1% uranyl acetate for staining. Excess stain was removed by blotting, and the grids were air-dried. Specimens were visualized in a JEOL 1200EX electron

microscope operated at 80 kV and fitted with an AMT 4-megapixel digital camera (Advanced Microscopy Techniques, Woburn, MA).

2.16 Cryo-Electron Microscopy and Image Processing

Cryo-electron microscopy analysis was performed following similar protocols as previously described (Ni et al., 2016). 30S ribosomal particles purified from the Era-depleted *E. coli* strain were diluted to a concentration of ~70 nM in storage buffer (10mM Tris–HCl at pH 7.5, 10mM magnesium acetate, 60mM NH_4Cl and 3mM 2-mercaptoethanol). Holey carbon electron microscopy grids (c-flat CF-2/2-2C-T) were freshly coated with an additional layer (5–10 nm) of thin carbon and grids were then glow discharged at 5 mA for 15 seconds. Approximately 3.6 µl of the diluted $30S_{Era\text{-}depleted}$ sample was applied to the freshly coated holey carbon grids and vitrification of the specimen was performed in a Vitrobot (FEI) with the blotting chamber maintained at 25 °C and 100% relative humidity. The grids were blotted twice, for 15 seconds each time, with an offset of -1.5 before they were plunged into liquid ethane. Grids were loaded using a Gatan 626 single tilt cryo-holder into the FEI Tecnai F20 electron microscope (FEI) operated at 200 kV and equipped with a Gatan K2 Summit direct electron detector device camera. This detector was used in counting mode with five electrons per pixel per second for 15 second exposures and 0.5 seconds per frame. This method produced movies containing 30 frames with an exposure rate of one electron per square angstrom per frame. Movies were collected using a range of defocus from -1 to -3.5 µm and a nominal magnification of 25,000x, which produces images with a calibrated pixel size of

1.45Å. The 30 frames in each movie were aligned using the program alignframesleastsquares_list (Rubinstein and Brubaker, 2015) and averaged into one single micrograph with the shiftframes_list program (Rubinstein and Brubaker, 2015). These micrographs were used to determine the parameters of the contrast transfer function using CTFFIND3 (Mindell and Grigorieff, 2003) and also to select for the coordinates of ~100 particles per image using the autopicking procedure in Relion 1.3 (Scheres, 2012a). The obtained coordinates were used to extract and produce a stack of candidate particle images. The initial number of particles extracted from the dataset for the $30S_{Era\text{-}depleted}$ sample was 29,217. This dataset was processed using the two-dimensional (2D) and 3D classification implemented by Relion 1.3 (Scheres, 2012a). Particles images obtained from the 2D classification step that resembled projections of 30S subunits and contained high-resolution features were chosen for further analysis. The 3D structures generated from the single particle analysis of the $30S_{Era\text{-}depleted}$ particles were built from 28,878 particle images that were assigned into twelve distinct classes. Twelve classes were requested for the 3D classification step to ensure that distinct and unique conformations were appropriately classified without the potential for them being grouped together. After the 3D classification, the three classes containing the majority (69%) of the total particles were selected for subsequent refinement and post-processing. Image processes were calculated using the hdos cluster at McMaster University. 3D cryo-electron density maps were generated using UCSF Chimera.

CHAPTER THREE

IMMATURE 30S PARTICLES IN Δ*yjeQ* AND Δ*rimM E. COLI* STRAINS ARE COMPETENT FOR MATURATION

3.1 Author's Preface

This chapter contains a subset of experiments that were conducted for a published manuscript in the journal *Nucleic Acids Research*. This manuscript aimed to characterize two main features about the nature of immature 30S particles that accumulate in the Δ*yjeQ* and Δ*rimM E.coli* strains. We first wanted to determine the fate of 30S particles that accumulate in these strains to determine if they are capable of assembling into mature 30S subunits and can form 70S ribosomes. Next, we wanted to analyze the binding interactions of assembly factors with these particles. This chapter focuses on the first part of the published manuscript and assesses if these immature 30S particles are competent for maturation. This thesis chapter has been modified from the original published manuscript and is not an exact copy. The contributions and full citations are listed below:

Thurlow, Brett., Davis, Joseph., Leong, Vivian., Moraes, Trevor., Williamson, James., Ortega, Joaquin. (2016). *Binding properties of YjeQ (RsgA), RbfA, RimM and Era to assembly intermediates of the 30S subunit*. Nucleic Acids Research. Epub ahead of print.

I performed all *in vitro* maturation assay experiments (Fig. 1.1) and prepared the samples used for the RNA analysis (Fig. 1.2). Vivian Leong performed all pulse-chase labelling experiments (Fig. 1.4) and ran the agarose gels for the RNA analysis (Fig. 1.2).

All authors contributed to the analysis of the data. Dr. Joaquin Ortega and I wrote the manuscript with feedback and contributions from other authors.

3.2 Introduction

One of the most utilized methods for studying putative ribosome biogenesis factors has been using assembly factor knockout or depletion bacteria strains to disrupt the maturation pathway and cause an accumulation of *in vivo* assembled precursors (Leong et al., 2013) (Jomaa et al., 2011b) (Guo et al., 2013) (Clatterbuck Soper et al., 2013) (Yang et al., 2014) (Goto et al., 2011) that typically remain in extremely low abundance under wild type conditions (Lindahl, 1975) (Lindahl, 1973) (Sykes et al., 2010). These studies have been instrumental in building upon our knowledge about ribosome assembly by providing a source of immature 30S particles for investigation. However, a major question that has remained is what the ultimate fate of these particles in the cell is. It has generally been assumed that these particles represent actual intermediates of the assembly pathway that accumulate because the process has been delayed, but can ultimately complete their maturation and enter the pool of translating ribosomes. Alternatively, these particles can represent dead-end products of a dysfunctional assembly pathway that cannot progress into mature 30S subunits and would ultimately be targeted for degradation within the cell. Prior to the work performed for this PhD project there had been no published studies that aggressively sought to answer this question and confirm whether these immature 30S particles are competent for maturation.

To address this question we used both *in vitro* and *in vivo* approaches to determine the possible fates of 30S particles that accumulate upon deletion of the assembly factors YjeQ or RimM. First, we used an *in vitro* maturation assay (see 2.9) to assess if immature 30S particles that accumulate in the Δ*yjeQ* ($30S_{\Delta yjeQ}$) and Δ*rimM* ($30S_{\Delta rimM}$) strains can associate with 50S subunits to form 70S ribosomes. We next used an *in vivo* pulse labelling method (see 2.8) to track the fate of a discrete population of 17S rRNA in the Δ*yjeQ* and Δ*rimM* strains and monitor its progression into mature 16S rRNA in a time dependent manner. In this study, we found that the immature 30S particles that accumulate in the Δ*yjeQ* and Δ*rimM* strains can progress into mature 30S subunits that can associate with 50S subunits to form 70S ribosomes, although at a slower rate than the wild type cells. Therefore, this study helps to shed light on the fate of the immature 30S particles that accumulate in these strains and provides assurance that studying these particles provides physiological relevant information about the assembly process.

3.3 Immature 30S ribosomal particles that accumulate in the Δ*rimM* and Δ*yjeQ* strains progress into 30S subunits that can associate with 50S particles

Evidence that at least a significant portion of the immature 30S ribosomal particles accumulating in Δ*rimM* and Δ*yjeQ* strains progress to the mature state was obtained by performing *in vitro* maturation assays (see 2.9) using cell lysates from the Δ*yjeQ* and Δ*rimM E.coli* strains. Previous cryo-EM structural characterization of the accumulated immature 30S particles isolated from the Δ*rimM* and Δ*yjeQ* strains have revealed that essential inter-subunit bridges and the 3' minor domain are present in a

distorted, flexible conformation that prevents their association with the 50S subunit (Leong et al., 2013) (Jomaa et al., 2011b) (Guo et al., 2013) (Yang et al., 2014). Accordingly, we tested whether the assembling 30S particles that accumulate in the null strains are able to mature by measuring the ability of 30S particles to form 70S ribosomes upon different incubation conditions of cell lysates. The premise of this assay was that only the 30S subunits that adopt a mature structure would be able to associate with 50S subunits to form 70S ribosomes.

Briefly, these experiments were performed by clarifying cell lysates from exponentially growing wild type, Δ*yjeQ* and Δ*rimM E.coli* strains. The cell lysates were then concentrated in a centrifugal device and incubated for 1 hour at 4 ºC or at 37 ºC. After incubation, the crude ribosomes were collected by pelleting the concentrated cell lysates with an ultracentrifuge followed by a series of clarification and high salt wash steps. The crude ribosome suspension was then layered on top a sucrose gradient and the individual components were separated by ultracentrifugation allowing for the distribution of free 30S and 50S subunits and the amount of 70S ribosomes to be analyzed (detailed methods in 2.9).

Initially, control experiments were performed using cells harvested from exponentially growing wild type cells (Fig. 3.1A). Incubation of cell lysates from wild type cells at 37 ºC for 1 hour led to no substantial change in the amount of free 30S and 50S subunits or 70S ribosomes compared to when the incubation was done at 4 ºC for 1 hour (Figure 3.1A). This control experiment was important for ensuring that concentration and incubation of the cell lysates did not alter the distribution of particles in

the ribosome profile, increase the amount of 70S ribosomes or cause degradation of subunits (Fig. 3.1A). Furthermore, it confirmed that the total amount of the free subunits is small relative to the total amount of 70S ribosomes.

Concentration of cell lysates from the Δ*rimM* (Fig. 3.1B) and Δ*yjeQ* (Fig. 3.1C) strains led to a significant reduction in the amount of free 30S and 50S subunits and a concurrent increase in the amount of 70S ribosomes when incubated at 37 °C compared to 4 °C. The percentage of free 30S subunits in the Δ*yjeQ* strain when cell lysates were maintained at 4 °C was 31% and decreased to 14% upon incubation at 37 °C. Similarly for the free 50S subunits, their percentage also decreased from 41% to 25% and the total amount of 70S ribosomes increased by 25% (Fig. 3.1C). In the case of the Δ*rimM* strain we found that a 1-hour incubation at 37 ºC only induced a minor effect on the distribution of ribosomal particles of the cell lysates compared to the 4 ºC control (data not shown). However, when the incubation time was increased to 2 hours, the percentages of free 30S subunits decreased from 51% to 44% and the percentage of 50S subunits decreased from 63% to 53% (Fig. 3.1B). Furthermore, there was a corresponding increase in the amount of 70S ribosomes by 24% at 37 °C versus 4 °C (Fig. 3.1B). These results suggest that a significant portion of the immature 30S subunits that accumulate in the null strains are capable of maturing into 30S subunits that can associate with 50S subunits to form 70S ribosomes.

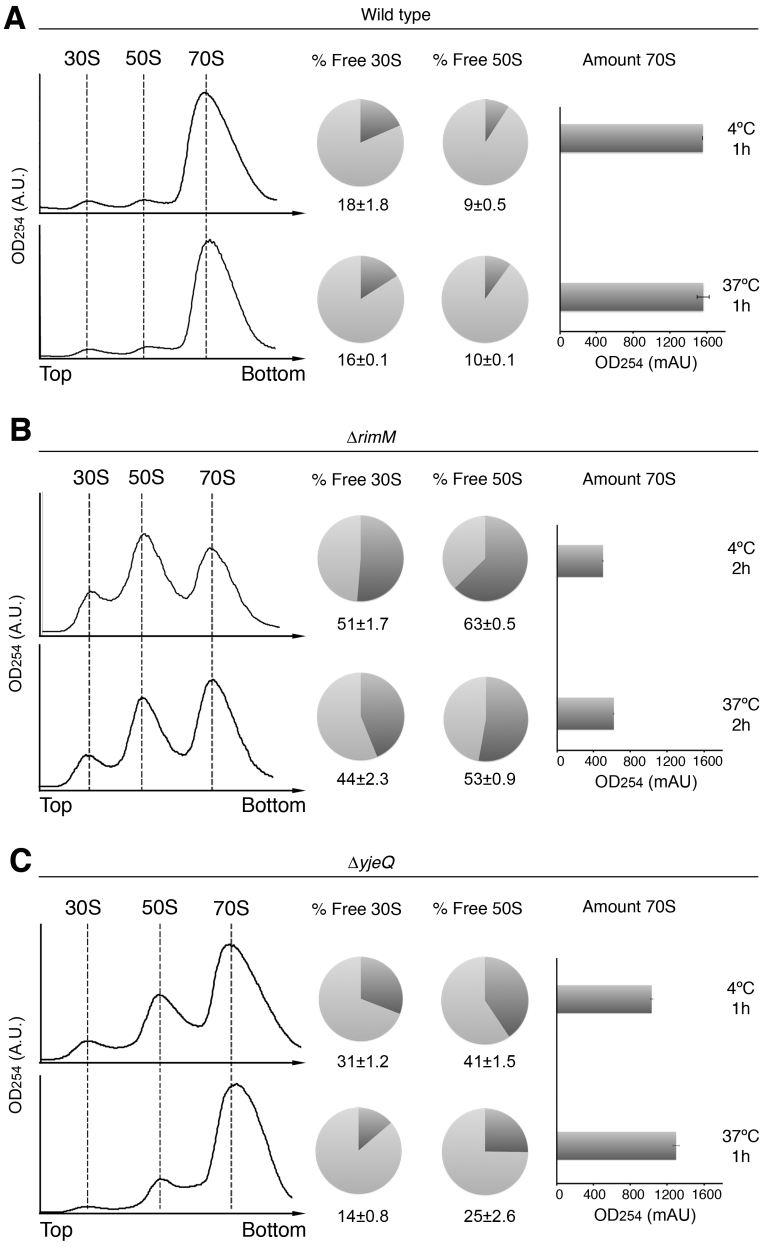

Figure 3.1. The immature 30S$_{\Delta yjeQ}$ or 30S$_{\Delta rimM}$ particles are able to associate with 50S subunits to form 70S ribosomes.

Concentrated cell lysates of wild type (A), Δ*rimM* (B) and Δ*yjeQ* (C) strains were incubated for 1 or 2 hours at 37 °C. After the treatment, crude ribosomes were purified from these cell extracts and layered onto sucrose gradients for separation of the 30S and 50S subunits and the 70S ribosomes, enabling the distribution of each subunit to be calculated. Panels in the figures show the results for the wild type (A), Δ*rimM* (B) and Δ*yjeQ* (C) strains. The standard deviations shown correspond to three replicas of the experiment. We performed an unpaired t-test for each strain to determine the statistical

significance of the changes observed in the percentages of free 30S and 50S subunits and amount of 70S ribosomes upon incubation. The obtained P-values for the changes during incubation in the free 30S, free 50S and total 70S ribosomes for wild type were $p>0.05$. In the case of the Δ*yjeQ* strain the obtained P-values were $p<0.0001$ (free 30S) and $p<0.001$ (free 50S and 70S). Finally, for the Δ*rimM* strain the P-values were $p<0.05$ (free 30S) and $p<0.0001$ (free 50S and 70S).

3.4 Immature 30S ribosomal subunits that accumulate in the *yjeQ* and *rimM* null strains are competent for maturation

We next tested whether the $30S_{\Delta yjeQ}$ and $30S_{\Delta rimM}$ particles were true assembly intermediates that are competent for maturation or instead, were dead-end products of the assembly pathway. It has previously been suggested that some 17S rRNA containing immature 30S particles assemble into 70S ribosomes (Roy-Chaudhuri et al., 2010) (Clatterbuck Soper et al., 2013) (Mangiarotti et al., 1974) (Hayes and Vasseur, 1976). Therefore, it was first necessary to analyze the distribution of rRNA amongst the free subunits and ribosomes to ensure that conversion of 17S rRNA to 16S rRNA was an appropriate parameter for assessing maturation in the Δ*yjeQ* and Δ*rimM* strains. To determine the distribution of the unprocessed 17S rRNA and mature 16S rRNA in these strains, the cell cultures were grown to early exponential growth phase (OD_{600}=0.2) and then harvested cultures were used to obtain ribosomal profiles by sucrose gradient ultracentrifugation. Ribosome profiles (Fig. 3.2) were consistent with previously published work (Jomaa et al., 2011b) (Leong et al., 2013) (Guo et al., 2013) showing that both null strains have a severe reduction in 70S ribosomes and a corresponding increase in the level of free 30S and 50S subunits compared to the parental strain.

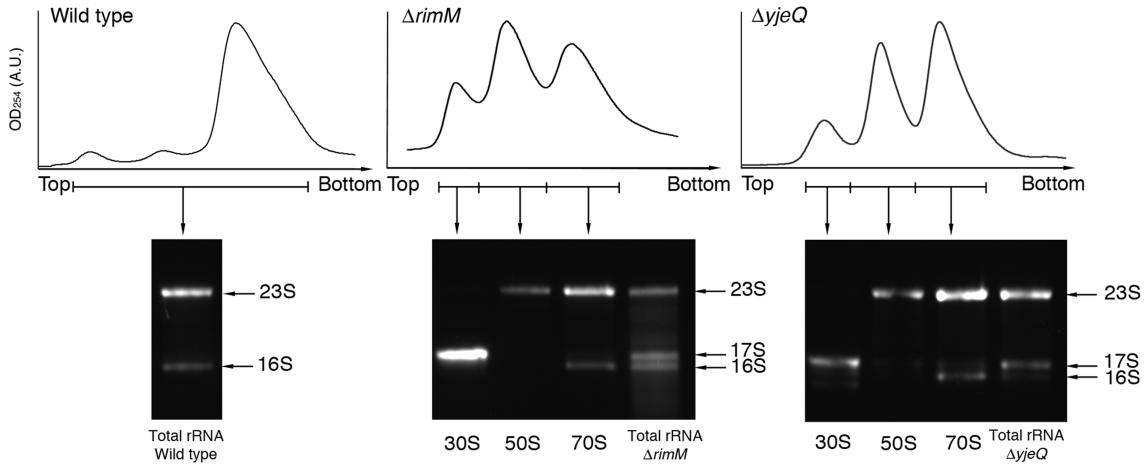

Figure 3.2. rRNA analysis in wt, Δ*yjeQ* and Δ*rimM* strains
The immature $30S_{\Delta yjeQ}$ or $30S_{\Delta rimM}$ particles accumulating in the Δ*yjeQ* and Δ*rimM* strains contain exclusively unprocessed 17S rRNA. Ribosomes from wild type, *yjeQ* and *rimM* null strains were resolved on 10-30% sucrose gradients. Fractions from each peak of the sucrose gradients were collected for total rRNA extraction and resolved by modified agarose gel electrophoresis. Total rRNA content in the three strains was also determined as a control. Gels were stained with ethidium bromide.

RNA extractions and agarose gel electrophoresis (see 2.7) were then used to assess the distribution of 17S and 16S rRNA in the $30S_{wt}$, $30S_{\Delta yjeQ}$ and $30S_{\Delta rimM}$ particles, as well as the 70S ribosomes and total RNA from these three strains (Fig. 3.2). We found that the total RNA in the Δ*yjeQ* strain mainly contained 17S rRNA, whereas in the case of the Δ*rimM* strain 17S and 16S rRNA existed in similar proportions (Fig. 3.2). In contrast, the parental strain had only a small proportion of dissociated subunits and contained entirely 16S rRNA (Fig. 3.2). Analysis of the rRNA content corresponding to the three types of particles in each ribosome profile, revealed that in the Δ*yjeQ* and Δ*rimM* strains, the 17S rRNA is contained almost exclusively in the immature 30S particles and all of the 16S rRNA is found within the mature 70S ribosomes (Figure 3.2).

Therefore, we used the amount of 17S/16S rRNA as a proxy to estimate the proportion of immature 30S subunits that progressed to mature 30S subunits.

In these experiments a discrete population of 17S rRNA that accumulated in the Δ*yjeQ*, Δ*rimM* and wild type strains was labelled by adding ^{3}H (tritium)-uracil to the growing culture. Following a two-minute "pulse", unlabelled uracil was added to the culture ("chase") and samples were harvested at the indicated time points (see 2.8). The total rRNA in these samples was extracted and resolved with gel electrophoresis. If the immature 30S particles were dead-end products of the assembly process, their 17S rRNA would not be expected to undergo further maturation and thus, it should persist over the time-course as 17S rRNA or would disappear due to degradation and recycling (Fig. 3.3). In contrast, if the accumulated 30S subunits progress to mature subunits we should observe the time-dependent loss of labelled 17S rRNA and the simultaneous appearance of labelled 16S rRNA (Fig 3.3).

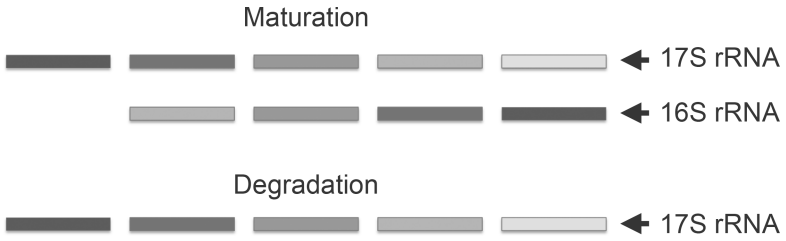

Figure 3.3. Pulse chase experiments
Diagram showing the expected results from the analysis of 17S rRNA maturation into 16S rRNA using pulse chase experiments with tritium labelled uracil. If the rRNA is processed into 16S rRNA by the removal of additional nucleotides on the 5' and 3' end then there will be a transition of the radiolabelled rRNA from the higher molecular weight 17s rRNA species into 16s rRNA over the time course of the experiment. Alternatively, if the rRNA is unable to mature, then over time it will be degraded and there will be a loss of the radiolabelled rRNA.

In the wild type strain the radiolabelled rRNA showed a rapid, monotonic disappearance of the 17S rRNA band with the concomitant emergence of the 16S rRNA band, consistent with rapid conversion of the immature species to the mature form in wild-type cells (Fig. 3.4A). Nearly all of the labelled 17S rRNA was converted to 16S rRNA in approximately 15 min of the initial pulse (Fig. 3.4A). In Δ*rimM* (Fig. 3.4A) and Δ*yjeQ* (Fig. 3.4B) cells, the 17S rRNA persists substantially longer than it did in the parental strain. Even after 2 hours of growth ~50% of the initial 17S rRNA was still present in both null strains. There was, however, a clear emergence of 16S rRNA over the course of growth suggesting that a substantial proportion of the immature particles progress to fully mature 30S subunits. Interestingly, in the Δ*yjeQ* strain, there was an additional band indicating the formation of a low molecular weight aberrantly processed rRNA species (Fig. 3.4B). This band likely represents an rRNA degradation product that has previously been characterized in the Δ*yjeQ* strain (Himeno et al., 2004) (Jomaa et al., 2011b) (Leong et al., 2013).

To corroborate that the delay on the processing of the 17S rRNA in the null strains was caused by the absence of YjeQ and RimM, the null strains were transformed with an IPTG-inducible copy of the *yje*Q and *rimM* gene, respectively. Expression of these genes was initiated with 10 μM IPTG at the beginning of the "chase" phase of the experiment. The transformed Δ*yjeQ* (Fig. 3.4B) and Δ*rimM* (Fig 3.3A) strains showed almost a complete processing of the radiolabelled 17S rRNA to 16S rRNA in an incubation time similar to the parental strain. Transforming the Δ*rimM* (Fig 3.4A) and Δ*yjeQ* (Fig 3.4B) strains with the empty IPTG-inducible vector also showed slow

processing of 17S rRNA into 16S rRNA, similar to the assembly factor knockout strains with no overexpression plasmid.

Overall, these data were consistent with the progression of a large portion of the $30S_{\Delta yjeQ}$ or $30S_{\Delta rimM}$ immature particles into mature 30S subunits. The remaining particles may eventually undergo transformation into mature particles beyond the two hours incubation of our assay or alternatively, represent dead-end products of the assembly process that are eventually degraded.

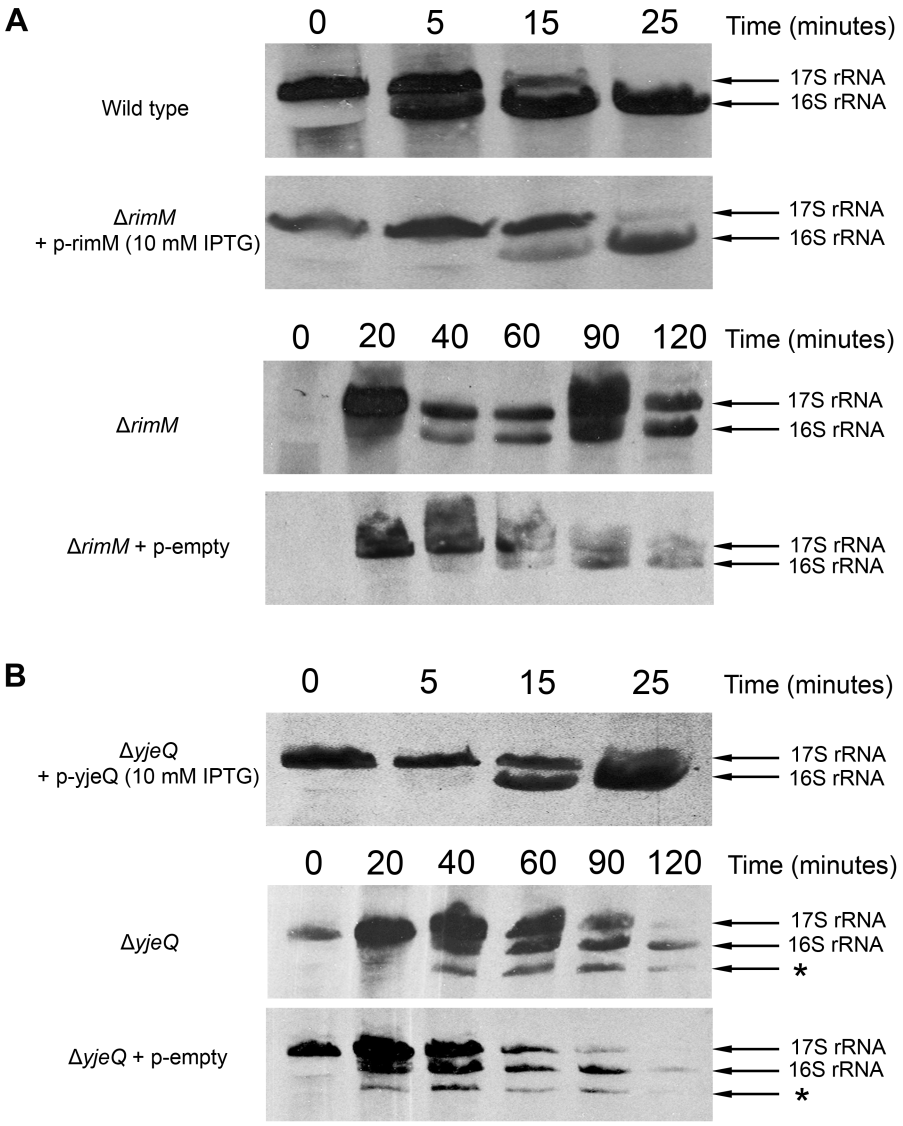

Figure 3.4. Progress of radiolabelled 17S rRNA in the Δ*yjeQ* and Δ*rimM* strains. (A) Cells were grown at 37 ºC with shaking and then pulsed with 125 µCi of ^{3}H (tritium) for 2 min. Cultures were subsequently chased with non-labelled uracil and samples were collected at the indicated times. At each time point the rRNA was extracted and resolved in 8% urea + 4% polyacrylamide gels by electrophoresis. The radiogram of the gels shows that initially only the 17S rRNA precursor is detected, but it is processed and converted to 16S rRNA in ~25 min for the wild type strain and the Δ*rimM* strain containing an IPTG-inducible copy of *rimM*. In the case of the Δ*rimM* strain substantial levels of precursor rRNA and mature 16S rRNA are visible throughout the time course that had to be expanded to 120 min. (B) Equivalent pulse-chase labelling experiment performed with the Δ*yjeQ* strain. In the Δ*yjeQ* strain 17S rRNA processing is delayed

relative to wild type strain, however the delayed processing can be rescued by overexpression of *yjeQ* from and IPTG inducible plasmid. The asterisk indicates an additional band that represents an aberrantly processed rRNA that typically appears in this strain.

3.5 Discussion

The final stages of 30S biogenesis are characterized by organization of the functional core and intersubunit bridges (Jomaa et al., 2011b) (Leong et al., 2013) (Guo et al., 2013) (Clatterbuck Soper et al., 2013), as well as processing of 17S rRNA into 16S rRNA (Mangiarotti et al., 1975). In fact, structural investigations have demonstrated that late stage assembly intermediates in maturation factor null strains have a distorted conformation that would render the particles incapable of associating with 50S subunits and engaging in translation (Jomaa et al., 2011b) (Leong et al., 2013) (Guo et al., 2011) (Clatterbuck Soper et al., 2013). Accordingly, we used *in vitro* and *in vivo* techniques to assess canonical features typically associated with 30S maturation. We have shown here using *in vitro* maturation assays and pulse-chase experiments that the immature 30S subunits that accumulate in the Δ*rimM* and Δ*yjeQ* strains are competent for maturation, although assembly takes longer in the knockout strains. This conclusion is supported by the ability of accumulated immature particles in the null strains to be able to associate with 50S subunits (Fig 3.1) and process 17S rRNA into 16S rRNA (Fig 3.4).

Based on the previous structural characterizations of the $30S_{\Delta yjeQ}$ and $30S_{\Delta rimM}$ particles, it seems likely that the formation of 70S ribosomes during incubation of cell lysates is because the accumulated particles are able to complete their maturation and subsequently associate with 50S subunits. Given that these assembly factors are

functionally related, it is possible that maturation of the immature particles is mediated by the remaining factors. For example, Era suppresses ribosome assembly defects in Δ*yjeQ* cells (Campbell and Brown, 2008) and RbfA can compensate for deletion of *rimM* (Bylund et al., 2001). Nonetheless, when *in vitro* maturation assays were performed by adding various combinations and concentrations of assembly factors to the Δ*rimM* and Δ*yjeQ* concentrated cell lysates, there was no effect on the formation of 70S ribosomes (data not shown). This may be a result of not having the ideal concentrations of each factor when exogenously adding them to the cell lysates, which is consistent with the observation that when assembly factor concentrations become too high they can prevent 30S and 50S subunit association (Himeno et al., 2004) (Sharma et al., 2005). This suggests there is an optimal concentration of maturation factor required in the cell to facilitate efficient ribosome assembly, but not perturb the association of 30S and 50S subunits. 30S subunits can also assemble *in vitro* at permissible temperatures without the aid of auxiliary factors (Traub and Nomura, 1969b). Therefore, at the temperatures used for incubation of cell lysates in this study (37 °C), it would be plausible that the maturation of the accumulated $30S_{\Delta yjeQ}$ and $30S_{\Delta rimM}$ particles is factor independent.

Interestingly, formation of 70S ribosomes took longer and was less pronounced in the Δ*rimM* strain compared to the Δ*yjeQ* strain. Perhaps this indicates that the $30S_{\Delta rimM}$ particles are at an earlier stage in the assembly pathway compared to the $30S_{\Delta yjeQ}$ particles and thus require more time for the incorporation of the remaining s-proteins and processing of immature rRNA. Supporting this, previous qMS analysis has shown that $30S_{\Delta rimM}$ particles contain less s-proteins than $30S_{\Delta yjeQ}$ particles (Leong et al., 2013).

Furthermore, the ribosome profiles in the Δ*yjeQ* strain are less perturbed and more reminiscent of wild type cells than the Δ*rimM* strain (Leong et al., 2013). This could indicate that the assembly defects are greater in the Δ*rimM* strain, resulting in the decreased 70S formation and increase in free 30S and 50S subunits relative to the Δ*yjeQ* strain.

The Δ*rimM* and Δ*yjeQ* strains display a substantial delay in 17S rRNA processing, which can be rescued upon addition of the removed factor (Fig 3.4). This would suggest that YjeQ and RimM could have a role on the rRNA processing steps required for the formation of functional 30S subunits. Perhaps, these maturation factors could directly facilitate the recruitment of RNAses to the processing site or stabilize the 30S subunit in a specific conformation that ensures efficient processing. It is also likely that these processing steps are mediated by multiple assembly factors in conjunction. Finally, it is plausible that a subset of the labelled 17S rRNA is able to progress into 16S rRNA through a YjeQ or RimM-independent parallel assembly pathway and therefore does not pass through the pool of accumulated $30S_{\Delta yjeQ}$ or $30S_{\Delta rimM}$ particles, respectively.

Ultimately, these findings provide reassurance that analysis of the immature 30S particles that accumulate in the Δ*rimM* and Δ*yjeQ* strains are competent for maturation and represent an assembly precursor. Therefore, investigations of these strains render physiologically relevant information about the late stages of assembly facilitated by YjeQ and RimM.

CHAPTER FOUR

BINDING PROPERITES OF YJEQ, ERA, RBFA AND RIMM TO 30S ASSEMBLY INTERMEDITATES

4.1 Author's Preface

This chapter contains experiments that were conducted for two published manuscripts in the journals *RNA* and *Nucleic Acids Research*. The first manuscript aimed to characterize a known functional interplay between the putative 30S assembly factors YjeQ and RbfA. The second manuscript assessed the fate of immature $30S_{\Delta yjeQ}$ and $30S_{\Delta rimM}$ particles and their interactions with multiple 30S assembly factors. This chapter focuses on experiments performed for the two publications that ultimately characterized the binding interactions of functionally related assembly factors with mature 30S subunits and immature 30S particles. This thesis chapter has been modified and adapted from the two original published manuscripts. The contributions and full citations are listed below:

Jeganathan, Ajitha., Razi, Aida., Thurlow, Brett., Ortega, Joaquin. (2015). *The C-terminal helix in the YjeQ zing-finger domain catalyzes the releases of RbfA during 30S ribosome subunit assembly*. RNA. 21(6):1203-1216.

Thurlow, Brett., Davis, Joseph., Leong, Vivian., Moraes, Trevor., Williamson, James., Ortega, Joaquin. (2016). *Binding properties of YjeQ (RsgA), RbfA, RimM and Era to assembly intermediates of the 30S subunit*. Nucleic Acids Research. Epub ahead of print.

For the portions of the *RNA* publication modified for this chapter (Fig. 4.2 & 4.3), I created the *rbfA* overexpression plasmid, developed the purification protocol for the RbfA protein and optimized the conditions for the filtration-binding assay. I also performed the salt stringency experiments (Fig 4.2) and contributed samples for the

assays describing the functional interplay between YjeQ and RbfA (Fig. 4.3). Aida Razi also contributed samples and ran the experiments describing the functional interplay between YjeQ and RbfA (Fig. 4.3). All authors contributed to the analysis and interpretation of data, and writing of the manuscript.

I performed all experiments and provided all samples for the experiments adapted from the *Nucleic Acids Research* publication (Figs. 4.6 – 4.12) for this chapter under the supervision of Dr. Joaquin Ortega. The work was completed in the labs of either Drs. Joaquin Ortega or Trevor Moraes. Dr. Joseph Davis performed the qMS analysis (Fig 4.6). All authors contributed to the analysis and interpretation of the data. Dr. Joaquin Ortega and I wrote the manuscript with contributions and feedback from others authors.

All other unpublished results described in this chapter (Figs 4.1, 4.4 & 4.5) were obtained from experiments conducted by me.

4.2 Introduction

For the past decade multiple laboratories have been exploiting the fact that if you knockout 30S assembly factors in bacteria you can perturb the biogenesis process resulting in an accumulation of immature 30S particles (Jomaa et al., 2011b) (Leong et al., 2013) (Guo et al., 2013) (Yang et al., 2014) (Clatterbuck Soper et al., 2013) (Jeganathan et al., 2015). These 30S particles can then be isolated and the strains characterized to learn about the role of the deleted assembly factor, as well as biogenesis as a whole. Despite the frequent use of these strains and the valuable information they have provided, the ultimate fate of these particles in the cells and whether they can

interact directly with assembly factors has remained poorly understood. In the previous chapter, it was demonstrated that $30S_{\Delta yjeQ}$ and $30S_{\Delta rimM}$ particles are ultimately capable of assembling into mature 30S subunits and thus represent precursor particles that can be further processed. Although these particles are competent for maturation, whether they represent bona fide intermediates that can bind to the removed or other functionally related factors has not been shown. To address this question, we employed a combination of techniques to analyze the binding interactions of functionally related 30S assembly factors. Unexpectedly, we found that immature particles isolated from the Δ*yjeQ* and Δ*rimM* strains contain low amounts of bound assembly factor. Furthermore, we found that YjeQ and Era bind better to mature 30S subunits than immature $30S_{\Delta yjeQ}$ and $30S_{\Delta rimM}$ particles and that RbfA and RimM does not bind with high affinity to any of the particles. Therefore, this study brings new insights into the nature of the immature 30S particles that assembly factor knockout strains accumulate and helps to elucidate the general model governing the interactions of these particles with biogenesis factors.

4.3 Construction of Assembly Factor Overexpression Plasmids and Purification of Proteins

To begin interrogating the interactions of the assembly factors YjeQ, RbfA, RimM and Era with both mature and immature ribosomal species, it was first necessary to develop the overexpression strains and the purification protocols for each protein. For a detailed description of the plasmids and protein purification protocols see 2.2 & 2.5. To purify YjeQ, Era, RbfA and RimM, the overexpression plasmids were constructed (see

2.2) and a combination of precipitation and liquid chromatographic techniques (see 2.5) were employed. Purity of YjeQ (Fig. 4.1A), Era (Fig. 4.1B), RbfA (Fig 4.1C) and RimM (Fig. 4.1D) were monitored by SDS-PAGE followed by Coomassie staining.

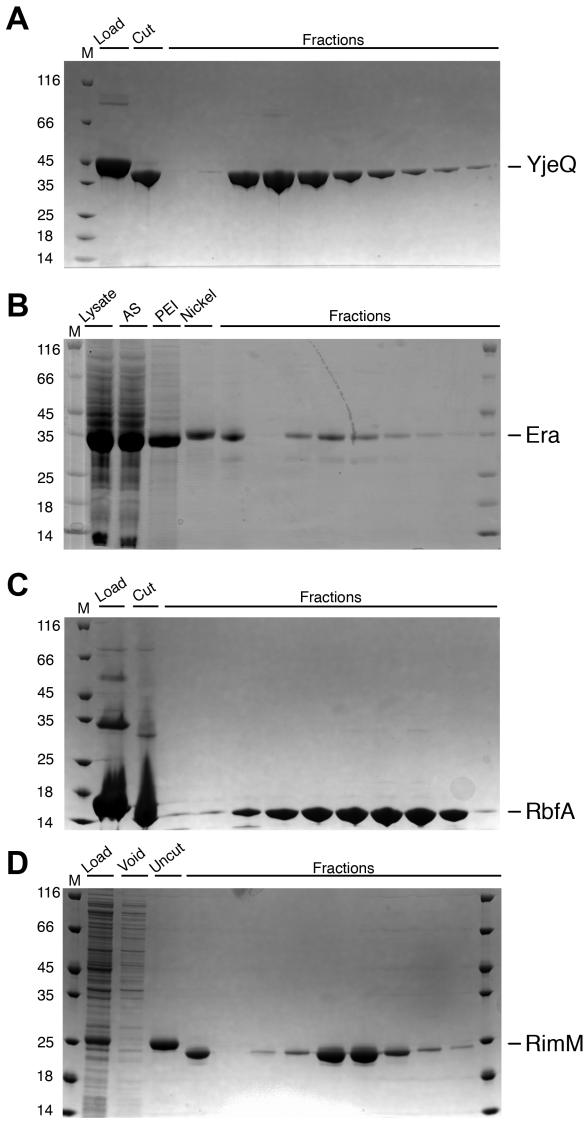

Figure 4.1. Purification of 30S assembly factors.
All four assembly factors were overexpressed in *E.coli* with a N-terminal His_6-tag and purified according to 2.6. (A) YjeQ was purified using nickel column chromatography. (B) Era was purified using a combination of ammonium sulfate (AS) and polyethylenimine (PEI) precipitations, followed by nickel and anion-exchange

chromatography. (C) RbfA was purified using a combination of nickel and anion exchange chromatography. (D) RimM was purified using a combination of nickel and anion exchange chromatography. Sample purity was assessed using 4%–12% bis–tris SDS-PAGE followed by Coomassie Brilliant Blue staining. For all four proteins, pure fractions were collected, pooled together and the His_6-tags were removed using either thrombin (Era, RbfA, RimM) or TEV (YjeQ) digestion. Pure and cleaved fractions were concentrated and dialyzed into protein storage buffer (50 mM Tris-HCl (pH=8), 5% [v/v] glycerol and stored at -80 °C.

4.4 Development of Filtration Binding Assay to Assess Functional Interplays amongst Assembly Factors

An important question that this thesis project sought to answer was to identify assembly factor interactions with mature and immature 30S particles, as well as any potential functional interplay amongst these factors. To address this question, we utilized a filtration-binding assay (see 2.10) that would allow us to visualize when proteins bound to the various 30S particles and ideally, identify if there were any changes in binding affinity upon the addition of other assembly factors. Briefly, filtration binding assays were performed by incubating a mixture of the 30S particles with assembly factors, followed by centrifugation through a 100 kDa MWCO filter device and analysis by SDS-PAGE. Given the size of the 30S subunit (~850 KDa) and the four assembly factors (15 – 39 kDa), the 100 kDa MWCO filter is capable of retaining only the factors that remain bound (B) to the 30S subunit, while any unbound proteins will pass into the flow-through (FT). Initially, we assessed the salt stringency of two previously identified 30S-assembly factor complexes to identify the optimal reaction conditions that enabled stable interactions, while ensuring specific binding. The YjeQ-$30S_{wt}$ (Himeno et al., 2004) (Daigle and Brown, 2004) (Jomaa et al., 2011a) complex has previously been established

to form stable interactions and accordingly this complex was used to assess the salt stringency of YjeQ. Conversely, RbfA has been shown to have stronger interactions with immature $30S_{\Delta yjeQ}$ particles compared to mature 30S subunits (Goto et al., 2011) and thus the RbfA-$30S_{\Delta yjeQ}$ complex was chosen to assess the salt stringency of this reaction.

Filtration assays using a salt concentration range from 60 – 600 mM NH_4Cl, along with standards containing a known amount of protein (not shown), were used to assess the YjeQ-$30S_{wt}$ complex in the presence GMP-PNP (Fig. 4.2). This experiment showed that at 300mM NH_4Cl, YjeQ-GMP-PNP bound to the 30S subunit at ~1:1 ratio, which is consistent with the stoichiometry that has been previously established for this complex (Himeno et al., 2004) (Daigle and Brown, 2004) (Jomaa et al., 2011b) (Guo et al., 2011). The salt stringency of the interaction of RbfA with the $30S_{\Delta yjeQ}$ particles was also assessed using filtration-binding assays. Specifically, RbfA bound to the $30S_{\Delta yjeQ}$ particles with a ~1:1 stoichiometry at 60 mM NH_4Cl. (Fig. 4.2). Therefore, the concentration of NH_4Cl in the reaction buffer is a critical parameter influencing the binding of these assembly factors to ribosomal particles with YjeQ and RbfA binding stoichiometrically at 300 mM and 60 mM NH_4Cl, respectively.

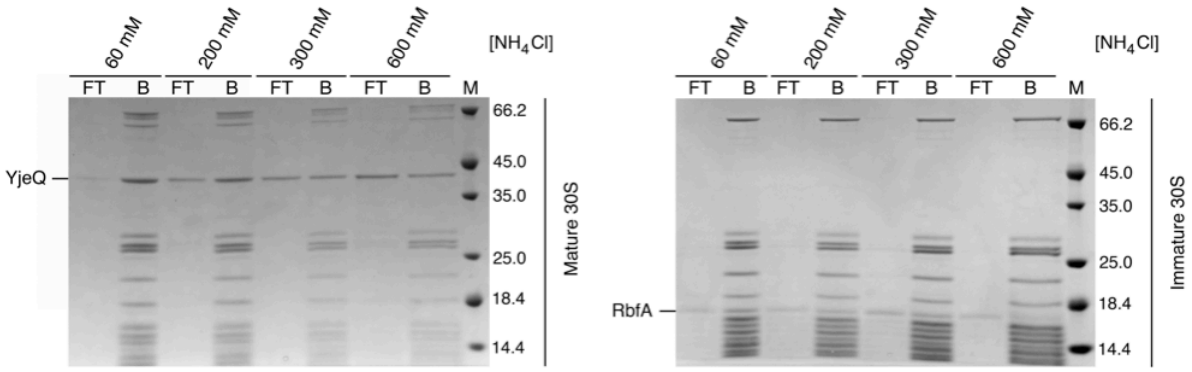

Figure 4.2. Filtration binding assay to assess the salt stringency of YjeQ and RbfA to mature and immature 30S subunits.
To establish the NH_4Cl concentration at which binding of YjeQ to the mature 30S subunit and RbfA to the immature $30S_{\Delta yjeQ}$ particles becomes stoichiometric, we tested the binding of these factors at different salt concentrations using filtration assays. These particular assembly reactions (YjeQ + mature 30S and RbfA + immature $30S_{\Delta yjeQ}$) were chosen because these are the most stable complexes YjeQ and RbfA have been previously shown to form. YjeQ and RbfA were added in 5-fold molar excess with respect to the 30S subunits in all reactions. Assembly reactions containing YjeQ were done in the presence of 1 mM GMP-PNP. The unbound protein was captured in the flow-through (FT) and the bound (B) protein was retained in the filter. Fractions were then resolved by 4-12% bis-tris SDS-PAGE and stained with Coomassie Brilliant Blue. Gels were scanned (Biorad ChemiDoc MP Imaging System) and the intensity of the protein bands was measured by densitometry (Image Lab Version 5.0-built 18; Biorad) and compared to the intensity of the bands from YjeQ, RbfA and ribosome standards in the same gel (not shown). Stoichiometric binding to the mature 30S subunit was observed at 300 mM and 60 mM NH_4Cl for YjeQ and RbfA, respectively. The molecular weight marker (M) is in kDa.

Next, we wanted to determine if the previously characterized functional interplay between YjeQ and RbfA (Goto et al., 2011) could be monitored using the filtration-binding assay at an appropriate salt concentration. It has been shown that YjeQ can facilitate the release of RbfA during the late stages of 30S maturation (Goto et al., 2011) and therefore we hoped to visualize this removal to confirm the robustness of the filtration binding assays. Consequently, for these assays we chose to use an NH_4Cl

concentration of 60 mM to ensure that binding of RbfA to the mature $30S_{wt}$ was still occurring, while minimizing non-specific binding of YjeQ. To assess these interactions, RbfA was initially incubated for 15 min at 37 °C with either mature or immature 30S particles, followed by the addition of YjeQ and an extended 15 min incubation. Under these conditions, YjeQ was able to efficiently displace RbfA from the mature 30S subunit and this removal was very effective in the presence of GTP (~95%) and GMP-PNP (~90%), but not GDP (~65%) (Fig. 4.3A). In the case of immature $30S_{\Delta yjeQ}$ particles, YjeQ could not release RbfA, regardless of the nucleotide present in the buffer (Fig. 4.3A). To establish that the inability of YjeQ to release RbfA from the immature 30S subunit was not due to the low salt concentration of the buffer, this experiment was repeated at a higher concentration in the presence of GMP-PNP. In this case, YjeQ still did not displace RbfA from the immature $30S_{\Delta yjeQ}$ particles (Fig. 4.3B). Control filtration assays performed in parallel using YjeQ, RbfA, or both proteins in low or high salt buffer, showed that the filter did not retain the proteins by themselves or when combined (Fig. 4.3A&B).

Although these filtration assay conditions were ideally suited to demonstrate the functional interplay between YjeQ and RbfA, it was apparent that the low salt concentration was causing YjeQ to bind suprastoichiometrically to the mature 30S particles. This could be seen by the presence of an increased intensity for the band corresponding to YjeQ relative the various s-protein bands of the 30S subunit (Fig. 4.3). This finding suggested that a small portion of YjeQ was non-specifically interacting with the membrane in the centrifugal filter device, despite rigorous blocking of the filter with

BSA (see 2.10). Therefore, when assessing the interactions of all four assembly factors with ribosomal particles, we chose to use the highest ammonium chloride (300 mM) concentration that still retained stoichiometric 1:1 binding of the well characterized YjeQ-30S complex (Himeno et al., 2004) (Daigle and Brown, 2004) (Jomaa et al., 2011a) (Guo et al., 2011), while minimizing any nonspecific interactions (Fig. 4.2).

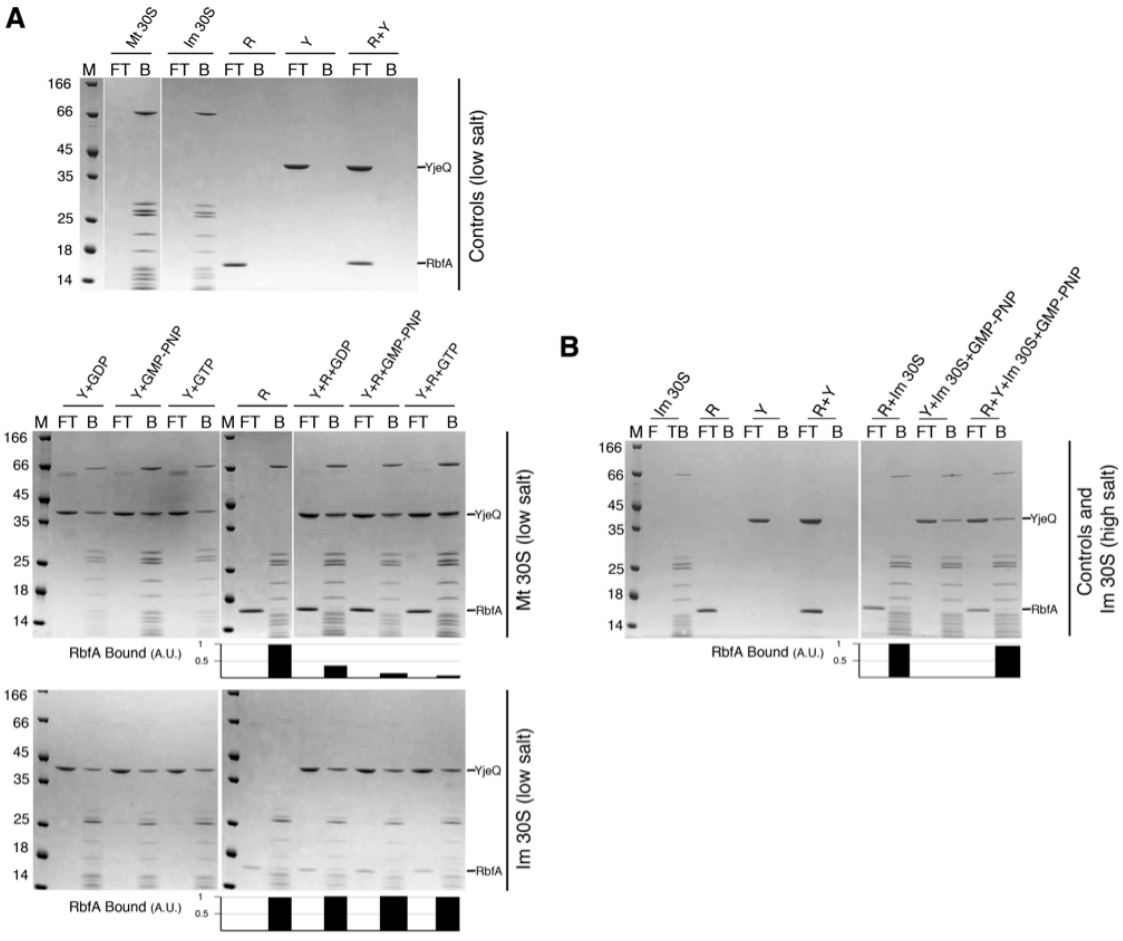

Figure 4.3. Functional interplay of YjeQ and RbfA.
(A) Filtration assays testing the ability of YjeQ (Y) to remove RbfA (R) bound to the mature (Mt) and immature (Im) 30S subunit in buffer containing 60 mM NH_4Cl (low salt). RbfA was first incubated with mature or immature 30S subunits at 37 ºC for 15 min. YjeQ and nucleotide (GDP, GMP-PNP or GTP) were then added where indicated and the mixtures were incubated for an additional 15 min. Proteins were added in five

fold molar excess to 30S particles. Flow-through (FT) and bound (B) fractions containing unbound and bound proteins retained on the filter respectively were separated by centrifugation through a 100-kDa cut-off centrifugal device. Fractions were resolved by 4-12% bis-tris SDS-PAGE and stained with Coomassie Brilliant Blue. The molecular weight for the markers (M) is in kDa. The SDS-PAGE in the top panel shows the control reactions containing YjeQ (Y), RbfA (R) or the 30S subunits (mature or immature) by themselves. We also tested a reaction containing both YjeQ and RbfA to ensure that combining the two proteins did not cause retention of some protein in the filtration device. (B) The 4-12% bis-tris SDS-PAGE stained with Coomassie Brilliant Blue in this panel shows the experiment in the bottom panel in (A) testing the ability of YjeQ to remove RbfA bound to the immature 30S subunit, but performed in buffer containing 300 mM NH_4Cl. The bar diagrams under the gels in (A) and (B) indicate the binding of the RbfA to the mature 30S subunit in each reaction as assessed by densitometry analysis in Image Lab. The observed binding of RbfA to the mature 30S subunit was defined as 1.

Under these buffer conditions, all four assembly factors were able to pass completely through the filter into the flow-through when incubated either alone or together in the absence of ribosomal particles (Fig. 4.4A). Conversely, the 30S subunits were entirely retained by the filter and appeared completely in the bound portion (Fig. 4.4B). Negative control reactions were assessed by testing binding of the 50S assembly factor, ribosome binding GTPase A (RbgA), to the mature 30S subunit (Fig. 4.4C) and binding of YjeQ to the 50S subunit (Fig. 4.4D). As expected, only a negligible portion (<2%) of either YjeQ or RbgA was found to bind to the 50S subunit or 30S subunit, respectively (Fig. 4.4C&D). Therefore, based on the salt profiles (Fig. 4.2) and the control experiments shown here (Fig. 4.4), these stringent buffer conditions ensured that the observed binding of YjeQ to ribosomal particles using the filtration assay was stoichiometric, yet still suitable for analyzing potential weak interactions, such as the RbfA-$30S_{\Delta yjeQ}$ complex (Fig. 4.4E).

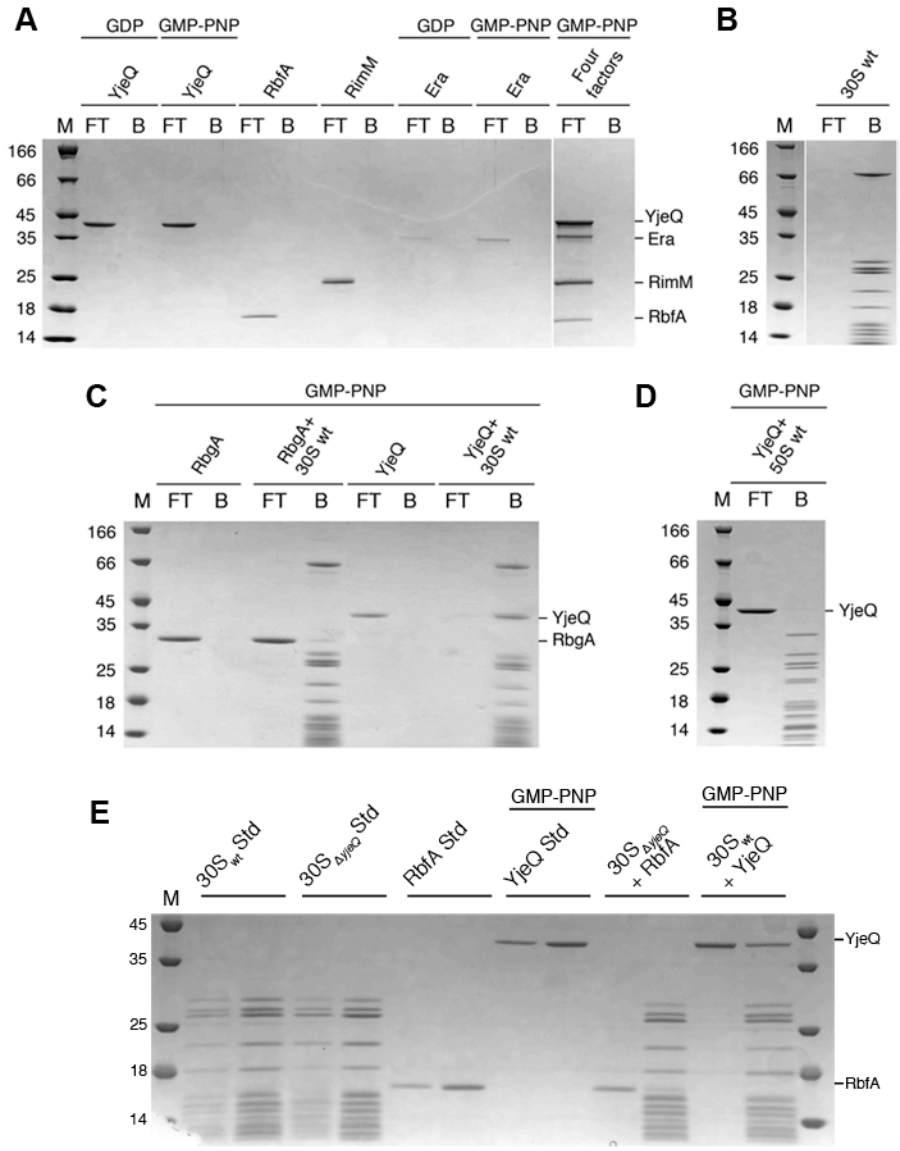

Figure 4.4. Filtration assays show specific binding of assembly factors to ribosomal subunits.

Filtration assays for these experiments were performed by incubating the assembly factors and 30S subunits in a 100 µl reaction in Binding Buffer (10 mM Tris-HCl at pH 8.0, 7 mM magnesium acetate, 300 mM NH_4Cl, 1 mM DTT) at 37 °C for 30 mins and then centrifuging the samples through a 100 kDa cut-off filter device blocked with 1% [w/v] bovine serum albumin. The flow-through (FT) and bound (B) portions were collected. Samples were resolved by 4-12% bis-tris SDS-PAGE and stained with Coomassie Brilliant Blue. The molecular marker (M) is in kDa. (A) Under these conditions, the filter membrane did not retain YjeQ, RbfA, RimM or Era when the factors were incubated either independently or in the same reaction. (B) Instead, the filter

retained all of the 30S ribosomal subunits. (C) and (D) Control experiments to evaluate the specificity of the filtration binding assay. (C) In this control experiment the binding of RbgA (an assembly factor that only binds to the 50S subunit) to the 30S subunit was assessed, along with a positive control reaction for YjeQ binding to mature 30S subunits. These reactions were performed by incubating equimolar amounts of assembly factor with the ribosomal particles. Under these conditions there was almost no detectable binding of RbgA to 30S subunits and YjeQ retained a stoichiometric interaction. (D) An additional negative control was performed by assessing the binding of YjeQ to the 50S subunit. For this reaction a five-fold molar excess of YjeQ was incubated with 50S subunits. There was almost no detectable binding of YjeQ to the 50S subunit under these reaction conditions. (E) Final optimized reaction conditions used for all subsequent filtration-binding assays. For these reactions, a five-fold molar excess of the assembly factors YjeQ or RbfA were incubated with $30S_{wt}$ or $30S_{\Delta yjeQ}$ particles, respectively. Standards (Std) with known concentrations of the assembly factors and ribosomal particles were also loaded into the polyacrylamide gel to enable absolute quantification of the intensity of the bands in the bound portion using Image Lab software. These optimized reaction conditions ensured stoichiometric binding of YjeQ to mature 30S subunits, while still being able to visualize the weaker binding reaction for the RbfA-$30S_{\Delta yjeQ}$ complex.

With several 30S intermediates and all of the assembly factors of interest purified, as well as an optimized system for analyzing interactions, we next assessed whether there was a notable hierarchy of binding of these factors to mature $30S_{wt}$ particles. We hypothesized that assembly factors could bind in an ordered manner similar to the association of s-proteins during 30S assembly (Mizushima and Nomura, 1970) or the sequential removal of factors from assembling 40S subunits in eukaryotes (Strunk et al., 2012). Primary assembly factors would be identified by their ability to bind directly to the ribosomal particle and a factor that requires the presence of a primary protein for binding would be considered a secondary factor. Furthermore, there would be the possibility that assembly factor removal could be dependent on the binding of other factors. By characterizing the binding dependencies of these factors we would be able to

develop a model for the association and disassociation of factors governing 30S subunit biogenesis.

YjeQ and Era were capable of binding individually and simultaneously to mature $30S_{wt}$ subunits in the presence of GMP-PNP (Fig. 4.5A). There was a small amount of YjeQ able to bind in the presence of GDP and the binding of Era was not affected by the nucleotide present in the buffer (Fig. 4.5A). Conversely, RbfA and RimM were unable to bind directly to the mature 30S subunit under the high salt conditions used for these experiments (Fig. 4.5A). YjeQ was unable to promote the secondary binding of any of the factors to $30S_{wt}$ particles (Fig. 4.4B), however Era had a minor ability to increase the binding of RbfA to mature 30S subunits (Fig. 4.5B). When performing the filtration assay by incubating three factors with mature 30S subunits to identify possible quaternary complexes, YjeQ, Era and RbfA were able to simultaneously bind (Fig. 4.5C). The addition of RimM to this assembly reaction did not have a substantial effect (Fig. 4.5D). RimM did not bind to mature 30S subunits either alone or in the presence of the other three assembly factors (Fig. 4.5). Together, these results indicate that multiple assembly factors can simultaneously bind to 30S ribosomal subunits. This is consistent with previous literature indicating that YjeQ (Jomaa et al., 2011a) (Guo et al., 2011), Era (Sharma et al., 2005) and RbfA (Datta et al., 2007) occupy non-overlapping binding sites on the 30S subunit, suggesting that all three proteins have the potential to bind simultaneously.

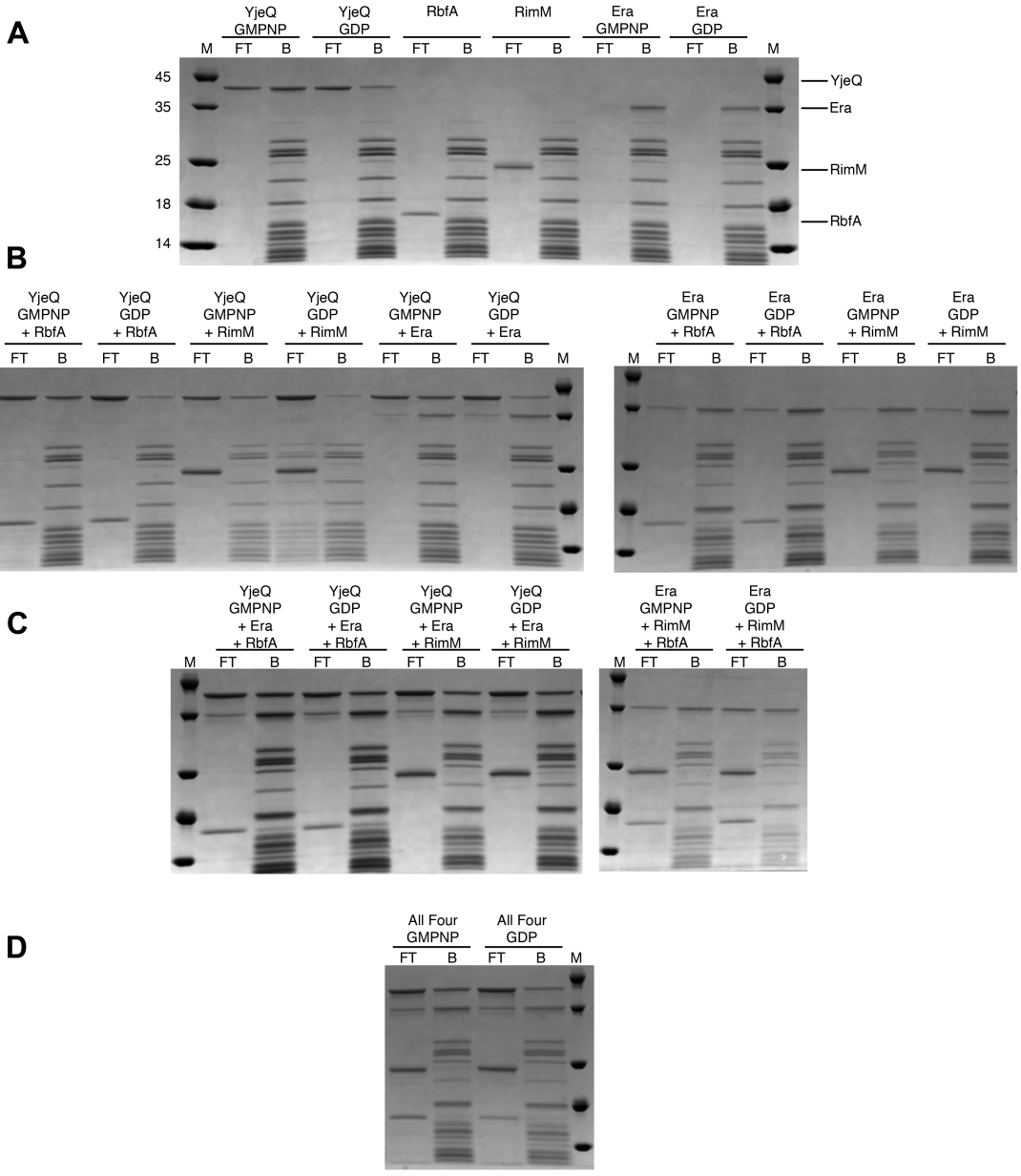

Figure 4.5. Assessing binding dependencies of assembly factors to mature 30S subunits.

Assembly factors were incubated with mature 30S subunits in 100 µl reactions with Binding Buffer containing 300 mM NH_4Cl for 30 minutes at 37 °C. A 30S subunit concentration of .4 µM and a 5-fold access of YjeQ, Era, Rbfa or RimM were used. The nucleotides GMP-PNP or GDP were added to the reaction buffer at a concentration of 0.4 mM where indicated. After incubation, the reactions mixtures were stopped by being cooled on ice, transferred to a Nanosep 100K Omega filter (Pall) and centrifuged at 12000*g* for ten minutes. The flow through (FT) volume was collected and the remaining bound (B) portion was washed twice by centrifugation using 100 µl of Binding Buffer.

The remaining bound portion was collected and all samples were analyzed using 4-12% bis-tris gel electrophoresis followed by Coomassie Brilliant Blue staining. (A) Filtration binding assay showing the interactions of a single factor with mature 30S subunits. YjeQ and Era are both able to bind to mature 30S subunits. (B) Filtration binding assays showing the interactions of two assembly factors simultaneously with mature 30S subunits. YjeQ and Era can both interact simultaneously with mature 30S subunits. Era can promote the binding of RbfA to mature 30S subunits. (C) Filtration binding assay showing the interactions of three factors simultaneously. YjeQ, Era and RbfA can simultaneously interact with mature 30S subunits. (D) Filtration binding assay showing the interaction of four factors simultaneously.

Although these results were able to confirm the previously characterized interactions of YjeQ (Jomaa et al., 2011a) (Daigle and Brown, 2004) (Himeno et al., 2004) (Guo et al., 2011) and Era (Sharma et al., 2005) (Tu et al., 2011) (Tu et al., 2009) with mature 30S subunits, it was difficult to use Coomassie Brilliant Blue stained polyacrylamide gels to observe potentially minor changes in binding affinities as a result of assembly factor functional interplays. Furthermore, due to the extremely large sample consumption of these assays and the multitude of potential binding dependencies, it was decided that these filtration binding assays would be best suited for determining qualitatively if a factor can bind independently to mature or immature ribosomal particles.

4.5 The Immature $30S_{\Delta yjeQ}$ and $30S_{\Delta rimM}$ Particles Accumulating in Bacterial Cells Have Substoichiometric Amounts of YjeQ, Era, RimM and RbfA Bound

To determine the occupancy level of YjeQ, Era, RimM and RbfA in the immature particles and mature 30S subunit *in vivo*, we purified mature 30S subunits from wild type cells, and immature $30S_{\Delta yjeQ}$ and $30S_{\Delta rimM}$ particles from the null strains using a modified

low-salt purification procedure (see 2.6). By working under these low-salt conditions (60 mM NH_4Cl), we hoped to maintain native interactions between the small subunit particles (SSU) and the assembly factors. The purified particles were then spiked with stoichiometric ^{15}N-labelled 70S ribosomes and purified assembly factors (Era, RbfA, RimM and YjeQ). Samples were digested with trypsin and peptide abundances were analyzed via quantitative mass spectrometry (qMS) using a targeted multiple reaction monitoring (MRM-HR) approach. To determine the reproducibility of our measurements, the immature subunits were assayed in duplicate.

Consistent with previous qMS analysis (Jomaa et al., 2011a) (Leong et al., 2013) (Guo et al., 2011) both immature particles were severely depleted of r-protein uS2 and bS21 (Fig. 4.6A). A subtle depletion of uS3 was also observed in both immature particles. Additionally, the $30S_{\Delta rimM}$ particles were partially depleted of uS13 and uS14 in both replicates (Figure 4.6A). Notably, control reactions from wild-type strains with either mature 30S subunits or 70S particles exhibited stoichiometric binding of each small subunit r-protein. Given the low abundance of uS2 and bS21 in the immature small subunit particles, we next asked whether these proteins freely accumulated in the cell or alternatively, if their abundance was regulated in the mutant strains.

To this end, we grew wild type (WT), Δ*rimM*, and Δ*yjeQ* strains in ^{14}N-labelled media. We then spiked these cell lysates as described above and measured the whole cell protein levels for small subunit ribosomal particles using qMS. Interestingly, we found that uS2 and bS21 were significantly depleted from the whole cell lysates (Figure 4.6B) indicating that these proteins, which are not bound to the immature particles, do not

accumulate as free proteins in the cell. This whole cell depletion effect may result from downregulated synthesis or up regulated degradation of these particular proteins when they are not bound to a ribosomal particle. Interestingly, degradation of bS21 has been observed in wild-type cells previously (Chen and Williamson, 2013). Additionally, we see more subtle depletion of proteins uS3, uS10, uS13, and uS14, specifically in the Δ*rimM* strain cell lysate.

We next extended our qMS method to measure the abundance of assembly factors Era, RbfA, RimM, and YjeQ. To determine the linearity of our approach, we first titrated purified ^{14}N-labelled factors against a fixed concentration of ^{15}N-labelled factors in the presence of both ^{14}N- and ^{15}N-labelled 70S subunits. Plotting the ^{14}N-labelled protein added against the measured ^{14}N/^{15}N ratio revealed the linearity of the approach (Fig. 4.6C). We then measured the factor occupancy in either purified subunits (Fig. 4.6D) or in whole cell lysates (Fig. 4.6E). With the exception of RbfA, factor occupancy was extremely low and below our quantitation limit in all particles tested (~5%) (Fig. 4.6D). We found low, but measurable (~15%) occupancy of RbfA in the $30S_{wt}$ and in the $30S_{\Delta rimM}$ particles. Additionally, RbfA was found at ~5% occupancy in the $30S_{\Delta yjeQ}$ particles, as well as the wild type 70S (Fig. 4.6D).

Analysis of the protein levels in cell lysates of parental and null strains revealed that YjeQ, RbfA, RimM and Era are not highly abundant when immature particles accumulate in the cell (Fig. 4.6E). Consistent with the factor occupancy levels found in the ribosomal particles purified under low salt buffer conditions, the measured protein levels in the cell lysates indicated that YjeQ, RimM and Era were present at levels less

than 5% that of the total quantity of ribosomal proteins in the cell (Fig. 4.6E). In contrast, RbfA was present at higher levels in each strain although the overall abundance was still less than 10% of the total r-proteins (Fig. 4.6E). Taken together, the observed low factor abundance is consistent with recent protein abundance measures in wild-type cells by ribosome footprinting (Li et al., 2014).

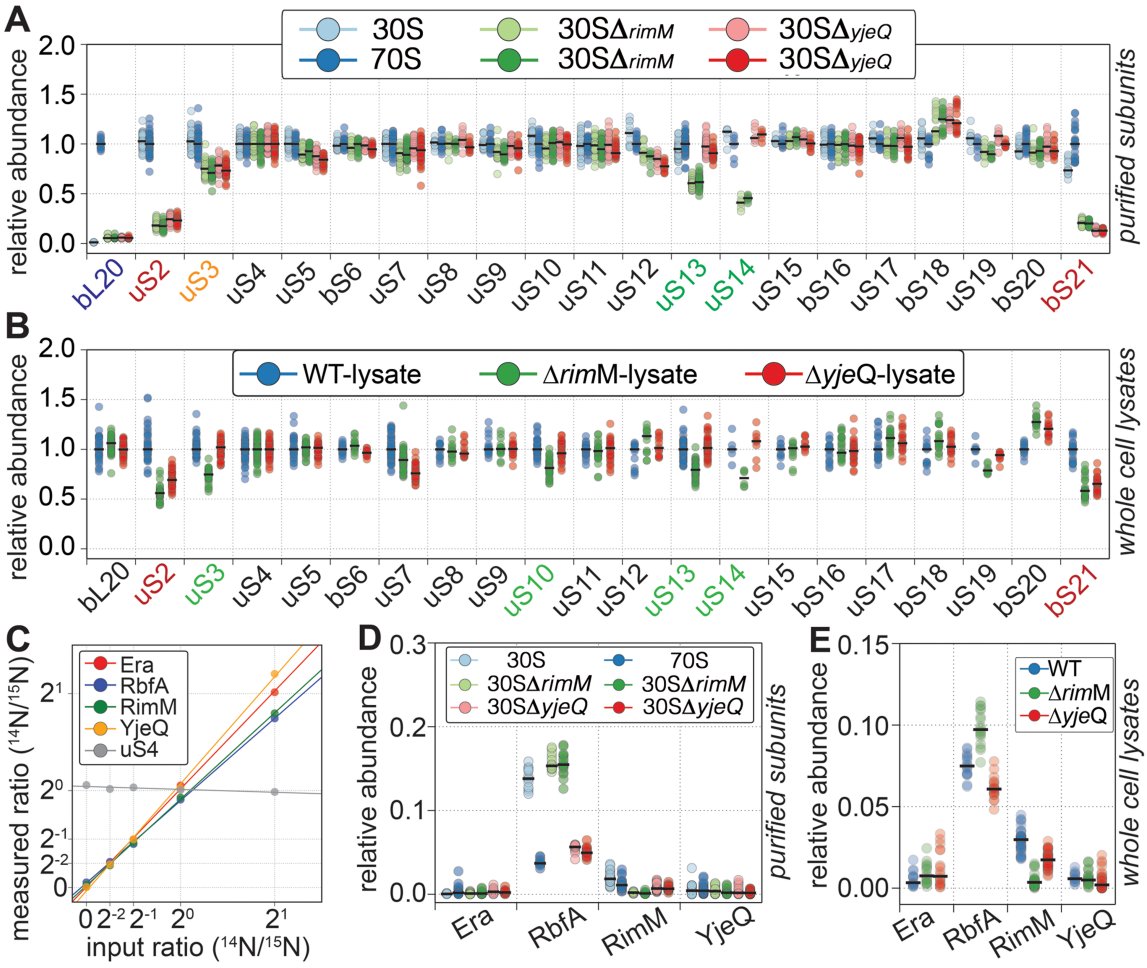

Figure 4.6. Ribosomal protein and assembly factor quantitation in mature and immature ribosomal particles.
(A) ^{14}N-labelled subunits are quantified against a fixed ^{15}N-labelled 70S standard. Protein abundance is calculated as the ^{14}N/^{15}N ratio from extracted ion chromatograms of

product ions, normalized to that of protein uS4. To highlight the different relative abundance of each protein relative to a fully mature 70S particle, for each protein, the abundance ratio is then normalized to that of the 70S ribosome. Circles denote a single product ion transition; black lines mark the median value. Replicates using 6 pmol or 12 pmol of $30S_{\Delta rimM}$ (greens) and $30S_{\Delta yjeQ}$ particles (reds) small subunits are plotted in light and dark colors, respectively. Control mature 30S subunits and 70S ribosomes are shown in blues. Proteins significantly depleted from all immature subunits are labelled red, those slightly depleted are labelled orange and those specifically depleted in the $30S_{\Delta rimM}$ particles are in green. For reference, a single large subunit protein is denoted with blue text. (B) R-protein quantitation in whole cell lysates. ^{14}N-labelled whole cell lysates were spiked with ^{15}N-labelled 70S particles. $^{14}N/^{15}N$ relative abundance calculated from extracted ion chromatograms is normalized to that of protein uS4 and, to highlight strain specific differences, finally normalized relative to the wild-type lysate. Labels and colors are the same as in (A). (C) Assembly factor quantitation calibration curve. Purified ^{14}N-labelled factors were added at various concentrations (0 pmol to 12 pmol) to a fixed amount of purified ^{15}N-labelled factors (6 pmol), as well as both ^{14}N- and ^{15}N-labelled 70S particles (6 pmol each). For each targeted product ion transition, ion chromatograms were extracted for ^{14}N- and ^{15}N-labelled species. The median ratio is plotted for each protein at each measured concentration. Assembly factor quantitation in purified subunits (D) or in whole cell lysates (E). Samples prepared as described in (A) with the addition of ^{15}N-labelled purified assembly factors (6 pmol). Protein abundance is calculated as the $^{14}N/^{15}N$ ratio, normalized to that of protein uS4. This approach allows for direct comparison between r-protein and assembly factor abundance.

4.6 YjeQ Binds to the Mature 30S Subunit with Higher Affinity than to the Immature 30S Particles

We first used pelleting assays (see 2.11) to test the binding of YjeQ to the mature 30S subunit and to the $30S_{\Delta yjeQ}$ and $30S_{\Delta rimM}$ immature particles. To this end, we incubated YjeQ in the presence of GMP-PNP with the ribosomal particles, ultracentrifuged the reaction mixture through a sucrose cushion and analyzed the supernatant and pellet by SDS-PAGE. The premise of this assay is that any assembly factors that interact with the ribosome will pellet with the ribosomal particles during centrifugation and any unbound factors will be retained in the supernatant. We found a

band corresponding to YjeQ in the pellet fraction of all the reactions containing ribosomal particles (Fig. 4.7A). Densitometry analysis determined that the intensity of this band was approximately two-fold stronger in the reaction with the mature 30S subunit compared to those containing the $30S_{\Delta yjeQ}$ and $30S_{\Delta rimM}$ immature particles. In control reactions containing only YjeQ with no ribosomal particles, all of the protein appeared in the flow through (Fig. 4.7A). These results indicate that YjeQ exhibits stronger binding affinity to the mature 30S subunit than to the immature particles.

In addition to the pelleting assays, we used filtration-binding assays (see 2.10) to assess the interactions of YjeQ with the mature and immature ribosomal particles. In the filtration assay for YjeQ (Fig. 4.7B), the assembly factor was incubated with the mature 30S subunit or with one of the immature 30S particles ($30S_{\Delta yjeQ}$ or $30S_{\Delta rimM}$) in buffer containing GMP-PNP. We found that in all of these reactions there was a band corresponding to YjeQ in the bound fraction (Fig. 4.7B). Consistently with the pelleting assay, the intensity of this band was approximately two-fold stronger in the reaction with the mature 30S subunit compared to those containing the immature 30S particles. In control reactions containing YjeQ in the absence of 30S particles, all of the YjeQ appeared in the flow through (Fig. 4.3B & 4.4A). Together, the results of the pelleting (Fig. 4.7A) and filtration assays (4.7B) indicated that YjeQ exhibits stronger binding to the mature 30S subunit than to the immature particles.

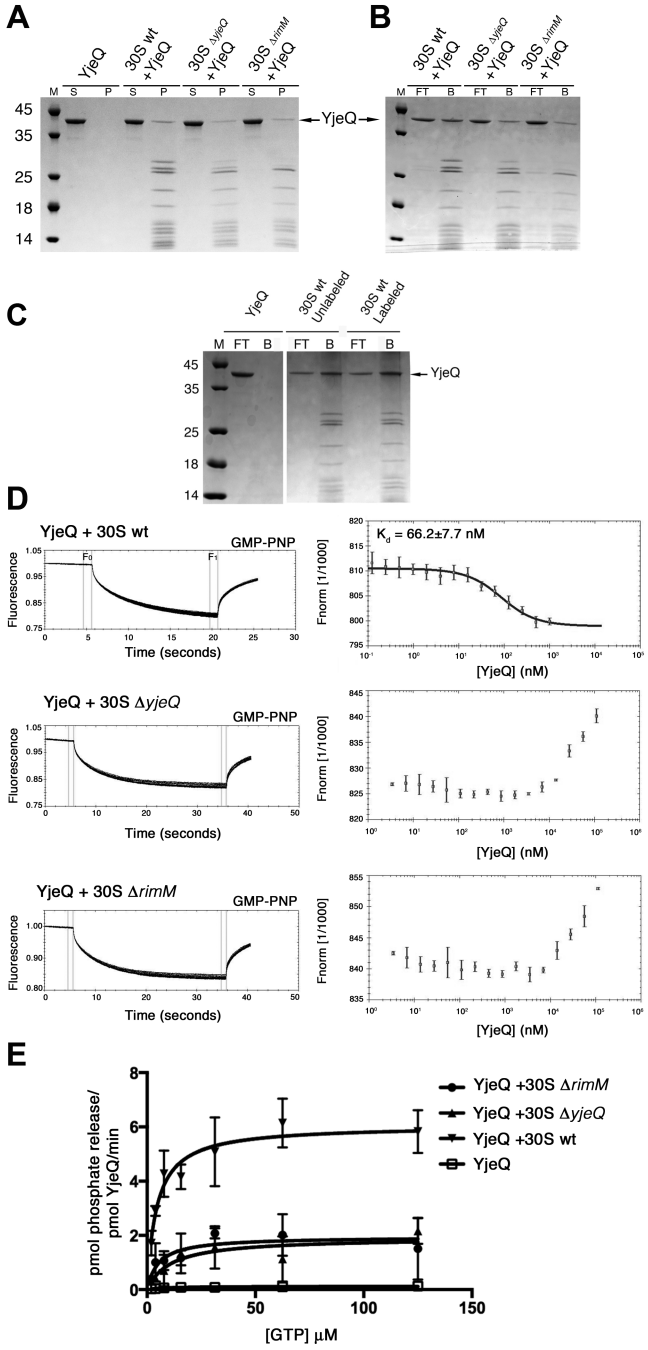

Figure 4.7. Binding of YjeQ to the mature 30S subunit and immature 30S$_{\Delta yjeQ}$ and 30S$_{\Delta rimM}$ particles.

(A) Pelleting assay testing the binding of YjeQ to the mature and immature 30S particles. A sevenfold excess of YjeQ was incubated with either the mature 30S subunits or one of the immature 30S particles for 30 min at 37 ºC. Following the incubation, reactions were

laid over a sucrose cushion and subjected to ultracentrifugation. Proteins that were unbound were collected in the supernatant (S), while proteins that bound to the 30S particle were found in the pellet (P). The molecular weight (M) is in kDa. The pellet and supernatant were resolved by 4%–12% bis–tris SDS-PAGE and stained with Coomassie blue. The bands for YjeQ are indicated. (B) Filtration assay testing the binding of YjeQ to the mature and immature 30S particles. Reactions contained 2 μM of assembly factor and 0.4 μM of 30S particle in 100 μl of Binding Buffer (10 mM Tris-HCl at pH 8.0, 7 mM magnesium acetate, 300 mM NH_4Cl, 1 mM DTT). Assembly reactions were incubated for 30 min at 37 °C in the presence of GMP-PNP. Following incubation, the reactions were centrifuged through a BSA blocked 100 kDa Nanosep Omega device at 12000*g* for 10 min to separate 30S particles and 30S-bound proteins that were retained by the filter from unbound proteins in the flow-through (FT) fraction. The flow-through was collected and the filter was gently washed twice with 100 μl of Binding Buffer followed by a 5 min spin at 12,000*g*. Finally, the 30S particles and 30S-bound proteins retained by the filter were vigorously resuspended in 100 μl of Binding Buffer and collected as the bound fraction (B). To resolve the FT and B fractions, samples were mixed with 6X SDS-PAGE loading buffer and loaded into a 4-12% Criterion™ XT Bis-tris gel (Bio-Rad). Samples were run in XT MOPS buffer (Bio-Rad). Gels were stained with Coomassie Brilliant Blue and visualized using a ChemiDoc MP system (Bio-Rad). (C) Effect of Red-Maleimide labelling of the 30S subunit on YjeQ binding. Filtration assay indicating that labelling of the 30S subunit with Red-Maleimide does not have a significant impact on YjeQ binding. Binding reactions were prepared by incubating 200 pmoles of YjeQ with 30 pmoles of mature 30S subunits in a 100 μl reaction in MST Binding Buffer (20 mM Tris-HCl pH=7.5, 150 mM NaCl, 10 mM $MgCl_2$, 1 mM DTT, 0.05% Tween-20, 0.4 mg/ml BSA, 1mM GMP-PNP). Experiment was performed as described in (B) using MST Binding Buffer. (D) Analysis of the interactions of YjeQ with the mature 30S subunit and immature particles by MST in the presence of 1 mM GMP-PNP. In these experiments the concentration of the fluorescently labelled ribosomal particles was constant, while the concentration of unlabelled YjeQ was varied. After a short incubation the samples were loaded into MST hydrophobic glass capillaries, and the thermophoretic mobility of the labelled ribosomal particles (left panels) was measured using the Monolith.NT.115 instrument (NanoTemper). Measured changes in the MST response were used to produce curves that plotted the F_{norm} (‰)=F_1/F_0 versus YjeQ concentration. The F_1 and F_0 regions of the fluorescence time traces used to calculate F_{norm} (‰) are indicated in the panel. The F_{norm} (‰) curves were fit using the law of mass action to yield a K_d value. (E) Stimulation of the GTPase activity of YjeQ by the mature 30S subunit and immature $30S_{\Delta yjeQ}$ or $30S_{\Delta rimM}$ particles. The GTP hydrolysis rates of YjeQ in the presence and absence of the ribosomal particles were measured at different concentrations of GTP to determine steady-state kinetic parameters.

We next used microscale thermophoresis (MST) to measure the dissociation constants (K_d values) of YjeQ binding to these ribosome particles. This technique has

been shown to be a robust approach for measuring binding affinities in macromolecular assemblies made of proteins and DNA/RNA, including the ribosome (Zillner et al., 2012) (Godinic-Mikulcic et al., 2014). We fluorescently labelled the ribosomal particles on cysteine residues using the Red-Maleimide Protein Labelling Kit (NanoTemper Technologies) and tested that the labelling was not impeding YjeQ binding (Fig. 4.7C). For each K_d measurement, YjeQ was titrated against a fixed concentration of the labelled 30S particles (40 nM) in the presence of GMP-PNP. After 10-min incubations, the reactions were loaded into hydrophobic MST capillaries and the thermophoretic mobility of the fluorescently labelled ribosomal particles was analyzed. Consistent with the observations in the pelleting and filtration assays, YjeQ exhibited high binding affinity to the mature 30S subunit with a K_d value of 66.2 ± 7.7 nM (Fig. 4.7D). Conversely, when YjeQ was incubated with the $30S_{\Delta yjeQ}$ and $30S_{\Delta rimM}$ particles it was not possible to reach saturation even at the highest concentration tested (112 μM) (Fig. 4.7D). Consequently, a K_d value for YjeQ binding to the immature particles was not obtained. These experiments suggested that the affinity of YjeQ to the immature particles is much weaker than to the mature 30S subunit.

To measure the effect of the nucleotide on the YjeQ K_d values, identical reactions were tested in the presence of GDP. In the reaction with the mature 30S subunit, binding of YjeQ was not detected at the highest concentration tested (4 μM) (Fig. 4.8), indicating a large drop in affinity with respect to the equivalent binding reaction in the presence of GMP-PNP (Fig. 4.7D). Binding of YjeQ to the immature particles was only detected at the highest concentrations of YjeQ tested (>112 μM), but it was not possible to saturate

the binding reaction (Fig. 4.8). These results indicate that in the presence of GDP, the binding affinity of YjeQ to the immature subunits is also extremely low.

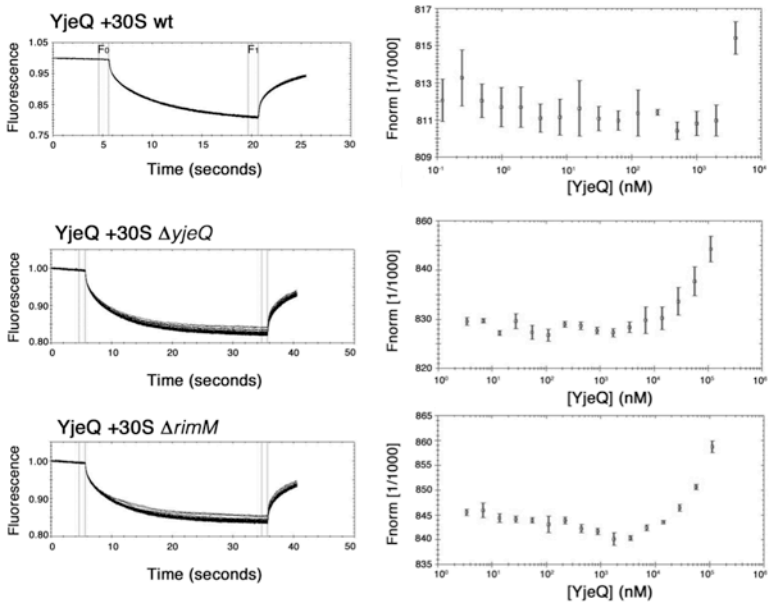

Figure 4.8. Effect of the nucleotide on the binding of YjeQ to the mature 30S subunit and immature 30S$_{\Delta yjeQ}$ and 30S$_{\Delta rimM}$ particles.
MST analysis of YjeQ binding to the mature and immature particles in the presence of 1 mM GDP. Left panel shows the fluorescence time traces for the binding reactions and the right panel displays the F_{norm} (‰)=F_1/F_0 curves for the three binding reactions derived from these traces. The F_1 and F_0 regions of the fluorescence time traces used to calculate F_{norm} (‰) are indicated in one of the traces on the left.

Next, we tested whether the binding of YjeQ to the mature 30S subunit at a protein concentration in the range of the K_d value obtained for the YjeQ+30S subunit complex constitutes a specific interaction. We also tested whether at this concentration range a specific interaction between YjeQ and the 30S$_{\Delta yjeQ}$ and 30S$_{\Delta rimM}$ particles is measurable. To this end, we took advantage of the low intrinsic GTPase activity of YjeQ, which increases upon specific interaction with ribosomal particles (Daigle et al.,

2002). In these experiments (Figure 4.7E), both the ribosomal particle and YjeQ were kept at 50 nM and the YjeQ GTPase activity was monitored with the malachite green assay at increasing concentrations of GTP (see 2.12). The GTPase activity exhibited by each ribosomal particle alone at each GTP concentration was subtracted from the total GTPase activity measured in the corresponding reactions containing YjeQ and the ribosomal particles. This background subtraction ensured accuracy in the calculations by removing all background phosphate production not due to YjeQ. A steady-state kinetic analysis (Table 4.1) showed that YjeQ had a similar K_M for GTP when the protein was by itself or in the presence of any of the ribosomal particles. Consistent with previous literature (Daigle et al., 2002), YjeQ GTPase activity exhibited a significant stimulation (>100 fold increase in k_{cat} / K_M) in the presence of the mature 30S subunit (Fig. 4.7E). Reactions containing immature $30S_{\Delta yjeQ}$ or $30S_{\Delta rimM}$ particles incubated with YjeQ also exhibited stimulation over the intrinsic YjeQ GTPase activity, albeit this stimulation was substantially smaller (10-30 fold increase in k_{cat} / K_M) compared to that shown by the mature 30S subunit (Fig. 4.7E).

Overall, the filtration, pelleting, MST and GTPase assays suggest that YjeQ is able to bind both the mature and immature 30S particles, however affinity for the mature 30S subunit is much higher than for the $30S_{\Delta yjeQ}$ or $30S_{\Delta rimM}$ particles.

Table 4.1. Kinetic parameters of YjeQ in the presence and absence of the mature 30S subunit and immature 30S$_{\Delta yjeQ}$ and particles.

	K_M (μM)	kcat (h^{-1})	kcat/K_M ($\mu M^{-1} h^{-1}$)	Increase in kcat/K_M
YjeQ	10.07	0.1327	219.63	1
30S$_{wt}$	4.47	6.059	2.256×10^4	103
30S$_{\Delta yjeQ}$	10.98	1.912	2.902×10^3	13
30S$_{\Delta rimM}$	5.36	1.949	6.060×10^3	27

4.7 Binding Affinity of Era, RimM and RbfA to the Mature 30S Subunits and Immature 30S Particles is Much Weaker than that of YjeQ

We analyzed the interactions of Era with 30S$_{wt}$, 30S$_{\Delta yjeQ}$ and 30S$_{\Delta rimM}$ particles using a combination of filtration and pelleting binding assays. Experiments using the pelleting assay demonstrated that when Era was incubated with either mature or immature ribosomal particles in the presence of GMP-PNP, the factor appeared in the pellet for each reaction (Fig. 4.9A). In control reactions containing Era in the absence of ribosome, less than 10% of the loaded protein appeared in the pellet fraction (Fig. 4.9A). When using the filtration assay to test binding of Era to either mature or immature ribosomal particles in the presence of GMP-PNP, Era was capable of interacting with all three ribosomal particles (Fig. 4.9B). Control reactions containing Era in the absence of ribosomal particles showed that Era passed into the flow through, however a large portion of the protein appeared to get stuck within the filter membrane and could therefore increase the likelihood of obtaining false positive results (Fig. 4.4A). These results

indicate that this factor has the ability to bind both the mature and immature ribosomal particles, however it was unclear from the qualitative assessment of the gels whether there was any difference in binding affinity amongst the different ribosomal particles.

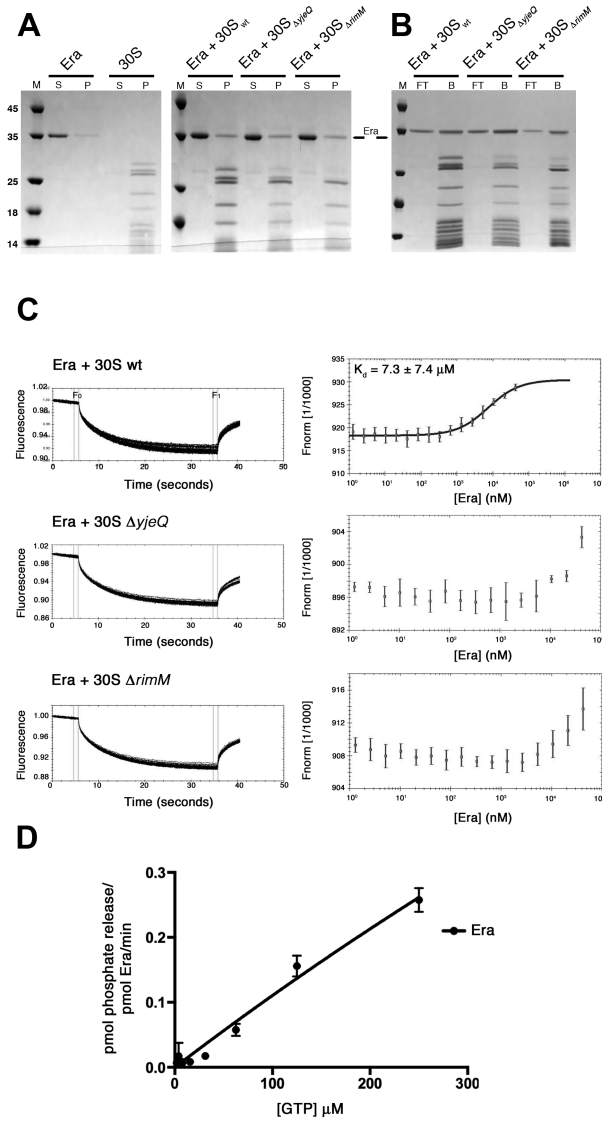

Figure 4.9. Binding of Era to the mature 30S subunit and immature 30S$_{\Delta yjeQ}$ and 30S$_{\Delta rimM}$ particles.
(A) Pelleting assay testing the binding of Era to the mature and immature 30S particles. A sevenfold excess of Era was incubated with either the mature 30S subunits or one of the immature 30S particles for 30 min at 37 ºC. Following the incubation, reactions were

laid over a sucrose cushion and subjected to ultracentrifugation. Proteins that were unbound were collected in the supernatant (S), while proteins that bound to the 30S particle were found in the pellet (P). The molecular weight (M) is in kDa. The pellet and supernatant were resolved by 4%–12% bis–tris SDS-PAGE and stained with Coomassie Brilliant Blue. The bands for Era are indicated. (B) Filtration assay testing the binding of Era to the mature and immature 30S particles. Reactions contained 2 μM of assembly factor and 0.4 μM of 30S particle. Assembly reactions were incubated for 30 min at 37 °C in the presence of GMP-PNP. Following incubation, the reactions were passed through a 100 kDa cut-off filter using centrifugation to obtain the FT and B fractions and samples were resolved by 4%–12% bis–tris SDS-PAGE and stained with Coomassie Brilliant Blue. (C) Analysis of the interactions of Era with the mature 30S subunit and immature particles by MST in the presence of 1 mM GMP-PNP. Fluorescence time traces and derived F_{norm} (‰)=F_1/F_0 curves for the three binding reactions are shown. In these experiments the concentration of the fluorescently labelled ribosomal particles was constant, while the concentration of unlabelled Era was varied. (D) Intrinsic GTPase activity of Era at different concentrations of GTP.

To identify any differences in the binding affinity of Era to the mature $30S_{wt}$ and immature $30S_{\Delta yjeQ}$ or $30S_{\Delta rimM}$ particles, a combination of MST experiments and GTPase assays were performed. MST experiments revealed that the K_d of Era to the mature 30S subunit in the presence of GMP-PNP was 7.3 ± 7.4 μM (Fig. 4.9C). Reactions to measure the K_d of Era with the immature particles did not reach saturation at concentrations of Era as high as 42 μM (Fig. 4.9C). Thus, a K_d value for Era binding to the immature particles was not obtained. Interestingly, performing the assembly reactions in the presence of GDP had no significant effect on the MST results for this factor (Fig. 4.10).

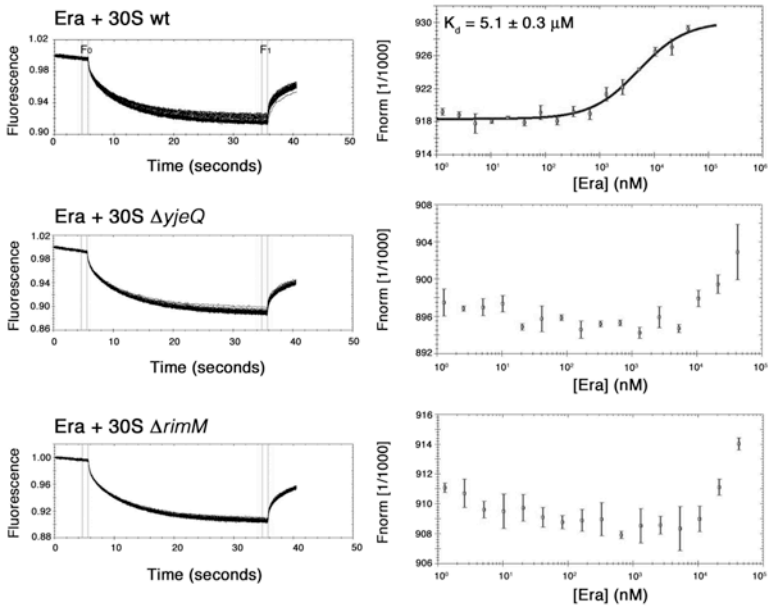

Figure 4.10. Nucleotide dependency on the binding of Era to the mature 30S subunit and immature 30S$_{\Delta yjeQ}$ and 30S$_{\Delta rimM}$ particles.
The left panel shows the thermophoretic mobility from the binding reactions of Era with the mature and immature particles. The F_{norm} (‰)=F_1/F_0 curves on the right panel are derived from the fluorescence time traces on the left. The F_1 and F_0 regions used to calculate F_{norm} (‰) are indicated in one of the traces on the left.

Finding that the binding affinity of Era to the mature 30S subunit was much weaker than that of YjeQ, led us to test using GTPase assays (see 2.12), whether at a protein concentration in the range of the K_d values obtained for the YjeQ+30S$_{wt}$ complex (66.2 ± 7.7 nM), a specific interaction between Era and the ribosomal particles occurs. Consistent with previous literature, Era (Johnstone et al., 1999) was shown to have low intrinsic GTPase activity (Fig.4.9D). In the steady-state kinetic analysis of this reaction, we used a GTP concentration range from 0 to 250 mM, which was the highest permitted concentration for the assay. The reactions did not saturate and k_{cat} and K_M values could not be determined (Fig. 4.9D), which is consistent with Era previously being reported to

have a high K_M (Hang and Zhao, 2003) (Meier et al., 1999) (Meier et al., 2000). Reactions containing Era at a 50 nM concentration and either mature or immature 30S particles at the same concentration did not show any enhancement of Era GTPase activity. Indeed, we did not detect any measurable phosphate being formed above background level (data not shown); thus, a steady-state kinetic analysis for these reactions was not possible. Background subtraction of intrinsic GTP hydrolysis and GTPase activity exhibited by the ribosomal particles themselves was applied as described in the case of YjeQ.

In the case of RimM and RbfA, their binding to the mature 30S subunits and to the $30S_{\Delta yjeQ}$ or $30S_{\Delta rimM}$ immature particles was tested by filtration assays (see 2.10). Despite the high concentration of factor used, only a weak interaction of RbfA with the $30S_{\Delta yjeQ}$ and $30S_{\Delta rimM}$ immature particles was observed and there was no appreciable binding to the mature 30S subunit (Fig. 4.11A). In the case of RimM, we did not observe substantial binding to any of the ribosomal particles (Fig. 4.11A). Consistent with the filtration assays, MST experiments used to measure the K_d values of RimM (Fig. 4.11B) and RbfA (Fig. 4.11C) to the ribosomal particles found there was low affinity of these factors to the ribosomal particles and that the reactions mostly did not reach saturation in spite of using concentrations of 217 μM and 1 mM for RimM and RbfA, respectively. However, there was notably more binding of RimM to the mature 30S subunits than to the immature 30S particles, indicating a K_d of 116 +/- 8.93 μM (Fig. 4.11B). Nonetheless, a K_d value for binding of RimM and RbfA to the immature particles was not obtained.

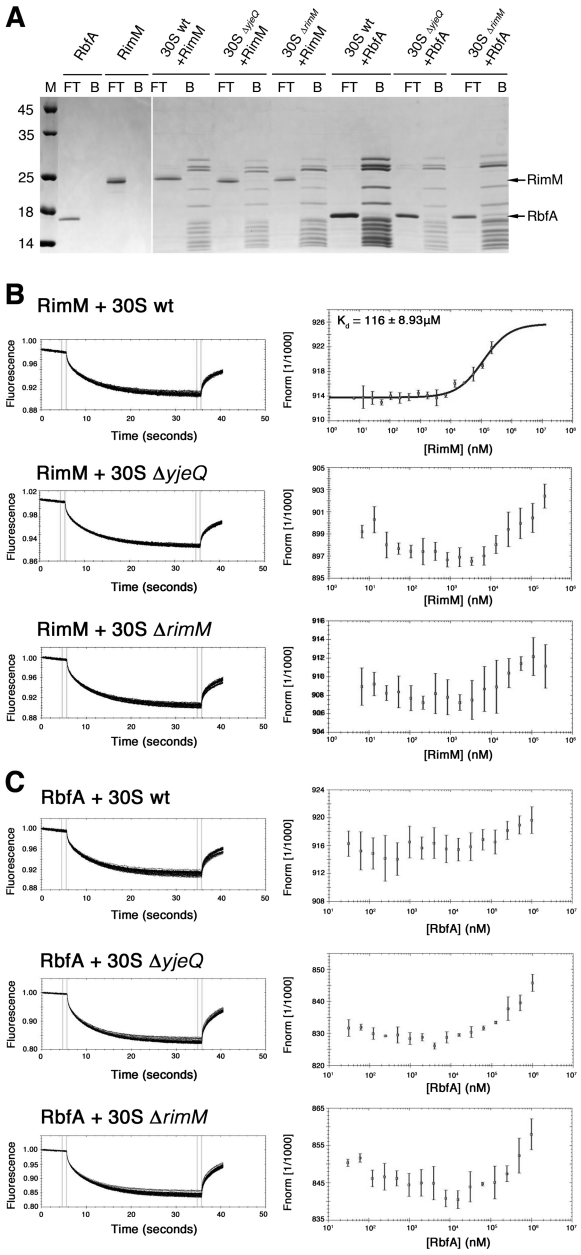

Figure 4.11. Binding of RbfA and RimM to mature 30S subunits and immature 30S$_{\Delta yjeQ}$ and 30S$_{\Delta rimM}$ particles.

Filtration assay testing the binding of RbfA (A) or RimM (C) to the mature and immature 30S particles. Reactions contained 2 µM of assembly factor and 0.4 µM of 30S particle. Assembly reactions were incubated for 30 min at 37 °C in the presence of GMP-PNP. Following incubation, the reactions were passed through a 100 kDa cut-off filter using centrifugation to obtain the FT and B fractions and samples were resolved by 4%–12% bis–tris SDS-PAGE and stained with Coomassie Brilliant Blue. MST analysis of the interactions of RbfA (B) or RimM (D) with the mature and immature 30S$_{\Delta yjeQ}$ the

$30S_{\Delta rimM}$ particles. Fluorescence time traces and derived F_{norm} (‰)=F_1/F_0 curves for the binding reactions are shown.

Overall, these experiments revealed that the binding affinity of Era, RimM and RbfA to both the mature 30S subunits and immature particles is much weaker than that of YjeQ to the mature 30S subunit. Most importantly, none of the factors showed a high binding affinity towards the immature 30S particles that accumulate in the Δ*yjeQ* and Δ*rimM* strain.

4.8 Discussion

Until now there have been no rigorous examinations of the binding interactions of functionally related maturation factors with the immature 30S particles that accumulate in assembly factor knockout strains. Interestingly, we found that YjeQ and Era bind to the mature 30S subunit with much higher affinity than to the $30S_{\Delta yjeQ}$ or $30S_{\Delta rimM}$ particles. Based on the observation that all four assembly factors analyzed had extremely low affinity to the immature 30S particles and the low abundance of ribosomal precursor particles in cells, it is likely that binding to the accumulated particles does not occur under physiological conditions. Consistent with these affinity measurements, we found substoichiometric occupancy of YjeQ, Era, RbfA and RimM on the immature 30S particles that accumulate in null cells. The binding affinity results are also in agreement with existing cryo-EM structures demonstrating a stable interaction of YjeQ (Jomaa et al., 2011a) (Guo et al., 2011), Era (Sharma et al., 2005) or RbfA (Datta et al., 2007) with the mature 30S subunit. In these structural studies, protein concentrations in the

micromolar range were used to assemble and visualize these complexes and we detected interactions between factors and mature 30S subunits at these concentrations.

These experiments also demonstrated that RbfA has the strongest interaction with immature $30S_{\Delta rimM}$ particles based on both the filtration (Fig. 4.11A) and qMS analysis (Fig. 4.6D). This is in agreement with previous literature demonstrating that the deleterious phenotypes caused by deletion of *rimM* can be suppressed by overexpression of *rbfA* (Bylund et al., 2001) (Bylund et al., 1998). Perhaps in the Δ*rimM* strain, the immature particles that accumulate have the ability to associate with RbfA to help facilitate downstream maturation into the functional 30S subunit. It is likely that this shared role in 30S assembly could involve the removal of the additional nucleotides on the 5' and 3' ends, which is consistent with previous literature indicating that both proteins are needed for 17S rRNA processing (Bylund et al., 1998). This redundancy in assembly factor functions could provide cells with a robust mechanism for sustaining efficient biogenesis.

It has previously been shown that YjeQ interacts preferentially with 30S subunits when bound to GTP compared to GDP (Himeno et al., 2004) (Jeganathan et al., 2015) (Daigle and Brown, 2004). This has led researchers to speculate that YjeQ's release from the 30S subunit is facilitated by its increased stimulation of GTPase activity upon association with the ribosome. The data presented in this thesis showing that YjeQ binds to the mature 30S subunit with high affinity in its GTP, but not GDP bound state (Fig. 4.8 & 4.9), is in good agreement with the hypothesis that the release mechanism is regulated by GTP hydrolysis. Conversely, Era's affinity to the mature 30S subunit was not

dependent on its nucleotide bound state (Fig 4.10 & 4.11). Era exhibited a low micromolar K_d in both its GMP-PNP and GDP bound states. Perhaps the release for Era from assembling 30S particles is facilitated by other maturation factors or s-proteins. Interestingly, the 30S binding sites for both Era and bS1 overlap (Sharma et al., 2005), which indicates that bS1 could be involved in the removal of Era during subunit assembly. The differences in the nucleotide associated affinity of YjeQ and Era to mature 30S subunits highlights potentially distinct mechanisms in how assembly factor release is mediated.

The low abundance of assembly factors in cells compared to ribosome components (Fig. 4.6) suggests that not all assembling particles require direct association with factors to achieve maturation into functional 30S subunits. This observation is further highlighted by the fact that YjeQ, RimM and RbfA are dispensable for the cell and fully matured 30S subunits can assemble into 70S ribosomes even in the absence of any of these factors (Leong et al., 2013) (Jomaa et al., 2011b) (Guo et al., 2013) (Yang et al., 2014). This would imply that the assembling particles could proceed down factor-independent pathways *in vivo* to achieve maturation. This is consistent with early work on ribosome assembly demonstrating that all of the information necessary for assembly is encoded within the s-proteins and rRNA themselves (Traub and Nomura, 1968) (Culver and Noller, 1999).

Given that these putative factors have been implicated in assisting in the folding of rRNA (reviewed in (Connolly and Culver, 2009) (Shajani et al., 2011) (Pyle, 2013) (Wilson and Nierhaus, 2007)), it is possible that they are required to lower the activation

energy along the folding landscape to increase the kinetics of assembly. Accordingly, these factors would be more crucial to assembly and perhaps in greater abundance during low temperature growth conditions when there is less thermal energy present to overcome the activation barriers. Consistent with this hypothesis, RbfA was originally identified as a ribosome assembly factor by its ability to suppress the cold-sensitivity phenotype of a C23U mutation in rRNA (Dammel and Noller, 1995). It is tempting to speculate that there would be a substantial increase in the abundance of these factors in cell lysates and association with assembling particles under cold growth conditions.

The qualitative binding assays (pelleting and filtration) for Era and the MST results showed an apparent discrepancy in the affinity of Era towards the immature subunits. The pelleting and filtration assays (Fig. 4.9A&B) suggest that Era binds to both mature and immature subunits with similar affinity, however the MST results (Fig. 4.9C) indicate that Era has much higher affinity to mature 30S subunits. This finding emphasizes that although Coomassie stained polyacrylamide gels can identify possible interactions, they are not ideally suited to determine differences in binding affinity. It seems that in the case of Era, the pelleting and filtration assays have a tendency to overestimate the amount of binding to the ribosomal particles. Nonetheless, this potential for false positive results did not apply to the other three proteins (YjeQ, RbfA and RimM) tested. Moreover, the filtration and binding assays were able to distinctly visualize the difference in binding of YjeQ to the mature 30S subunit relative to immature 30S particles, thus reinforcing that large changes in affinity could be detected from the gels.

Results from chapter 3 demonstrated that the accumulated immature 30S particles from the Δ*yjeQ* and Δ*rimM* strains have a delay in 17S rRNA processing that can be rescued by induction of YjeQ and RimM, respectively (Fig. 3.4). This suggests that the increased expression of YjeQ or RimM is able to facilitate processing of the additional nucleotides on the terminal ends of 17S rRNA. This increased processing of rRNA could be a result of direct interactions of either YjeQ or RimM with their respective accumulated assembly intermediates. This is an interesting contrast to the binding data presented in this chapter indicating that $30S_{\Delta yjeQ}$ or $30S_{\Delta rimM}$ particles are not bound by assembly factors when isolated from cells (Fig. 4.6) and also do not bind to the factors *in vitro* (Fig. 4.8 – 4.11). It is likely that during the pulse chase experiments the expression of the assembly factors in the null strains is restored immediately upon labelling of the particles and therefore they would be at the early stages of the assembly process. The factors would then be able to interact with these early stage intermediates to help facilitate downstream processing.

In conclusion, this study brings new insights into the nature and binding interactions of the immature ribosomal particles that assembly factor single knockout strains accumulate.

CHAPTER FIVE

GENERATION AND CHARACTERIZATION OF AN ERA-DEPLETED STRAIN AND AN RBFA KNOCKOUT STRAIN

5.1 Author's Preface

This chapter contains unpublished results regarding the generation of an essential gene depletion strain for *era* and an *rbfA* knockout strain. The main goal of this project was to generate unique 30S assembly factor depletion/deletion strains that have never been previously studied in Dr. Joaquin Ortega's lab. Furthermore, it was important to provide an initial biochemical and structural characterization of these strains to lay the groundwork in which further studies could be developed. The ultimate goal is that this work will be incorporated into a manuscript for a future co-first author publication.

I created both strains discussed in this chapter under the supervision of Dr. Joaquin Ortega and with consultation from Dr. Jean Philippe Cote in Dr. Eric Brown's laboratory at McMaster University. The recombineering plasmid used for inducing integration of genes into the chromosome was a kind gift from Dr. Eric Brown's lab. All other biochemical procedures including the generation of the *era* depletion culture conditions, purification of the ribosomal subunits and analysis of the sucrose profiles was performed by me. All electron microscopy was performed by me with direct oversight from Dr. Joaquin Ortega. Negative staining electron microscopy was performed at McMaster University using the JEOL 1200 EX. Cryo-electron microscopy was

performed using the FEI Tecnai F20 at SickKids Hospital in Toronto in the laboratory of Dr. John Rubinstein.

5.2 Introduction

To gain a more comprehensive understanding of how late stage assembly factors mediate 30S maturation, it is important to expand on the available 30S intermediates that can be isolated for investigation. Chapters 3 and 4 further characterized the fate and binding interactions of the 30S particles that accumulate in the Δ*yjeQ* and Δ*rimM* strains. Furthermore, there have only been previous electron microscopy structural analyses of the immature 30S particles that accumulate in Δ*yjeQ* (Jomaa et al., 2011b), Δ*rimM* (Leong et al., 2013) (Guo et al., 2013) and Δ*yjeQ*Δ*rbfA* (Yang et al., 2014) bacterial strains. These strains have proven to be a powerful tool for investigating the late stages of 30S assembly and have enabled detailed visualization of assembling particles. By further exploiting this technique and generating novel strains that expand on the list of immature 30S particles, we hope to gain a more comprehensive understanding of the late stages of 30S subunit maturation. Importantly, there remains to be any investigation of the structural defects that occur in assembling 30S subunits upon depletion of essential 30S assembly factors.

Accordingly, we developed two additional *E.coli* strains with late stage assembly factors either depleted or removed. We created an arabinose-inducible essential gene depletion strain for the *era* gene (Era-depleted) and an *rbfA* knockout strain (Δ*rbfA)*. These two 30S assembly factors have been previously shown to contain highly similar

RNA binding C-terminal KH domains (Swapna et al., 2001) (Huang et al., 2003) (Johnstone et al., 1999) and have overlapping functions in ribosome assembly (Inoue et al., 2006) (Inoue et al., 2003). Furthermore, perturbation of either assembly factor leads to a common phenotype consisting of slowed growth, an increase in unprocessed 17S rRNA, an accumulation of free 30S and 50S subunits and a concomitant decrease in 70S ribosomes and polysomes (Dammel and Noller, 1995) (Sayed et al., 1999) (Inoue et al., 2003). Despite previous genetic and biochemical studies involving these strains, there remains to be any structural studies of the 30S particles that accumulate. Therefore, for this work we aimed to generate and perform the first structural characterization of 30S particles that assemble in the absence of the essential GTPase Era.

5.3 Creation of Era-Depleted and Δ*rbfA E.coli* Strains

The first step of this project was to create both an Era-depleted stain and *rbfA* knockout strain (see 2.3). Briefly, the *era* gene was PCR amplified from the previously generated pET15b-*era* overexpression plasmid and then cloned it into the pBS-*araBAD*flank*kan* plasmid (Campbell and Brown, 2002) (Fig. 5.1 A &B). The recombineering pSim6 plasmid (Datta et al., 2006), was then used to insert *era* into the bacterial chromosome at the *araBAD* promoter. Replacement of the *araBAD* genes with *era* was confirmed using two sets of primers for PCR screening that only produce a product if *era* is inserted in the correct orientation in the chromosome at *araBAD* (Fig. 5.1C). After insertion of *era* at *araBAD*, the native *era* gene was deleted and replaced with an apramycin^{r} cassette using pSim6 and the *era* knockout cassette (see 2.3). Two

sets of oligonucleotides were used to confirm the precise deletion of *era* at its native locus (Fig. 5.1D). The resulting *E.coli* strain was called "Era-depleted".

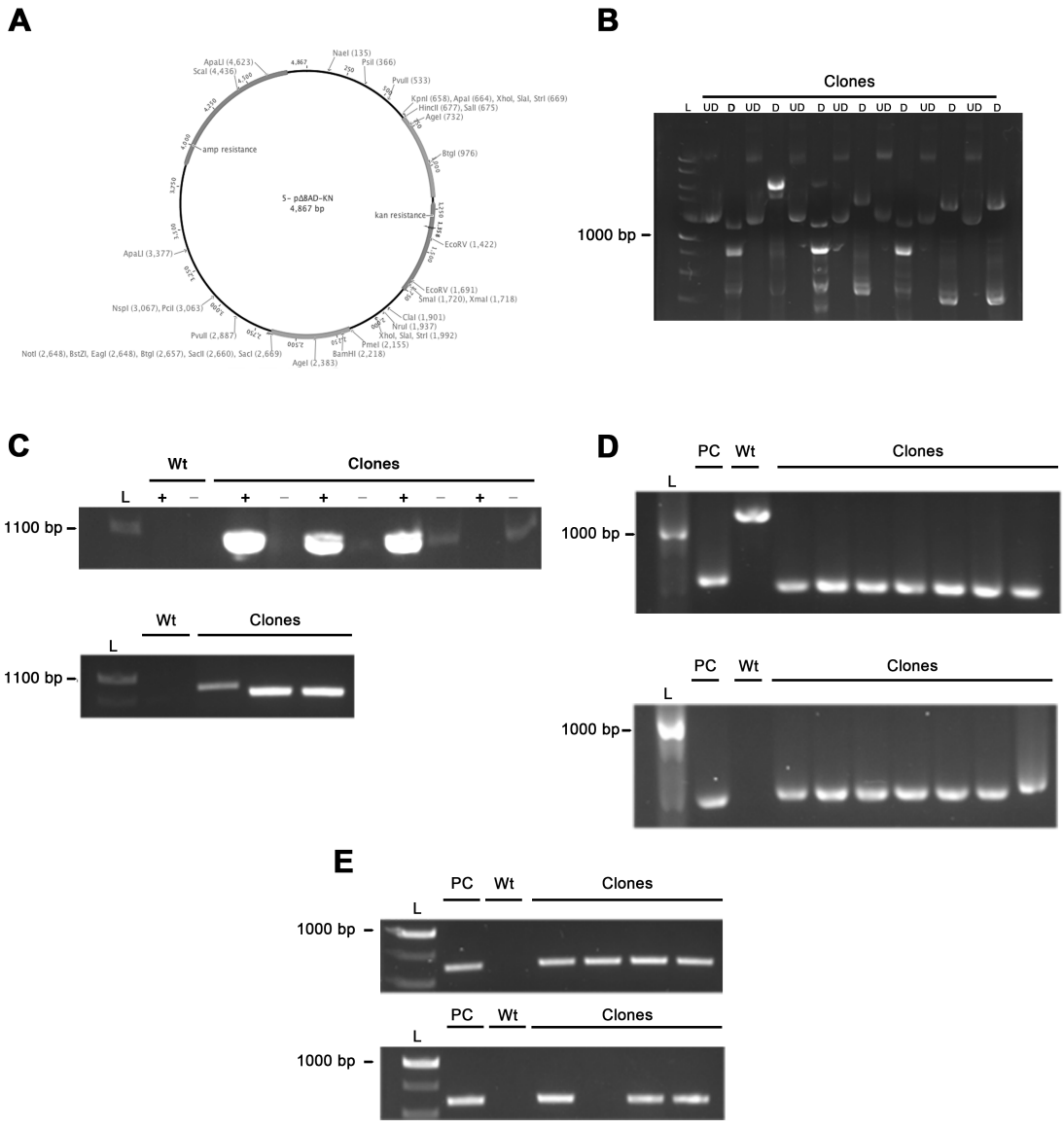

Figure 5.1. Generation of Era-depleted and Δ*rbfA E.coli* strains.
(A) Diagram of pBS-*araBAD*flank*kan* plasmid used for insertion of Era at the *araBAD* locus. (B) Restriction enzyme double digestion (D) using *NdeI* and *XhoI t*o screen for ligation of Era PCR product into pBS-*araBAD*flank*kan* to create pBS-*araBAD*flank*erakan.* Undigested (UD) plasmid products are also shown. Expected PCR

products confirming ligation of Era in the correct orientation were 2.4 kb and 3.4 kb. Positive transformants containing pBS-*araBAD*flank*erakan* with *era* inserted into the correct orientation were confirmed by sequencing (Mobix, McMaster University). Molecular ladder (L) in number of base pairs is shown. (C) Two sets of PCR screening results using ara_up-R and Era_down-F oligonucleotides (+) (insertion in correct orientation) or ara_up-R and Era_up-R oligonucleotides (-) (insertion in wrong orientation) (top panel) or kan_int and ara_int oligonucletodies (confirms insertion) (bottom panel). These PCR results demonstrate insertion of the double digested (*NotI* and *PsiI*) linearized DNA fragment from the pBS-*araBAD*flank*erakan* into the chromosome of *E.coli* BW25113 cells to generate an *araBAD*::*era* strain. (D) Two sets of PCR screening results using apra_int-F and EraKO_confirm-R primers (top panel) and apra_int-R and EraKO_confirm-F (bottom panel) to confirm the precise knockout of Era and insertion of apramycin^r at the *era* locus in *araBAD*::*era E.coli* BW25113 cells to generate *araBAD*::*era*, *era*::*apr*^{r}. The top panel show a PCR amplicon for the wild type (Wt) strain using the EraKO_confirm-F and EraKO_confirm-R oligonucleotides with an expected product of ~1100 bp. The bottom panel shows the PCR results for the wild type (Wt) using the apra_int-R and EraKO_confirm-F oligonucleotides, which is not expected to produce an amplicon of the native *era* locus. A positive control (PC) was used to ensure optimal PCR amplification for the apramycin^r cassette. (E) Two sets of PCR screening results using apra_int-F and RbfAKO_confirm-R oligonucleotides (top panel) and apra_int-R and RbfAKO_confirm-F (bottom panel) to confirm the precise knockout of *rbfA* and insertion of apramycin^r at the *rbfA* locus in *E.coli* BW25113 cells to generate *rbfA*::*apr*^{r}. The PCR results for the wild type (Wt) strain are shown, which are not expected to produce an amplicon of the native *rbfA* locus. A positive control (PC) was used to ensure optimal PCR amplification of the apramycin^r cassette. See table 2.1 in section 2.3 for oligonucleotide sequences.

The deletion of *rbfA* was performed by transforming the PCR amplicon containing an apramycin^r cassette with flanking regions homologous to the upstream and downstream regions of the native *rbfA* gene into the parental BW25113 cells (see 2.3). Two sets of primers used for PCR screening confirmed the insertion of apramycin^r at the native *rbfA* locus (Fig. 5.1E). The resulting strain was called "Δ*rbfA"*.

5.4 Era-Depleted and Δ*rbfA* Strains Have a Slow Growth Phenotype

To assess the optimal culture conditions for the Era-depleted strain, overnight cultures were diluted in LB media containing different arabinose concentrations and growth rate was monitored relative to the wild type strain (see 2.4). Complementation was most efficient in LB media supplemented with 1% arabinose (data not shown) and all subsequent Era-depleted culture conditions were maintained at this arabinose concentration until initiation of the era-depletion protocol (see 2.4). Consistent with previous literature (Lerner and Inouye, 1991) (Inoue et al., 2003), the growth rates at 37 °C of the Era-depleted strain in the absence of arabinose and the Δ*rbfA* strain were drastically reduced relative to the wild type strains (Fig. 5.2A). When the Era-depleted strain was grown in the presence of arabinose, there was an extended lag period and the culture reached the stationary phase at a lower optical density compared to the wild type strain, suggesting that full complementation was not achieved (Fig. 5.2A). Growth at 15 °C of the Era-depleted strain without arabinose and the Δ*rbfA* strain was completely inhibited (Fig. 5.2A), which is indicative of the cold-sensitivity phenotype classically associated with ribosome assembly defects (Stokes et al., 2014). Additionally, the Era-depleted strain did not grow even in the presence of 1% arabinose at 15 °C, further supporting the notion that full complementation was not achieved under the arabinose inducible system.

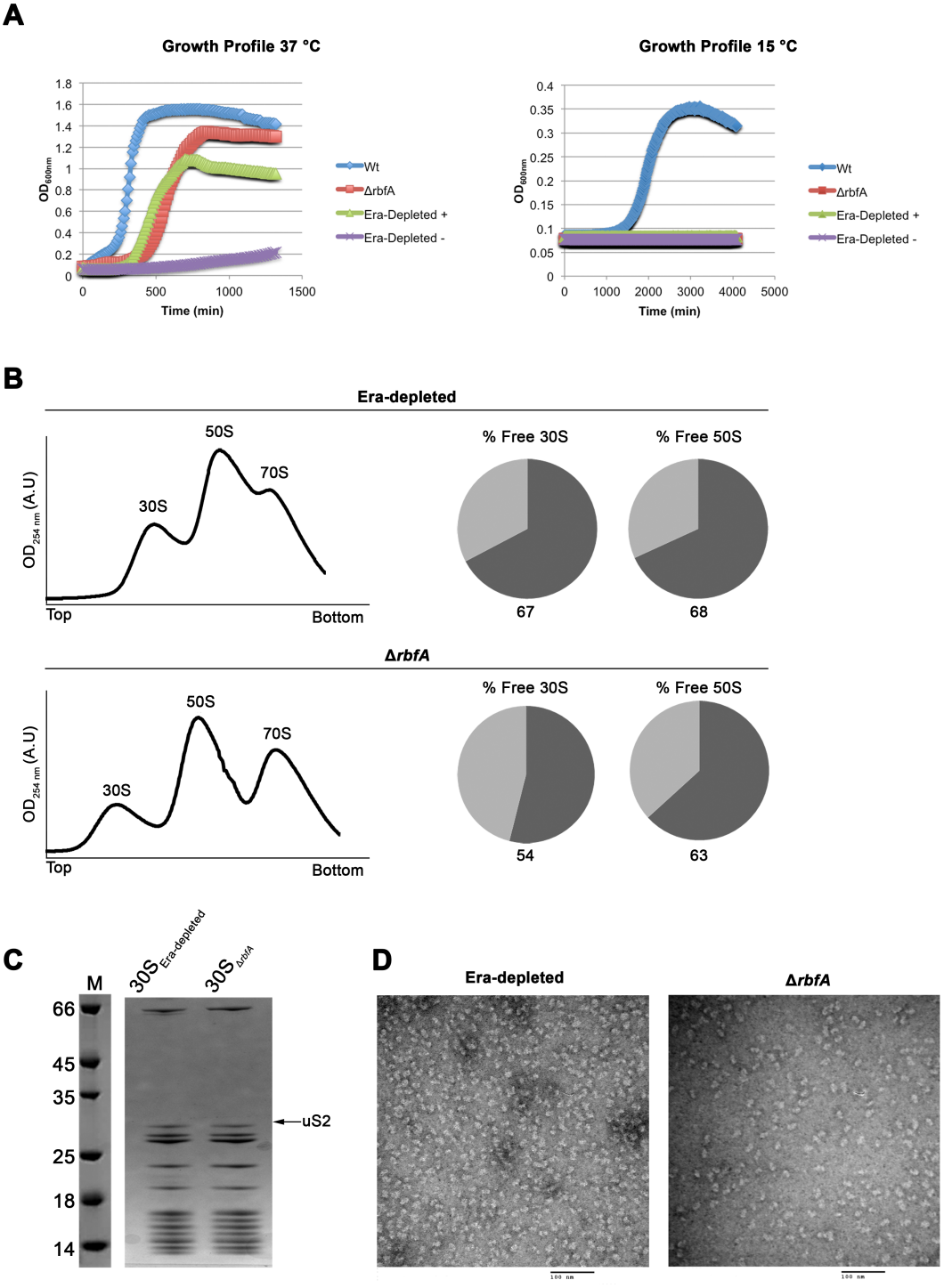

Figure 5.2. Characterization of Era-depleted and Δ*rbfA* strains.
(A) Growth profiles of the wild type, Era-depleted and Δ*rbfA* strains incubated at either 37 °C or 15 °C in liquid media. Overnight cultures grown in LB media at 37 °C were diluted 1/10,000 in fresh LB media and incubated at either 37 °C for 24 hours or 15 °C

for 72 hours. The profile for the Era-depleted strain grown in LB media with 1% arabinose (+) and without arabinose (-) is shown. Growth at 37 °C for the Era-depleted strain in the absence of arabinose is severely compromised and is delayed in the Δ*rbfA* strain. There is no growth of the Era-depleted or Δ*rbfA* strains at 15 °C. Growth curves represent absorbance taken at 600 nm every ten minutes in a 96-well plate using a Tecan Sunrise plate reader. Experiment was performed with five replicates for each culture condition. (B) Ribosome profile showing distribution of 30S, 50S and 70S particles in Era-depleted and Δ*rbfA* strains. The Era-depleted strain was grown overnight in 1% arabinose and then subcultured into LB media without arabinose to initiate the Era depletion protocol (see 2.6). Crude ribosomes were extracted from lysates of the Era-depleted and Δ*rbfA* cells, layered onto a 10-30% sucrose gradient and subjected to ultracentrifugation overnight to separate the ribosomal particles. In both strains there is an increase in free 30S and 50S subunits and decrease in 70S ribosomes relative to wild type BW25113 strain. (C) SDS-PAGE analysis in 4 – 12% bis-tris polyacrylamide gel of purified 30S subunits samples isolated from Era-depleted and Δ*rbfA* strains. There is a subtle depletion in the late binding uS2 protein. Molecular marker (M) is shown in kDa. (D) Electron microscopy images of negative stained 30S particles isolated from the Era-depleted and Δ*rbfA E.coli* strains. Particles were purified as previously described, diluted to ~47 nM in ribosome storage buffer (10 mM Tris-HCl (pH=7.5), 10 mM Mg Acetate, 60 mM NH_4Cl, 3 mM β-mercaptoethanol), stained with 1% uranyl acetate solution and applied to freshly carbon coated continuous layer grids immediately after glow discharge. Images were collected using a JEOL 1200EX electron microscope operated at 80 kV.

5.5 Era-Depleted and Δ*rbfA* Strains Contain an Altered Ribosome Profile

To confirm if the Era-depleted and Δ*rbfA* strains had a ribosome assembly defect similar to what has been previously described (Dammel and Noller, 1995) (Sayed et al., 1999) (Inoue et al., 2003), we purified the 30S particles that accumulate in these strains and examined the ribosome profiles (see 2.6). Ribosome assembly in wild type bacteria cells is extremely efficient and assembly intermediates do not accumulate (Lindahl, 1975), resulting in the majority of subunits being associated to form 70S ribosomes with few free 30S and 50S subunits (Fig. 3.1 & 3.3). Conversely, a well-known hallmark of perturbed ribosome assembly is that there is an accumulation of free 30S and 50S

subunits relative to 70S ribosomes (Lovgren et al., 2004) (Leong et al., 2013) (Jomaa et al., 2011b) (Guo et al., 2013) (Inoue et al., 2003) (Yang et al., 2014).

Prior to isolating 30S particles from the Era-depleted strain, it was first necessary to deplete Era from the cells following the detailed protocol described in 2.6. Analysis of the ribosome profiles generated by sucrose gradient ultracentrifugation for the Era-depleted and Δ*rbfA* strains revealed an assembly defect characterized by a severe accumulation of free 30S and 50S subunits relative to 70S ribosomes (Fig 5.2B). In the Era-depleted and Δ*rbfA* strains, 67% and 54% of the 30S particles respectively, were not associated with 50S subunits. These values of free 30S subunits are higher than what has typically been reported in the past for other assembly factor deletion strains (Leong et al., 2013), perhaps suggesting a more substantial defect in the assembly process. In comparison, only ~18% of the 30S subunits are not bound to 50S subunits in wild type cells (Fig. 3.1). Furthermore, the protein complement of the $30S_{\Delta rbfA}$ and $30S_{\text{Era-depleted}}$ particles was assessed by SDS-PAGE to confirm the purity of the samples and identify any possible depletion in s-proteins (Fig. 5.2C). The Coomassie stained gels showed a mostly typical protein profile for *E.coli* 30S subunits, with a subtle depletion in uS2 for both the $30S_{\Delta rbfA}$ and $30S_{\text{Era-depleted}}$ particles. The abnormal ribosome profiles and depletion of a late binding s-protein in the Era-depleted and Δ*rbfA* strain is consistent with numerous other studies confirming that Era and RbfA are involved in 30S subunit biogenesis (Sharma et al., 2005) (Datta et al., 2007) (Goto et al., 2011) (Inoue et al., 2003) (Inoue et al., 2006).

5.6 Depletion of Era Leads to an Accumulation of 30S Precursors at Different Stages of the Assembly Process

Structural characterizations of immature 30S particles from several assembly factor knockout strains have provided insight into the specific roles implemented by assembly factors, as well as general features of the maturation process (Jomaa et al., 2011b) (Leong et al., 2013) (Guo et al., 2013) (Yang et al., 2014) (Clatterbuck Soper et al., 2013). Although numerous studies have implicated Era in 30S subunit assembly (Sayed et al., 1999) (Sharma et al., 2005) (Inoue et al., 2003) (Inoue et al., 2006), there have been no high-resolution structures solved of the immature 30S particles that accumulate upon depletion of Era or any other essential 30S factor. Accordingly, to assess the structural defects in the $30S_{Era\text{-}depleted}$ particles a combination of negative staining and cryo-EM was used (see 2.15 & 2.16).

It was necessary to assess the morphology of the $30S_{Era\text{-}depleted}$ particles and ensure that the sample was pure before proceeding to cryo-EM. Several samples of $30S_{Era\text{-}depleted}$ particles were prepared at various concentrations for negative staining and the distribution of particles was analyzed using transmission electron microscopy (see 2.15). Analysis of the negative stained $30S_{Era\text{-}depleted}$ particles revealed that the particles had morphological features that are typical of 30S subunits and that the sample was suitable for cryo-EM analysis (Fig. 5.2D).

The $30S_{Era\text{-}depleted}$ particles were prepared for cryo-EM by loading the diluted samples onto freshly-coated holey carbon grids, vitrifying the samples in liquid ethane and imaging them using a Tecnai F20 electron microscope (FEI) operated at 200 kV and

fitted with a K2 direct electron detector (see 2.16). Micrographs (Fig. 5.3A) were processed using the single particle reconstruction methods provided in Relion software (version 1.3) (Scheres, 2012b) (Scheres, 2012a) and initially ~30,000 particles were selected to generate 2D (Fig. 5.3B) and 3D class averages (Fig. 5.3C) of the $30S_{Era\text{-}depleted}$ particles. Given the relatively low number of particles selected, the structural characterization of the $30S_{Era\text{-}depleted}$ particles described here is only preliminary.

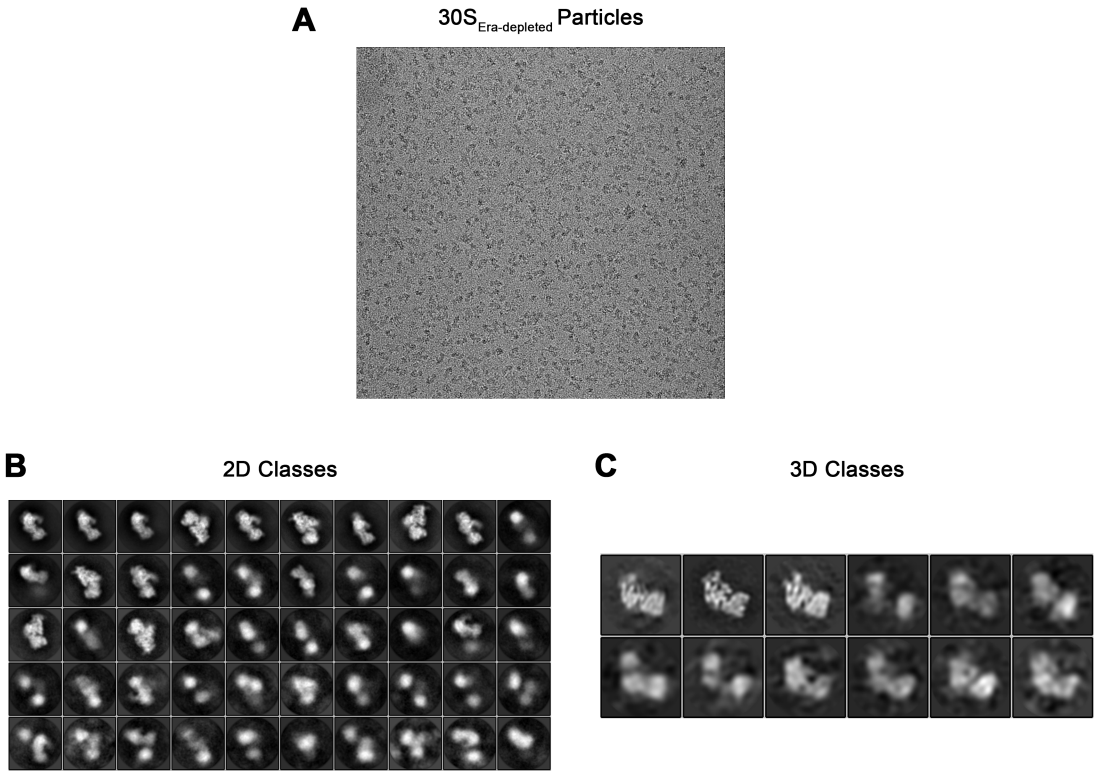

Figure 5.3. 2D and 3D image classification of 30S particles isolated from Era-depleted strain.
(A) Typical micrograph of 30S particles isolated from the Era-depletion strain. Image was taken using a Tecnai F20 (FEI) electron microscope operated at 200 kV. (B) 2D classification using maximum likelihood methods provided in Relion software suite. 29,217 particles were selected, CTF-corrected and 2D averages were generated representing different views and conformations of the $30S_{Era\text{-}depleted}$ particles. Classes that contained distinct morphological features of the 30S subunit with high signal to noise

ratio were selected for subsequent 3D classification. 100 classes were requested for this step and 25 iterations of image classification. The classes are sorted according to the distribution of particles in descending order. Only the top 50 classes are shown. (C) 3D classification performed in Relion using 28,878 particles that were selected after the 2D classification step. 12 classes were requested for this step and 25 iterations of image classification. The classes are sorted according to distribution of particles in descending order.

Analysis of the preliminary 3D cryo-EM density maps of the various 30S particle classes that accumulate upon depletion of Era revealed a strikingly heterogeneous sample (Fig. 5.4A). Interestingly, the $30S_{Era\text{-}depleted}$ particles appeared to be in different stages of the assembly pathway ranging from early intermediates to mature 30S subunits. At one end of the spectrum, classes representing early assembly intermediates contained a partially formed 30S body with varying amounts of distortion in the head and platform region. In some instances the head appeared to be completely detached from the platform and body, suggesting high flexibility in the interdomain regions. The major domains in these early 30S assembly intermediates were apparent, however the landmark features were still being assembled and in some instances were absent or unrecognizable. For instance, the spur and h44 were not apparent in the early stage 30S intermediates. As the level of maturation progressed, the interdomain regions became less flexible and electron density became more pronounced. Furthermore, landmark features started to adopt a similar conformation to that observed in the mature 30S subunit and structural components such as the spur and h44 become identifiable. Notably, the three most abundant classes (Fig. 5.4B) also happened to be those that most closely resembled the mature 30S subunit. Together, this data indicates that depletion of Era leads to an accumulation of 30S precursors at different stages of the assembly pathway.

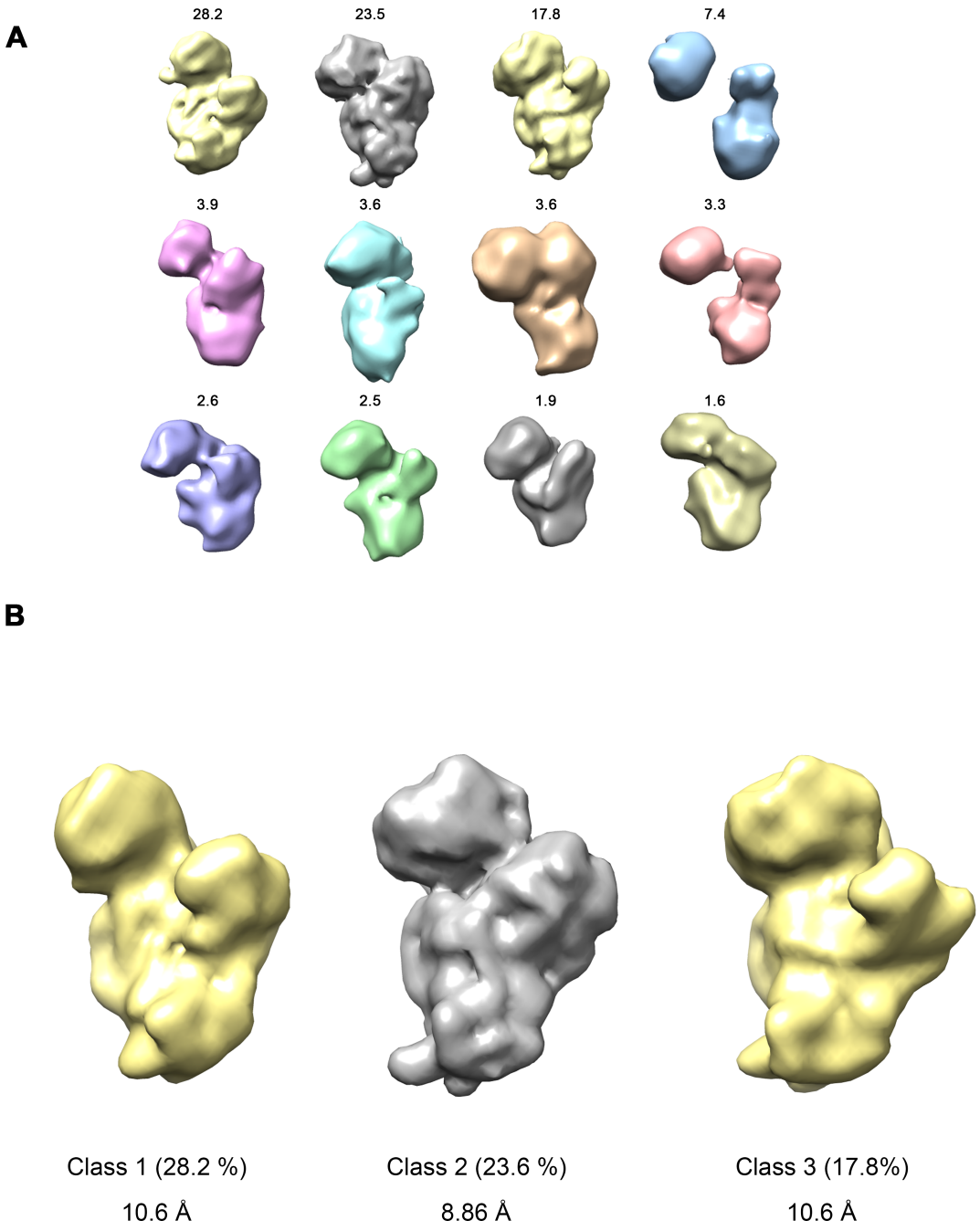

Figure 5.4. Cryo-EM density maps of Era-depleted 30S particles.
(A) Cryo-EM density maps of 12 classes depicting the three dimensional structures of the $30S_{Era\text{-}depleted}$ particles. Images were taken using a Tecnai F20 (FEI) electron microscope operated at 200 kV. Micrographs were processed using Relion and 28,878 projections showing different views and conformations of the 30S particles were selected for 3D classification. Classes were organized based on the particle distribution in descending

order with the percentage of particles attributed to each class shown. The classes demonstrate 30S intermediates at various stages of the maturation process based on the architecture of the landmark features of the mature 30S subunit. (B) The top three classes (classes 1, 2 and 3) containing the large majority of the $30S_{Era\text{-}depleted}$ particles (69%) were submitted for 3D refinement and post-processing generating cryo-EM density maps between 8.86 – 10.6 Å resolution. One of these classes (class 2) that constitute 24% of the total particles has morphological features that resemble the fully matured 30S subunits. The other two classes have structural features that contain all three major domains of the 30S subunit; however the domains are not properly oriented relative to one another.

5.7 Discussion

The structural heterogeneity in the $30S_{Era\text{-}depleted}$ particles indicates that Era could be involved during the early stages of 30S assembly and facilitate a global maturation event. Era has previously been shown to cause a modest increase in the rates of association of numerous s-proteins that span across all domains, but does not have any dramatic specific effects (Bunner et al., 2010b). Furthermore, it has been suggested that Era may bind to assembling 30S particles early on and remain bound until the very final stages of maturation (Bunner et al., 2010b). In this work we have shown that upon depletion of Era there is an accumulation of immature 30S particles from the early to final stages of the assembly process, rather than just one specific intermediate (Fig. 5.4). These accumulated $30S_{Era\text{-}depleted}$ particles have varying levels of structural defects in all three major domains and in some cases the interdomain regions appear to be completely flexible. This observation is consistent with previous literature implicating that Era may have a general role throughout 30S assembly, such as inducing rRNA conformational changes (Bunner et al., 2010b). Furthermore, a large portion of the particles has a structure similar to the mature 30S subunit (class 2). It is tempting to speculate that the

various classes represent on-pathway intermediates that are in the process of assembling into mature 30S subunits.

Interestingly, the particles that accumulate in the Era-depleted strain are remarkably more diverse with greater structural defects than in other strains with non-essential 30S assembly factors knocked out. Previous biochemical and structural studies in Δ*yjeQ* (Jomaa et al., 2011b), Δ*rimM* (Leong et al., 2013) (Guo et al., 2013), and Δ*yjeQ*Δ*rbfA* (Yang et al., 2014) strains have demonstrated that the accumulated immature particles represent late stage intermediates that all share similar structural distortions (Fig. 1.8). Specifically, essential intersubunit bridges and the decoding centre are not properly structured, thus preventing the immature particles from associating with 50S subunits and engaging in translation. These findings suggest that the multiple parallel pathways of assembly converge into structurally related "common intermediates", as opposed to the mature state (Leong et al., 2013). Perhaps these non-essential factors have overlapping functions that specialize in assisting the final stages of maturation, including formation of the decoding centre and intersubunit bridges. This redundancy in their roles ensures immature particles have a robust system in place for assembling the most functionally important regions of the 30S subunit. Conversely, the finding that Era depletion leads to a diverse set of structurally distinct particles and may be involved in global maturation events throughout the entire assembly process could provide a reason for why it is indispensable for cell survival. Furthermore, although overexpression of Era can compensate for deletion of other factors (Campbell and Brown, 2008) (Inoue et al., 2003) (Inoue et al., 2006), no other factors have been shown to compensate for the deleterious

phenotypes in Era depletion strains. Therefore, it is conceivable that Era does not lead to an accumulation of "common intermediates" because it is involved in multiple stages of assembly early on, whereas YjeQ, RbfA and RimM have overlapping roles during a specific late stage maturation event.

Regardless of what stage Era is required during 30S biogenesis, it is clear from results in chapter 4 of this thesis (Fig. 4.9) and previous literature (Sharma et al., 2005) (Tu et al., 2011) (Tu et al., 2009) that Era can stably bind to mature 30S subunits. Era has been shown to bind to the cleft between the head and platform, near the anti-Shine-Dalgarno sequence in the 3' domain of the 30S subunit (Fig 1.6) (Sharma et al., 2005) (Tu et al., 2011) (Tu et al., 2009). A common characteristic of several of the accumulated 30S particles in the Era-depletion strain is that the region between the head and platform is extremely flexible resulting in the two domains being improperly oriented and other structural features being unresolved in this region (Fig. 5.4). Based on the previous literature demonstrating the binding site for Era and the structure of the $30S_{Era\text{-}depleted}$ particles, Era could bind this region to facilitate global rearrangements necessary for proper domain architecture during 30S biogenesis.

A technique recently exploited to visualize 30S biogenesis throughout multiple stages of assembly was to incubate 16S rRNA with all 21 s-proteins *in vitro* and then use time-resolved negative staining electron microscopy to assess the various complexes (Mulder et al., 2010). This group was able to successfully use this method to identify 14 assembly intermediates and monitor their population flux over time. A caveat of this study was that it was performed under *in vitro* conditions and may not necessarily reflect

what is occurring within the context of the cell. We have shown here that by perturbing the assembly factor Era, there is also an accumulation of precursor particles at different stages of the assembly process (Fig. 5.4). Therefore, it is interesting to consider that essential assembly factor depletion strains could be harnessed to increase the populations of *in vivo* assembled intermediates at various stages. These intermediates could then be exploited to help provide a complete framework of the events governing the specific stages of ribosome biogenesis.

CHAPTER SIX

CONCLUDING REMARKS

6.1 Author's Preface

This chapter contains statements and a figure (Fig. 6.1) describing the nature of immature $30S_{\Delta yjeQ}$ and $30S_{\Delta rimM}$ particles from a manuscript that was published in *Nucleic Acids Research*. The manuscript was written by Dr. Joaquin Ortega and me with contribution and feedback from other authors. The full citation is listed below:

Thurlow, Brett., Davis, Joseph., Leong, Vivian., Moraes, Trevor., Williamson, James., Ortega, Joaquin. (2016). *Binding properties of YjeQ (RsgA), RbfA, RimM and Era to assembly intermediates of the 30S subunit*. Nucleic Acids Research. Epub ahead of print.

6.2 Assembly Factors as Checkpoint Proteins during Biogenesis

In this thesis we characterized the fate (chapter 3) and binding interactions (chapter 4) of immature 30S particles that accumulate in Δ*yjeQ* and Δ*rimM E.coli* strains. Interestingly, it was shown that assembly factors generally bind better to the mature 30S subunit than to the immature particles. This finding raises an intriguing question of why factors involved in assembling ribosomal subunits can bind to the final product. In eukaryotic ribosome biogenesis late stage 40S intermediates can simultaneously be bound by seven different assembly factors, which contribute to a redundant and multi-pronged approach to chaperoning immature 40S subunits and preventing them from prematurely engaging in translation (Strunk et al., 2011). The assembly factors accomplish this by obstructing the binding sites for initiation factors, disrupting the decoding centre, inhibiting association with the large 60S subunit and preventing opening of the mRNA

channel (Strunk et al., 2011). Although bacteria lack all seven of these assembly factors, several prokaryotic factors have been proposed to have similar roles to the eukaryotic factors. Era binds to the anti-Shine-Dalgarno sequence near the 3' end of the 16S rRNA molecule (Sharma et al., 2005) (Tu et al., 2011) (Tu et al., 2009), positioning it in a location that would prevent mRNA recruitment and subunit association (Sayed et al., 1999). This function would be analogous to the roles implemented by the eukaryotic 40S checkpoint proteins Enp1 (essential nuclear protein 1) and Ltv1 (low temperature viability). Perhaps Era exhibits relatively high affinity to the mature 30S subunits to monitor the final stages of maturation and prevent premature subunits from entering the pool of translating ribosomes.

A quality control checkpoint exists during 40S maturation that involves a translation-like cycle, whereby pre-40S subunits associate with the 60S subunit to give 80S-like complexes (Strunk et al., 2012). These 80S-like complexes lack mRNA and initiator tRNA and are subsequently disassembled by termination factors to allow for dissociation of the assembly factors and subsequent translation initiation (Strunk et al., 2012). The purpose proposed for this translation-like cycle is to provide a functional test of 60S subunit association and assess the GTPase site before ribosomes engage in translation (Strunk et al., 2012). Despite this checkpoint mechanism being characterized in eukaryotic biogenesis, a similar process remains to be described in prokaryotes. In eukaryotes, the GTPase-like protein Tsr1 (twenty S rRNA accumulation) facilitates this quality control cycle by binding to the 40S interface near helix-44 (Strunk et al., 2011) (Strunk et al., 2012). This is analogous to the prokaryotic GTPase YjeQ, which also

interacts with the subunit interface near helix-44 (Jomaa et al., 2011a) (Guo et al., 2011) and can bind mature 30S subunits with high affinity (Fig. 4.7). It is intriguing to consider that a function for YjeQ could be to monitor the final stages of 30S assembly in a similar mechanism as the 40S-licensing step proposed for eukaryotic cells. Results from this thesis that shows factors can form high affinity interactions and preferentially bind mature 30S subunits relative to immature particles, could suggest a yet to be characterized role for these proteins as intrinsic checkpoint of the assembly process. Furthermore GTPase checkpoints could provide an effective means of coupling ribosome assembly to the energy needs of the cell by monitoring cytoplasmic GTP concentrations.

Alternatively, based on our findings that the assembling 30S particles in bacteria have a low occupancy of these factors (Fig. 4.6), it is tempting to speculate that in prokaryotes premature translation initiation may be achieved by the structure of the rRNA itself, rather than through assembly factors sterically obstructing the ligand sites. Consistently, the cryo-EM structures of the immature $30S_{\Delta rimM}$ and $30S_{\Delta yjeQ}$ subunits revealed that the upper domain of helix-44 is dislodged, thus preventing essential inter-subunit bridges from forming and sterically blocking association with the 50S subunit (Leong et al., 2013) (Jomaa et al., 2011b) (Guo et al., 2013). The rearrangements of h44 distort the decoding site, which is then unable to provide the minor groove interactions critical for productive recognition of amino-acylated tRNA during translation. Furthermore, YjeQ, RbfA, RimM and Era are not the bacterial homologs of any of the seven factors that stably bind to the 40S subunit during the late stages of assembly. Therefore, the low presence and occupancy of assembly factors in exponentially growing

E.coli cells may highlight a significant difference in the way prokaryotic and eukaryotic cells prevent premature ribosomal subunits from engaging in translation. It also likely that premature translation initiation in prokaryotes is prevented by a combination of both rRNA structure and factor mediated regulation.

6.3 The True Substrates for the Assembly Factors Precede the Accumulated $30S_{\Delta rimM}$ and $30S_{\Delta yjeQ}$ Particles

Considering that YjeQ, RbfA, RimM and Era are putative assembly factors; the weak binding of these factors to the immature particles was an unexpected result. However, this result reconciles well with a putative role of these factors in chaperoning the folding of rRNA. Similarly to the r-proteins that upon binding to the rRNA stabilize transient RNA conformations and keep the rRNA in a productive line of folding, it is likely that YjeQ, RbfA, RimM and Era may also play a role in stabilizing specific rRNA motifs at or near the decoding center (Jomaa et al., 2011a) (Guo et al., 2011) (Sharma et al., 2005) (Datta et al., 2007) (Lovgren et al., 2004). In the absence of any of these factors, the conformation of the rRNA motifs that these factors should bind may transition into a local energy minimum that is thermodynamically more stable. Our current thinking is that in the knockout strains the on-pathway intermediate that constitute the real substrate for each factor progresses to a downstream assembly intermediate that exhibits low affinity to the factors. Indeed, recent structural studies (Jomaa et al., 2011b) (Leong et al., 2013) (Guo et al., 2011) (Yang et al., 2014) found that the immature 30S particles accumulating in the Δ*rimM* and Δ*yjeQ* null strains are structurally similar.

Therefore, it seems that in the knockout strains the different on-pathway intermediates that are recognized by the specific assembly factors may be progressing into a structurally similar local energy minimum intermediate.

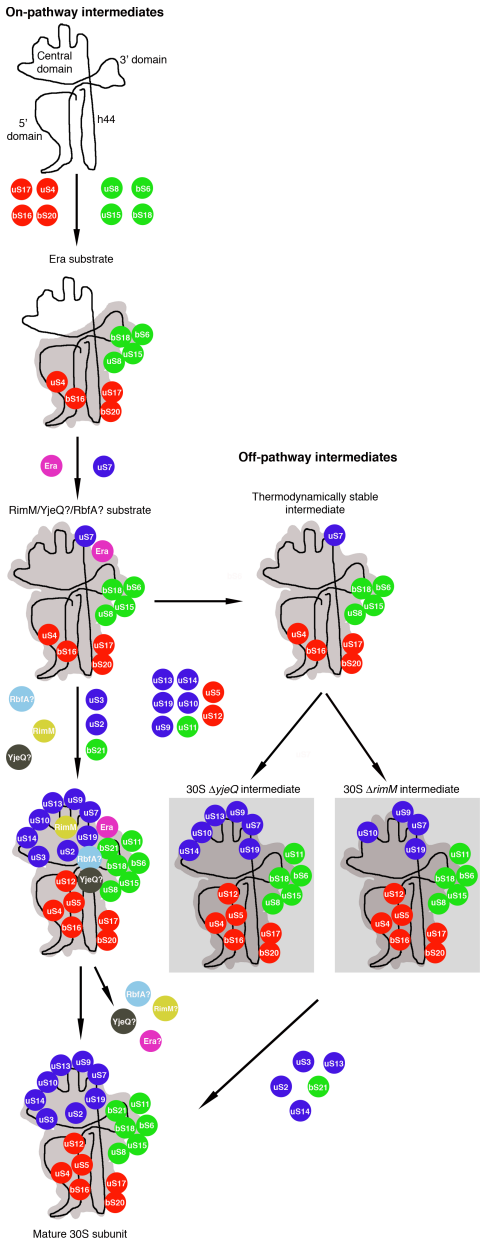

Figure 6.1. Model describing the placement of the 30S$_{\Delta yjeQ}$ or 30S$_{\Delta rimM}$ immature particles in the assembly pathway of the 30S subunit.

The four domains of the 16S rRNA are labelled in the top left cartoon. Ribosomal proteins that belong to the 5', central and 3' domains are colored in red, green and blue, respectively. The entry of the r-proteins in the cartoon is shown according to the Nomura assembly map. Era and RimM point of entry in the assembly line is marked according to previous work (Bunner et al. 2010) that helps define the actual substrate for these two factors (semi-transparent boxes). Points of entry for RbfA and YjeQ are displayed arbitrarily (denoted with a '?') as they are unknown. Similarly, the release point of the four factors has been displayed arbitrarily as it is also unknown (denoted with a '?'). In the presence of YjeQ, RbfA, RimM and Era assembly progresses through on-pathway intermediates recognized by the factors until the mature 30S subunit is formed. In the absence of the assembly factors, the immature particles evolve into a more energetically stable folding state (labelled as 'Thermodynamically stable intermediate'). This intermediate continues to incorporate most of the remaining r-proteins, except those that we found depleted in our qMS analysis, and evolves into the $30S_{\Delta yjeQ}$ or $30S_{\Delta rimM}$ immature particles (highlighted by semi-transparent boxes) that accumulate and exhibit low affinity to the assembly factors. These accumulated particles can eventually mature into complete 30S subunits.

These results imply that the true substrates of YjeQ, RbfA, RimM and Era are assembling 30S particles that precede the immature intermediates accumulating in the knockout strains. This is consistent with recent work (Bunner et al., 2010b) testing the effect of Era and RimM on the kinetics of incorporation of r-proteins to the assembling 30S subunit *in vitro*. This study found that Era causes acceleration of the binding rates of r-proteins uS5, uS9, uS11 and uS12. There was also a more subtle increase in the kinetics of incorporation of uS7, uS10, uS13, uS14 and uS19. RimM affected the rates of incorporation r-proteins uS3, uS9, uS10, uS12, uS13 and uS19. This information along with the Nomura assembly map (Mizushima and Nomura, 1970) (Held et al., 1974) establishing the hierarchy of s-protein binding, allows one to estimate a point of entry of Era and RimM into the assembly line of the 30S subunit (Figure 4.12). The qMS analysis presented here (Fig 4.6A) also allowed us to put an estimated time stamp on the $30S_{\Delta yjeQ}$ and $30S_{\Delta rimM}$ immature particles and position them within this assembly line. All of the r-

proteins with incorporation kinetics that are affected by the presence of Era or RimM (Bunner et al., 2010b) were present in the immature particles in full occupancy. The only exceptions were uS3 that was partially depleted in both particles and uS13 and uS14 were slightly depleted in the $30S_{\Delta rimM}$ particles. This protein complement placed the $30S_{\Delta yjeQ}$ or $30S_{\Delta rimM}$ immature particles that accumulate in the Δ*yjeQ* and Δ*rimM* null strains at the very late stages of the assembly pathway and more importantly, downstream of the particles recognized by YjeQ and RimM as substrates. Our current hypothesis is that the thermodynamically more stable intermediate to which the true substrate particle for RimM and YjeQ evolve to (labelled as 'Thermodynamically stable intermediate' in Figure 6.1), still continues to incorporate most of the remaining s-proteins except those that we found depleted in our qMS analysis (Figure 6.1A). These are the $30S_{\Delta yjeQ}$ or $30S_{\Delta rimM}$ immature particles that we see accumulating in the Δ*yjeQ* and Δ*rimM* strains (shown enclosed in a semi-transparent box in Figure 6.1). Interestingly, data presented in chapter 3 indicates that these immature particles have the ability to progress into 30S subunits that can associate with 50S subunits to form 70S ribosomes.

6.4 Dual Roles of Assembly Factors and Promiscuous Proteins

Based on over a decade of research regarding the roles of 30S assembly factors, it has generally been accepted that these proteins can stably bind to precursor ribosomal particles to facilitate maturation. These studies have largely utilized genetic manipulation of the factors to impair the assembly process, thus implicating a role in biogenesis for the perturbed factor. Despite this hypothesis, direct interactions of 30S assembly factors with

immature precursor particles has remained elusive (Himeno et al., 2004) (Goto et al., 2011) (Guo et al., 2013) (Leong et al., 2013) (Thurlow et al., 2016). Based on the model proposed in this thesis (Fig. 6.1) and our findings that factors bind with high affinity to mature 30S subunits (chapter 4), it seems possible that these factors could have dual roles in the assembly process. Perhaps, during the early stages of assembly the factor binds to a yet to be characterized assembly intermediate and assists in the maturation of these particles by chaperoning rRNA and facilitating entry of s-proteins. The factor could then remain bound throughout the remainder of the assembly process and ultimately act as an intrinsic checkpoint protein during the final stages of maturation. Interestingly, RbfA has been proposed to have a dual role in 30S subunit assembly by acting on the 5' (body) region during the early stages of assembly and central pseudoknot during the late stages (Clatterbuck Soper et al., 2013). The ability of maturation factors to both build ribosomes and oversee the assembly process could provide cells with a robust mechanism for ensuring efficient assembly.

A dual function for factors throughout various stages of the assembly process would imply that certain factors could bind to multiple 30S particles with distinct structures. This is consistent with these assembly factors being promiscuous and capable of recognizing multiple binding partners, which has previously been characterized for numerous protein interactions (Schreiber and Keating, 2011). Furthermore, it has recently been shown that promiscuous binding of assembly factors occurs during the late stages of 50S subunit assembly to allow for the final steps to occur without a precise sequence (Ni et al., 2016).

6.5 A Need for New Approaches for Obtaining Ribosomal Precursors

At the onset of this thesis, a prevailing question in the field of ribosome biogenesis was how functionally related assembly factors work together to achieve 30S subunit maturation. Despite numerous studies implicating the factors YjeQ, Era, RbfA and RimM in ribosome assembly (Jeganathan et al., 2015) (Daigle and Brown, 2004) (Jomaa et al., 2011b) (Jomaa et al., 2011a) (Leong et al., 2013) (Himeno et al., 2004) (Sharma et al., 2005) (Datta et al., 2007) (Goto et al., 2011) (Lovgren et al., 2004) (Inoue et al., 2003) (Inoue et al., 2006) (Yang et al., 2014) (Guo et al., 2011) (Guo et al., 2013), a comprehensive understanding of the specific and interrelated functions of these proteins has remained elusive. Perhaps the most critical reason for the limited progress in understanding the mechanistic roles of these proteins is the lack of homogenous 30S precursor particles that can be harnessed to probe the functions of these enigmatic proteins. Indeed, the paucity of assembly intermediates has largely driven researchers to focus on using mature 30S subunits to investigate the interactions and mechanism of assembly factor mediated biogenesis (Jomaa et al., 2011a) (Guo et al., 2011) (Datta et al., 2007) (Sharma et al., 2005). This technique of using the final product to study assembly factors provides an inherent limitation on obtaining impactful information about the specific roles implemented by these factors. As such, methodologies to enrich for precursor 30S particles by utilizing assembly factor deletion strains were adopted by multiple groups (Himeno et al., 2004) (Goto et al., 2011) (Jomaa et al., 2011b) (Leong et al., 2013) (Guo et al., 2013) (Yang et al., 2014).

The work presented throughout this thesis expanded upon this approach by assessing the fate (chapter 3) and binding interactions (chapter 4) of precursor particles that accumulate in two assembly factor knockout strains, as well as generating additional strains that produce novel assembly intermediates (chapter 5). The purification methods used to isolate these ribosomal precursors involved sucrose gradient ultracentrifugation under associating (high magnesium) buffer conditions (see 2.6). The premise of this approach is that any mature 30S subunits will be able to associate with 50S subunits to form 70S ribosomes, whereas the immature particles will remain unbound and can thus be separated by ultracentrifugation. Although this approach is quite effective at enriching for immature precursor particles, it cannot completely exclude the possibility of some contamination with mature 30S subunits. These technical challenges make it difficult for performing and interpreting biochemical and structural studies aimed at exclusively investigating immature precursor particles and characterizing the specific roles and functional interplays implemented by these factors. Based on results from this thesis, it is evident that the field will need to move into a new direction to determine the functions and relationships amongst all assembly factors and ultimately develop a holistic view of ribosome biogenesis.

To address this daunting challenge, several groups have recently adopted new methodologies for isolating and purifying immature precursor particles that entirely exclude any possible mature 30S subunit contamination. In bacterial cells, affinity purification of immature 30S particles has been successfully achieved by inserting MS2 tags within different rRNA regions (Gupta and Culver, 2014) or by using

oligonucleotides complementary to the 5' leader sequence of 17S rRNA (Clatterbuck Soper et al., 2013) or the exposed central pseudoknot (Sashital et al., 2014). Utilizing affinity purification techniques with oligonucleotides designed to interact with only premature rRNA species provides a robust system for removing mature 30S subunit contamination and improving the yield of immature species. An extension of affinity purification methods has also been adapted for investigating eukaryotic ribosome biogenesis. In these studies, affinity tags have been used to purify assembly factors that are still bound to the precursor 40S (Strunk et al., 2011) (Strunk et al., 2012) or 60S (Wu et al., 2016) ribosomal particles. This technique has proven to be extremely useful for isolating and characterizing the actual *in vivo* substrates of the assembly factors (Strunk et al., 2011) (Strunk et al., 2012) (Wu et al., 2016). Furthermore, precursor ribosomal particles remain bound to multiple maturation factors simultaneously and therefore this technique can be exploited to assess functional interplays amongst assembly factors in the context of the actual precursor ribosomal substrates. Ultimately, improved methods for isolating homogenous samples of precursor ribosomal particles at high concentrations will be instrumental in advancing our understanding of ribosome biogenesis in cells.

A limitation of disrupting assembly factors by genetic perturbation to enrich for ribosomal intermediates is that the consequence and nature of the accumulated particles is currently not well understood. Indeed, genetic manipulation has little temporal resolution and can often lead to wide ranging cellular effects, making it difficult to tease out specific functions. Furthermore, results from this thesis demonstrate that although the particles that accumulate in assembly factor knockout strains are competent for maturation

(chapter 3) they do not bind with high affinity to the knocked out or functionally related assembly factors (chapter 4). Therefore, there is evidence supporting the notion that these accumulated precursor particles are not bona fide intermediates of the knocked out assembly factors. To circumvent these challenges a recent approach has been to increase cellular concentrations of *in vivo* assembled ribosome precursors with the use of small molecule inhibitors specific to ribosome assembly (Stokes et al., 2014) (Stokes et al., 2015). By screening a diverse collection of thousands of compounds for a cold-sensitivity growth phenotype, the anticonvulsant drug lamotrigine was identified to be a specific inhibitor of bacteria ribosome biogenesis (Stokes et al., 2015) (Stokes et al., 2014). Treatment of cells with lamotrigine led to an immediate increase in both 30S and 50S precursor particles that comprised of immature rRNA and an incomplete r-protein complement (Stokes et al., 2014). Therefore, the utility of small molecule inhibitors as chemical probes of ribosome biogenesis is promising and could provide an enriched source of *in vivo* assembled precursor particles.

6.6 Significance

The focus of this thesis was to determine the fates of the immature particles that accumulate in the Δ*yjeQ* and Δ*rimM* strains and characterize their binding interactions with YjeQ, Era, RbfA and RimM. Additionally, an Era-depletion and Δ*rbfA* strain was generated for subsequent biochemical and structural characterizations of novel ribosomal intermediates. Cryo-EM single particle analysis of the $30S_{Era\text{-}depleted}$ particles revealed that there is considerably more structural heterogeneity than in the Δ*yjeQ* and Δ*rimM*

strains, which is consistent with Era having a global effect on ribosome biogenesis. More importantly, results showed that although the $30S_{\Delta yjeQ}$ and $30S_{\Delta rimM}$ particles are competent for maturation, they do not exhibit high affinity to their respective knocked out protein or other functionally related factors. This indicates that the $30S_{\Delta yjeQ}$ and $30S_{\Delta rimM}$ particles represent thermodynamically stable off-pathway intermediates that can assemble into mature 30S subunits. This finding must give way to a paradigm shift in which the accumulated immature particles from 30S assembly factor single knockout strains do not represent the actual substrate of the removed factor. Although these immature particles have been informative on the assembly process and instrumental to our understanding of biogenesis, new approaches will need to be developed to enrich for novel sources of assembly intermediates. Ultimately, this work provides great insight into the nature of ribosomal precursor particles that assembly factor deletion/depletion strains accumulate and the feasibility of using these strains to advance our understanding of ribosome biogenesis as a whole.

REFERENCES

Adilakshmi, T., Ramaswamy, P., and Woodson, S.A. (2005). Protein-independent folding pathway of the 16S rRNA 5' domain. J Mol Biol *351*, 508–519.

Adilakshmi, T., Lease, R.A., and Woodson, S.A. (2006). Hydroxyl radical footprinting in vivo: mapping macromolecular structures with synchrotron radiation. Nucleic Acids Res. *34*, e64.

Adilakshmi, T., Bellur, D.L., and Woodson, S.A. (2008). Concurrent nucleation of 16S folding and induced fit in 30S ribosome assembly. Nature *455*, 1268–1272.

Agalarov, S.C., Zheleznyakova, E.N., Selivanova, O.M., Zheleznaya, L.A., Matvienko, N.I., Vasiliev, V.D., and Spirin, A.S. (1998). In vitro assembly of a ribonucleoprotein particle corresponding to the platform domain of the 30S ribosomal subunit. Proc Natl Acad Sci U S A *95*, 999–1003.

Alix, J.H., and Guérin, M.F. (1993). Mutant DnaK chaperones cause ribosome assembly defects in Escherichia coli. Proc. Natl. Acad. Sci. U. S. A. *90*, 9725–9729.

Arigoni, F., Talabot, F., Peitsch, M., Edgerton, M.D., Meldrum, E., Allet, E., Fish, R., Jamotte, T., Curchod, M.L., and Loferer, H. (1998). A genome-based approach for the identification of essential bacterial genes. Nat. Biotechnol. *16*, 851–856.

Arnold, R.J., and Reilly, J.P. (1999). Observation of Escherichia coli ribosomal proteins and their posttranslational modifications by mass spectrometry. Anal Biochem *269*, 105–112.

Baba, T., Ara, T., Hasegawa, M., Takai, Y., Okumura, Y., Baba, M., Datsenko, K.A., Tomita, M., Wanner, B.L., and Mori, H. (2006). Construction of Escherichia coli K-12 in-frame, single-gene knockout mutants: the Keio collection. Mol Syst Biol *2*, 2006 0008.

Ban, N., Nissen, P., Hansen, J., Moore, P.B., and Steitz, T.A. (2000). The complete atomic structure of the large ribosomal subunit at 2.4 A resolution. Science (80-.). *289*, 905–920.

Ban, N., Beckmann, R., Cate, J.H., Dinman, J.D., Dragon, F., Ellis, S.R., Lafontaine, D.L., Lindahl, L., Liljas, A., Lipton, J.M., et al. (2014). A new system for naming ribosomal proteins. Curr. Opin. Struct. Biol. *24*, 165–169.

Bellur, D.L., and Woodson, S.A. (2009). A minimized rRNA-binding site for ribosomal protein S4 and its implications for 30S assembly. Nucleic Acids Res *37*, 1886–1896.

Britton, R.A. (2009). Role of GTPases in bacterial ribosome assembly. Annu Rev Microbiol *63*, 155–176.

Britton, R.A., Powell, B.S., Court, D.L., and Lupski, J.R. (1997). Characterization of mutations affecting the Escherichia coli essential GTPase Era that suppress two temperature-sensitive dnaG alleles. J. Bacteriol. *179*, 4575–4582.

Britton, R.A., Powell, B.S., Dasgupta, S., Sun, Q., Margolin, W., Lupski, J.R., and Court, D.L. (1998). Cell cycle arrest in Era GTPase mutants: A potential growth rate-regulated checkpoint in Escherichia coli. Mol. Microbiol. *27*, 739–750.

Britton, R.A., Chen, S.M., Wallis, D., Koeuth, T., Powell, B.S., Shaffer, L.G., Largaespada, D., Jenkins, N.A., Copeland, N.G., Court, D.L., et al. (2000). Isolation and preliminary characterization of the human and mouse homologues of the bacterial cell cycle gene era. Genomics *67*, 78–82.

Brosius, J., Palmer, M.L., Kennedy, P.J., and Noller, H.F. (1978). Complete nucleotide sequence of a 16S ribosomal RNA gene from Escherichia coli. Proc Natl Acad Sci U S A *75*, 4801–4805.

Brosius, J., Dull, T.J., and Noller, H.F. (1980). Complete nucleotide sequence of a 23S ribosomal RNA gene from Escherichia coli. Proc Natl Acad Sci U S A *77*, 201–204.

Brosius, J., Dull, T.J., Sleeter, D.D., and Noller, H.F. (1981). Gene organization and primary structure of a ribosomal RNA operon from Escherichia coli. J Mol Biol *148*, 107–127.

Brown, E.D. (2005). Conserved P-loop GTPases of unknown function in bacteria: an emerging and vital ensemble in bacterial physiology. Biochem Cell Biol *83*, 738–746.

Bunner, A.E., Beck, A.H., and Williamson, J.R. (2010a). Kinetic cooperativity in Escherichia coli 30S ribosomal subunit reconstitution reveals additional complexity in the assembly landscape. Proc Natl Acad Sci U S A *107*, 5417–5422.

Bunner, A.E., Nord, S., Wikstrom, P.M., and Williamson, J.R. (2010b). The effect of ribosome assembly cofactors on in vitro 30S subunit reconstitution. J Mol Biol *398*, 1–7.

Bylund, G.O., Persson, B.C., Lundberg, L.A., and Wikstrom, P.M. (1997). A novel ribosome-associated protein is important for efficient translation in Escherichia coli. J Bacteriol *179*, 4567–4574.

Bylund, G.O., Wipemo, L.C., Lundberg, L.A., and Wikstrom, P.M. (1998). RimM and RbfA are essential for efficient processing of 16S rRNA in Escherichia coli. J Bacteriol *180*, 73–82.

Bylund, G.O., Lovgren, J.M., and Wikstrom, P.M. (2001). Characterization of mutations in the metY-nusA-infB operon that suppress the slow growth of a DeltarimM mutant. J Bacteriol *183*, 6095–6106.

Caldon, C.E., Yoong, P., and March, P.E. (2001). Evolution of a molecular switch:

universal bacterial GTPases regulate ribosome function. Mol Microbiol *41*, 289–297.

Campbell, T.L., and Brown, E.D. (2002). Characterization of the depletion of 2-C-methyl-D-erythritol-2,4-cyclodiphosphate synthase in Escherichia coli and Bacillus subtilis. J Bacteriol *184*, 5609–5618.

Campbell, T.L., and Brown, E.D. (2008). Genetic interaction screens with ordered overexpression and deletion clone sets implicate the Escherichia coli GTPase YjeQ in late ribosome biogenesis. J Bacteriol *190*, 2537–2545.

Campbell, T.L., Henderson, J., Heinrichs, D.E., and Brown, E.D. (2006). The yjeQ gene is required for virulence of Staphylococcus aureus. Infect Immun *74*, 4918–4921.

Chen, S.S., and Williamson, J.R. (2013). Characterization of the ribosome biogenesis landscape in E. coli using quantitative mass spectrometry. J Mol Biol *425*, 767–779.

Clatterbuck Soper, S.F., Dator, R.P., Limbach, P.A., and Woodson, S.A. (2013). In vivo X-ray footprinting of pre-30S ribosomes reveals chaperone-dependent remodeling of late assembly intermediates. Mol Cell *52*, 506–516.

Clemons Jr., W.M., May, J.L., Wimberly, B.T., McCutcheon, J.P., Capel, M.S., and Ramakrishnan, V. (1999). Structure of a bacterial 30S ribosomal subunit at 5.5 A resolution. Nature *400*, 833–840.

Comartin, D.J., and Brown, E.D. (2006). Non-ribosomal factors in ribosome subunit assembly are emerging targets for new antibacterial drugs. Curr Opin Pharmacol *6*, 453–458.

Connolly, K., and Culver, G. (2009). Deconstructing ribosome construction. Trends Biochem Sci *34*, 256–263.

Culver, G.M. (2003). Assembly of the 30S ribosomal subunit. Biopolymers *68*, 234–249.

Culver, G.M., and Noller, H.F. (1999). Efficient reconstitution of functional Escherichia coli 30S ribosomal subunits from a complete set of recombinant small subunit ribosomal proteins. RNA *5*, 832–843.

Daigle, D.M., and Brown, E.D. (2004). Studies of the interaction of Escherichia coli YjeQ with the ribosome in vitro. J Bacteriol *186*, 1381–1387.

Daigle, D.M., Rossi, L., Berghuis, A.M., Aravind, L., Koonin, E. V, and Brown, E.D. (2002). YjeQ, an essential, conserved, uncharacterized protein from Escherichia coli, is an unusual GTPase with circularly permuted G-motifs and marked burst kinetics. Biochemistry *41*, 11109–11117.

Dammel, C.S., and Noller, H.F. (1995). Suppression of a cold-sensitive mutation in 16S rRNA by overexpression of a novel ribosome-binding factor, RbfA. Genes Dev *9*, 626–

637.

Danilova, N., and Gazda, H.T. (2015). Ribosomopathies: how a common root can cause a tree of pathologies. Dis Model Mech *8*, 1013–1026.

Datsenko, K.A., and Wanner, B.L. (2000). One-step inactivation of chromosomal genes in Escherichia coli K-12 using PCR products. Proc Natl Acad Sci U S A *97*, 6640–6645.

Datta, P.P., Wilson, D.N., Kawazoe, M., Swami, N.K., Kaminishi, T., Sharma, M.R., Booth, T.M., Takemoto, C., Fucini, P., Yokoyama, S., et al. (2007). Structural aspects of RbfA action during small ribosomal subunit assembly. Mol Cell *28*, 434–445.

Datta, S., Costantino, N., and Court, D.L. (2006). A set of recombineering plasmids for gram-negative bacteria. Gene *379*, 109–115.

Davies, B.W., Kohrer, C., Jacob, A.I., Simmons, L.A., Zhu, J., Aleman, L.M., Rajbhandary, U.L., and Walker, G.C. (2010). Role of Escherichia coli YbeY, a highly conserved protein, in rRNA processing. Mol Microbiol *78*, 506–518.

Decatur, W.A., and Fournier, M.J. (2002). rRNA modifications and ribosome function. Trends Biochem Sci *27*, 344–351.

Dohme, F., and Nierhaus, K.H. (1976). Total reconstitution and assembly of 50 S subunits from Escherichia coli Ribosomes in vitro. J Mol Biol *107*, 585–599.

Donati, G., Montanaro, L., and Derenzini, M. (2012). Ribosome biogenesis and control of cell proliferation: p53 is not alone. Cancer Res *72*, 1602–1607.

Earnest, T.M., Lai, J., Chen, K., Hallock, M.J., Williamson, J.R., and Luthey-Schulten, Z. (2015). Toward a Whole-Cell Model of Ribosome Biogenesis: Kinetic Modeling of SSU Assembly. Biophys J *109*, 1117–1135.

Engelman, D.M., Moore, P.B., and Schoenborn, B.P. (1975). Neutron scattering measurements of separation and shape of proteins in 30S ribosomal subunit of Escherichia coli: S2-S5, S5-S8, S3-S7. Proc. Natl. Acad. Sci. U. S. A. *72*, 3888–3892.

Frank, J. (2003). Toward an understanding of the structural basis of translation. Genome Biol *4*, 237.

Freed, E.F., Bleichert, F., Dutca, L.M., and Baserga, S.J. (2010). When ribosomes go bad: diseases of ribosome biogenesis. Mol Biosyst *6*, 481–493.

Ginsburg, D., and Steitz, J.A. (1975). The 30 S ribosomal precursor RNA from Escherichia coli. A primary transcript containing 23 S, 16 S, and 5 S sequences. J Biol Chem *250*, 5647–5654.

Glaser, G., Sarmientos, P., and Cashel, M. (1983). Functional interrelationship between two tandem E. coli ribosomal RNA promoters. Nature *302*, 74–76.

Godinic-Mikulcic, V., Jaric, J., Greber, B.J., Franke, V., Hodnik, V., Anderluh, G., Ban, N., and Weygand-Durasevic, I. (2014). Archaeal aminoacyl-tRNA synthetases interact with the ribosome to recycle tRNAs. Nucleic Acids Res. *42*, 5191–5201.

Gollop, N., and March, P.E. (1991a). A GTP-binding protein (Era) has an essential role in growth rate and cell cycle control in Escherichia coli. J. Bacteriol. *173*, 2265–2270.

Gollop, N., and March, P.E. (1991b). Localization of the membrane binding sites of Era in Escherichia coli. Res. Microbiol. *142*, 301–307.

Goto, S., Kato, S., Kimura, T., Muto, A., and Himeno, H. (2011). RsgA releases RbfA from 30S ribosome during a late stage of ribosome biosynthesis. EMBO J *30*, 104–114.

Grondek, J.F., and Culver, G.M. (2004). Assembly of the 30S ribosomal subunit: positioning ribosomal protein S13 in the S7 assembly branch. RNA *10*, 1861–1866.

Gulati, M., Jain, N., Davis, J.H., Williamson, J.R., and Britton, R.A. (2014). Functional interaction between ribosomal protein L6 and RbgA during ribosome assembly. PLoS Genet. *10*, e1004694.

Guo, Q., Yuan, Y., Xu, Y., Feng, B., Liu, L., Chen, K., Sun, M., Yang, Z., Lei, J., and Gao, N. (2011). Structural basis for the function of a small GTPase RsgA on the 30S ribosomal subunit maturation revealed by cryoelectron microscopy. Proc Natl Acad Sci U S A *108*, 13100–13105.

Guo, Q., Goto, S., Chen, Y., Feng, B., Xu, Y., Muto, A., Himeno, H., Deng, H., Lei, J., and Gao, N. (2013). Dissecting the in vivo assembly of the 30S ribosomal subunit reveals the role of RimM and general features of the assembly process. Nucleic Acids Res *41*, 2609–2620.

Gupta, N., and Culver, G.M. (2014). Multiple in vivo pathways for Escherichia coli small ribosomal subunit assembly occur on one pre-rRNA. Nat. Struct. Mol. Biol. *21*, 937–943.

El Hage, A., Sbaï, M., and Alix, J.H. (2001). The chaperonin GroEL and other heat-shock proteins, besides DnaK, participate in ribosome biogenesis in Escherichia coli. Mol. Gen. Genet. *264*, 796–808.

Hang, J.Q., and Zhao, G. (2003). Characterization of the 16S rRNA- and membrane-binding domains of Streptococcus pneumoniae Era GTPase: Structural and functional implications. Eur. J. Biochem. *270*, 4164–4172.

Hang, J.Q., Meier, T.I., and Zhao, G. (2001). Analysis of the interaction of 16s rRNA and cytoplasmic membrane with the C-terminal part of the Streptococcus pneumoniae Era GTpase. Eur. J. Biochem. *268*, 5570–5577.

Hansen, J.L., Schmeing, T.M., Moore, P.B., and Steitz, T.A. (2002). Structural insights into peptide bond formation. Proc Natl Acad Sci U S A *99*, 11670–11675.

Harms, J., Schluenzen, F., Zarivach, R., Bashan, A., Gat, S., Agmon, I., Bartels, H., Franceschi, F., and Yonath, A. (2001). High resolution structure of the large ribosomal subunit from a mesophilic eubacterium. Cell *107*, 679–688.

Hase, Y., Yokoyama, S., Muto, A., and Himeno, H. (2009). Removal of a ribosome small subunit-dependent GTPase confers salt resistance on Escherichia coli cells. RNA *15*, 1766–1774.

Hayes, F., and Hayes, D.H. (1971). Biosynthesis of ribosomes in E. coli. I. Properties of ribosomal precursor particles and their RNA components. Biochimie *53*, 369–382.

Hayes, F., and Vasseur, M. (1976). Processing of the 17-S Escherichia coli precursor RNA in the 27-S pre-ribosomal particle. Eur. J. Biochem. *61*, 433–442.

Held, W.A., Mizushima, S., and Nomura, M. (1973). Reconstitution of Escherichia coli 30 S ribosomal subunits from purified molecular components. J Biol Chem *248*, 5720–5730.

Held, W.A., Ballou, B., Mizushima, S., and Nomura, M. (1974). Assembly mapping of 30 S ribosomal proteins from Escherichia coli. Further studies. J Biol Chem *249*, 3103–3111.

Herold, M., and Nierhaus, K.H. (1987). Incorporation of six additional proteins to complete the assembly map of the 50 S subunit from Escherichia coli ribosomes. J Biol Chem *262*, 8826–8833.

Himeno, H., Hanawa-Suetsugu, K., Kimura, T., Takagi, K., Sugiyama, W., Shirata, S., Mikami, T., Odagiri, F., Osanai, Y., Watanabe, D., et al. (2004). A novel GTPase activated by the small subunit of ribosome. Nucleic Acids Res *32*, 5303–5309.

Holmes, K.L., and Culver, G.M. (2005). Analysis of conformational changes in 16 S rRNA during the course of 30 S subunit assembly. J. Mol. Biol. *354*, 340–357.

Huang, Y.J., Swapna, G.V.T., Rajan, P.K., Ke, H., Xia, B., Shukla, K., Inouye, M., and Montelione, G.T. (2003). Solution NMR structure of ribosome-binding factor A (RbfA), a cold-shock adaptation protein from Escherichia coli. J. Mol. Biol. *327*, 521–536.

Inoue, K., Alsina, J., Chen, J., and Inouye, M. (2003). Suppression of defective ribosome assembly in a rbfA deletion mutant by overexpression of Era, an essential GTPase in Escherichia coli. Mol Microbiol *48*, 1005–1016.

Inoue, K., Chen, J., Tan, Q., and Inouye, M. (2006). Era and RbfA have overlapping function in ribosome biogenesis in Escherichia coli. J Mol Microbiol Biotechnol *11*, 41–52.

Jacob, A.I., Kohrer, C., Davies, B.W., RajBhandary, U.L., and Walker, G.C. (2013). Conserved bacterial RNase YbeY plays key roles in 70S ribosome quality control and

16S rRNA maturation. Mol Cell *49*, 427–438.

Jankowsky, E., Gross, C.H., Shuman, S., and Pyle, A.M. (2001). Active disruption of an RNA-protein interaction by a DExH/D RNA helicase. Science *291*, 121–125.

Jeganathan, A., Razi, A., Thurlow, B., and Ortega, J. (2015). The C-terminal helix in the YjeQ zinc-finger domain catalyzes the release of RbfA during 30S ribosome subunit assembly. Rna *21*, 1203–1216.

Johnstone, B.H., Handler, A.A., Chao, D.K., Nguyen, V., Smith, M., Ryu, S.Y., Simons, E.L., Anderson, P.E., and Simons, R.W. (1999). The widely conserved Era G-protein contains an RNA-binding domain required for Era function in vivo. Mol. Microbiol. *33*, 1118–1131.

Jomaa, A., Stewart, G., Mears, J.A., Kireeva, I., Brown, E.D., and Ortega, J. (2011a). Cryo-electron microscopy structure of the 30S subunit in complex with the YjeQ biogenesis factor. RNA *17*, 2026–2038.

Jomaa, A., Stewart, G., Martin-Benito, J., Zielke, R., Campbell, T.L., Maddock, J.R., Brown, E.D., and Ortega, J. (2011b). Understanding ribosome assembly: the structure of in vivo assembled immature 30S subunits revealed by cryo-electron microscopy. RNA *17*, 697–709.

Jomaa, A., Jain, N., Davis, J.H., Williamson, J.R., Britton, R.A., and Ortega, J. (2014). Functional domains of the 50S subunit mature late in the assembly process. Nucleic Acids Res *42*, 3419–3435.

Jones, P.G., and Inouye, M. (1996). RbfA, a 30S ribosomal binding factor, is a cold-shock protein whose absence triggers the cold-shock response. Mol Microbiol *21*, 1207–1218.

Kaczanowska, M., and Ryden-Aulin, M. (2007). Ribosome biogenesis and the translation process in Escherichia coli. Microbiol Mol Biol Rev *71*, 477–494.

Kenerley, M.E., Morgan, E.A., Post, L., Lindahl, L., and Nomura, M. (1977). Characterization of hybrid plasmids carrying individual ribosomal ribonucleic acid transcription units of Escherichia coli. J Bacteriol *132*, 931–949.

Kim, H., Abeysirigunawarden, S.C., Chen, K., Mayerle, M., Ragunathan, K., Luthey-Schulten, Z., Ha, T., and Woodson, S.A. (2014). Protein-guided RNA dynamics during early ribosome assembly. Nature *506*, 334–338.

Kiss, A., Sain, B., and Venetianer, P. (1977). The number of rRNA genes in Escherichia coli. FEBS Lett *79*, 77–79.

Kitagawa, M., Ara, T., Arifuzzaman, M., Ioka-Nakamichi, T., Inamoto, E., Toyonaga, H., and Mori, H. (2005). Complete set of ORF clones of Escherichia coli ASKA library (a

complete set of E. coli K-12 ORF archive): unique resources for biological research. DNA Res *12*, 291–299.

Kowalak, J.A., and Walsh, K.A. (1996). Beta-methylthio-aspartic acid: identification of a novel posttranslational modification in ribosomal protein S12 from Escherichia coli. Protein Sci *5*, 1625–1632.

Lake, J.A. (1976). Ribosome structure determined by electron microscopy of Escherichia coli small subunits, large subunits and monomeric ribosomes. J Mol Biol *105*, 131–139.

Leong, V., Kent, M., Jomaa, A., and Ortega, J. (2013). Escherichia coli rimM and yjeQ null strains accumulate immature 30S subunits of similar structure and protein complement. RNA *19*, 789–802.

Lerner, C.G., and Inouye, M. (1991). Pleiotropic changes resulting from depletion of Era, an essential GTP-binding protein in Escherichia coli. Mol. Microbiol. *5*, 951–957.

Lerner, C.G., Sood, P., Ahnn, J., and Inouye, M. (1992). Cold-sensitive growth and decreased GTP-hydrolytic activity from substitution of Pro17 for Val in Era, an essential Escherichia coli GTPase. FEMS Microbiol. Lett. *95*, 137–142.

Levdikov, V.M., Blagova, E. V, Brannigan, J.A., Cladire, L., Antson, A.A., Isupov, M.N., Sror, S.J., and Wilkinson, A.J. (2004). The crystal structure of YloQ, a circularly permuted GTPase essential for Bacillus subtilis viability. J. Mol. Biol. *340*, 767–782.

Li, G.-W., Burkhardt, D., Gross, C., and Weissman, J.S. (2014). Quantifying absolute protein synthesis rates reveals principles underlying allocation of cellular resources. Cell *157*, 624–635.

Li, Z., Pandit, S., and Deutscher, M.P. (1999). RNase G (CafA protein) and RNase E are both required for the 5’ maturation of 16S ribosomal RNA. EMBO J *18*, 2878–2885.

Lindahl, L. (1973). Two new ribosomal precursor particles in E. coli. Nat New Biol *243*, 170–172.

Lindahl, L. (1975). Intermediates and time kinetics of the in vivo assembly of Escherichia coli ribosomes. J Mol Biol *92*, 15–37.

Linder, P. (2006). Dead-box proteins: A family affair - Active and passive players in RNP-remodeling. Nucleic Acids Res. *34*, 4168–4180.

Linder, P., Lasko, P.F., Ashburner, M., Leroy, P., Nielsen, P.J., Nishi, K., Schnier, J., and Slonimski, P.P. (1989). Birth of the D-E-A-D box. Nature *337*, 121–122.

Link, A.J., Phillips, D., and Church, G.M. (1997). Methods for generating precise deletions and insertions in the genome of wild-type Escherichia coli: Application to open reading frame characterization. J. Bacteriol. *179*, 6228–6237.

Lovgren, J.M., Bylund, G.O., Srivastava, M.K., Lundberg, L.A., Persson, O.P., Wingsle, G., and Wikstrom, P.M. (2004). The PRC-barrel domain of the ribosome maturation protein RimM mediates binding to ribosomal protein S19 in the 30S ribosomal subunits. RNA *10*, 1798–1812.

Lund, E., Dahlberg, J.E., Lindahl, L., Jaskunas, S.R., Dennis, P.P., and Nomura, M. (1976). Transfer RNA genes between 16S and 23S rRNA genes in rRNA transcription units of E. coli. Cell *7*, 165–177.

Machnicka, M.A., Milanowska, K., Oglou, O.O., Purta, E., Kurkowska, M., Olchowik, A., Januszewski, W., Kalinowski, S., Dunin-Horkawicz, S., Rother, K.M., et al. (2013). MODOMICS: A database of RNA modification pathways - 2013 update. Nucleic Acids Res. *41*, D262–D267.

MacLean, B., Tomazela, D.M., Shulman, N., Chambers, M., Finney, G.L., Frewen, B., Kern, R., Tabb, D.L., Liebler, D.C., and MacCoss, M.J. (2010). Skyline: an open source document editor for creating and analyzing targeted proteomics experiments. Bioinformatics *26*, 966–968.

Maguire, B.A. (2009). Inhibition of bacterial ribosome assembly: a suitable drug target? Microbiol Mol Biol Rev *73*, 22–35.

Mangiarotti, G., Turco, E., Ponzetto, A., and Altruda, F. (1974). Precursor 16S RNA in active 30S ribosomes. Nature *247*, 147–148.

Mangiarotti, G., Turco, E., Perlo, C., and Altruda, F. (1975). Role of precursor 16S RNA in assembly of E. coli 30S ribosomes. Nature *253*, 569–571.

Meier, T.I., Peery, R.B., Jaskunas, S.R., and Zhao, G. (1999). 16S rRNA is bound to era of Streptococcus pneumoniae. J. Bacteriol. *181*, 5242–5249.

Meier, T.I., Peery, R.B., McAllister, K.A., and Zhao, G. (2000). Era GTPase of Escherichia coli: Binding to 16S rRNA and modulation of GTPase activity by RNA and carbohydrates. Microbiology *146*, 1071–1083.

Michaels, G.A. (1972). Ribosome maturation of Escherichia coli growing at different growth rates. J Bacteriol *110*, 889–894.

Milanowska, K., Mikolajczak, K., Lukasik, A., Skorupski, M., Balcer, Z., Machnicka, M.A., Nowacka, M., Rother, K.M., and Bujnicki, J.M. (2013). RNApathwaysDB--a database of RNA maturation and decay pathways. Nucleic Acids Res *41*, D268–D272.

Mindell, J.A., and Grigorieff, N. (2003). Accurate determination of local defocus and specimen tilt in electron microscopy. J. Struct. Biol. *142*, 334–347.

Mizushima, S., and Nomura, M. (1970). Assembly mapping of 30S ribosomal proteins from E. coli. Nature *226*, 1214.

Mohr, S., Stryker, J.M., and Lambowitz, A.M. (2002). A DEAD-Box protein functions as an ATP-dependent RNA chaperone in group I intron splicing. Cell *109*, 769–779.

Montanaro, L., Trere, D., and Derenzini, M. (2012). Changes in ribosome biogenesis may induce cancer by down-regulating the cell tumor suppressor potential. Biochim Biophys Acta *1825*, 101–110.

Mulder, A.M., Yoshioka, C., Beck, A.H., Bunner, A.E., Milligan, R.A., Potter, C.S., Carragher, B., and Williamson, J.R. (2010). Visualizing ribosome biogenesis: parallel assembly pathways for the 30S subunit. Science (80-.). *330*, 673–677.

Nesterchuk, M. V, Sergiev, P. V, and Dontsova, O.A. (2011). Posttranslational Modifications of Ribosomal Proteins in Escherichia coli. Acta Naturae *3*, 22–33.

Ni, X., Davis, J.H., Motahhari, A., Razi, A., and Benlekbir, S. (2016). YphC and YSxC GTPases contribute to the maturation of the central protuberance and functional core of the 50S ribosomal subunit. Nucleic Acids Res. *Epub ahead*.

Nichols, C.E., Johnson, C., Lamb, H.K., Lockyer, M., Charles, I.G., Hawkins, A.R., and Stammers, D.K. (2007). Structure of the ribosomal interacting GTPase YjeQ from the enterobacterial species Salmonella typhimurium. Acta Crystallogr. Sect. F Struct. Biol. Cryst. Commun. *63*, 922–928.

Nissen, P., Hansen, J., Ban, N., Moore, P.B., and Steitz, T.A. (2000). The structural basis of ribosome activity in peptide bond synthesis. Science (80-.). *289*, 920–930.

Noller, H.F. (1991). Ribosomal RNA and translation. Annu Rev Biochem *60*, 191–227.

Noller, H.F., and Woese, C.R. (1981). Secondary structure of 16S ribosomal RNA. Science *212*, 403–411.

Noller, H.F., Kop, J., Wheaton, V., Brosius, J., Gutell, R.R., Kopylov, A.M., Dohme, F., Herr, W., Stahl, D.A., Gupta, R., et al. (1981). Secondary structure model for 23S ribosomal RNA. Nucleic Acids Res. *9*, 6167–6189.

Nomura, M., Traub, P., Guthrie, C., and Nashimoto, H. (1969a). The assembly of ribosomes. J Cell Physiol *74*, Suppl 1:241+.

Nomura, M., Mizushima, S., Ozaki, M., Traub, P., and Lowry, C. V (1969b). Structure and function of ribosomes and their molecular components. Cold Spring Harb Symp Quant Biol *34*, 49–61.

Ogle, J.M., and Ramakrishnan, V. (2005). Structural insights into translational fidelity. Annu Rev Biochem *74*, 129–177.

Ogle, J.M., Brodersen, D.E., Clemons Jr., W.M., Tarry, M.J., Carter, A.P., and Ramakrishnan, V. (2001). Recognition of cognate transfer RNA by the 30S ribosomal

subunit. Science (80-.). *292*, 897–902.

Palade, G. (1955). A small particulate component of the cytoplasm. J. Biophys. Biochem. Cytol. *1*, 59–68.

Paul, B.J., Ross, W., Gaal, T., and Gourse, R.L. (2004). rRNA transcription in Escherichia coli. Annu Rev Genet *38*, 749–770.

Poehlsgaard, J., and Douthwaite, S. (2005). The bacterial ribosome as a target for antibiotics. Nat Rev Microbiol *3*, 870–881.

Popova, A.M., and Williamson, J.R. (2014). Quantitative analysis of rRNA modifications using stable isotope labeling and mass spectrometry. J Am Chem Soc *136*, 2058–2069.

Powell, B.S., Court, D.L., Inada, T., Nakamura, Y., Michotey, V., Cui, X., Reizer, A., Saier, M.H., and Reizer, J. (1995). Novel proteins of the phosphotransferase system encoded within the rpoN operon of Escherichia coli: Enzyme IIANtr affects growth on organic nitrogen and the conditional lethality of an erats mutant. J. Biol. Chem. *270*, 4822–4839.

Powers, T., Daubresse, G., and Noller, H.F. (1993). Dynamics of in vitro assembly of 16 S rRNA into 30 S ribosomal subunits. J. Mol. Biol. *232*, 362–374.

Pyle, A.M. (2013). Coordinating the party: assembly factors and ribogenesis. Mol. Cell *52*, 469–470.

Ramakrishnan, V. (2002). Ribosome structure and the mechanism of translation. Cell *108*, 557–572.

Rohl, R., and Nierhaus, K.H. (1982). Assembly map of the large subunit (50S) of Escherichia coli ribosomes. Proc Natl Acad Sci U S A *79*, 729–733.

Roy-Chaudhuri, B., Kirthi, N., and Culver, G.M. (2010). Appropriate maturation and folding of 16S rRNA during 30S subunit biogenesis are critical for translational fidelity. Proc. Natl. Acad. Sci. U. S. A. *107*, 4567–4572.

Rubinstein, J.L., and Brubaker, M.A. (2015). Alignment of cryo-EM movies of individual particles by optimization of image translations. J. Struct. Biol. *192*, 188–195.

Samaha, R.R., O'Brien, B., O'Brien, T.W., and Noller, H.F. (1994). Independent in vitro assembly of a ribonucleoprotein particle containing the 3' domain of 16S rRNA. Proc Natl Acad Sci U S A *91*, 7884–7888.

Sarmientos, P., Sylvester, J.E., Contente, S., and Cashel, M. (1983). Differential stringent control of the tandem E. coli ribosomal RNA promoters from the rrnA operon expressed in vivo in multicopy plasmids. Cell *32*, 1337–1346.

Sashital, D.G., Greeman, C.A., Lyumkis, D., Potter, C.S., Carragher, B., and Williamson,

J.R. (2014). A combined quantitative mass spectrometry and electron microscopy analysis of ribosomal 30S subunit assembly in E. coli. Elife *3*, e04491.

Sayed, A., Matsuyama, S., and Inouye, M. (1999). Era, an essential Escherichia coli small G-protein, binds to the 30S ribosomal subunit. Biochem Biophys Res Commun *264*, 51–54.

Scheres, S.H.W. (2012a). RELION: implementation of a Bayesian approach to cryo-EM structure determination. J. Struct. Biol. *180*, 519–530.

Scheres, S.H.W. (2012b). A Bayesian view on cryo-EM structure determination. J. Mol. Biol. *415*, 406–418.

Schluenzen, F., Tocilj, A., Zarivach, R., Harms, J., Gluehmann, M., Janell, D., Bashan, A., Bartels, H., Agmon, I., Franceschi, F., et al. (2000). Structure of functionally activated small ribosomal subunit at 3.3 angstroms resolution. Cell *102*, 615–623.

Schreiber, G., and Keating, A.E. (2011). Protein binding specificity versus promiscuity. Curr. Opin. Struct. Biol. *21*, 50–61.

Shajani, Z., Sykes, M.T., and Williamson, J.R. (2011). Assembly of bacterial ribosomes. Annu Rev Biochem *80*, 501–526.

Sharma, M.R., Barat, C., Wilson, D.N., Booth, T.M., Kawazoe, M., Hori-Takemoto, C., Shirouzu, M., Yokoyama, S., Fucini, P., and Agrawal, R.K. (2005). Interaction of Era with the 30S ribosomal subunit implications for 30S subunit assembly. Mol Cell *18*, 319–329.

Shin, D.H., Lou, Y., Jancarik, J., Yokota, H., Kim, R., and Kim, S.-H. (2004). Crystal structure of YjeQ from Thermotoga maritima contains a circularly permuted GTPase domain. Proc. Natl. Acad. Sci. U. S. A. *101*, 13198–13203.

Shine, J., and Dalgarno, L. (1974). The 3'-terminal sequence of Escherichia coli 16S ribosomal RNA: complementarity to nonsense triplets and ribosome binding sites. Proc Natl Acad Sci U S A *71*, 1342–1346.

Steitz, T.A. (2008). A structural understanding of the dynamic ribosome machine. Nat Rev Mol Cell Biol *9*, 242–253.

Stokes, J.M., and Brown, E.D. (2015). Chemical modulators of ribosome biogenesis as biological probes. Nat. Chem. Biol. *11*, 924–932.

Stokes, J.M., Davis, J.H., Mangat, C.S., Williamson, J.R., and Brown, E.D. (2014). Discovery of a small molecule that inhibits bacterial ribosome biogenesis. Elife *3*, 1–22.

Stokes, J.M., Selin, C., Cardona, S.T., and Brown, E.D. (2015). Chemical inhibition of bacterial ribosome biogenesis shows efficacy in a worm infection model. Antimicrob.

Agents Chemother. *59*, 2918–2920.

Strunk, B.S., and Karbstein, K. (2009). Powering through ribosome assembly. RNA *15*, 2083–2104.

Strunk, B.S., Loucks, C.R., Su, M., Vashisth, H., Cheng, S., Schilling, J., Brooks 3rd, C.L., Karbstein, K., and Skiniotis, G. (2011). Ribosome assembly factors prevent premature translation initiation by 40S assembly intermediates. Science (80-.). *333*, 1449–1453.

Strunk, B.S., Novak, M.N., Young, C.L., and Karbstein, K. (2012). A translation-like cycle is a quality control checkpoint for maturing 40S ribosome subunits. Cell *150*, 111–121.

Sulthana, S., and Deutscher, M.P. (2013). Multiple exoribonucleases catalyze maturation of the 3' terminus of 16S ribosomal RNA (rRNA). J Biol Chem *288*, 12574–12579.

Suzuki, S., Tatsuguchi, A., Matsumoto, E., Kawazoe, M., Kaminishi, T., Shirouzu, M., Muto, Y., Takemoto, C., and Yokoyama, S. (2007). Structural characterization of the ribosome maturation protein, RimM. J Bacteriol *189*, 6397–6406.

Swapna, G. V, Shukla, K., Huang, Y.J., Ke, H., Xia, B., Inouye, M., and Montelione, G.T. (2001). Resonance assignments for cold-shock protein ribosome-binding factor A (RbfA) from Escherichia coli. J. Biomol. NMR *21*, 389–390.

Sykes, M.T., and Williamson, J.R. (2009). A complex assembly landscape for the 30S ribosomal subunit. Annu Rev Biophys *38*, 197–215.

Sykes, M.T., Shajani, Z., Sperling, E., Beck, A.H., and Williamson, J.R. (2010). Quantitative Proteomic Analysis of Ribosome Assembly and Turnover In Vivo. J. Mol. Biol. *403*, 331–345.

Talkington, M.W., Siuzdak, G., and Williamson, J.R. (2005). An assembly landscape for the 30S ribosomal subunit. Nature *438*, 628–632.

Tanner, N.K., Cordin, O., Banroques, J., Doere, M., and Linder, P. (2003). The Q motif: a newly identified motif in DEAD box helicases may regulate ATP binding and hydrolysis. Mol Cell *11*, 127–138.

Thurlow, B., Davis, J.H., Leong, V., F. Moraes, T., Williamson, J.R., and Ortega, J. (2016). Binding properties of YjeQ (RsgA), RbfA, RimM and Era to assembly intermediates of the 30S subunit. Nucleic Acids Res.

Tocilj, A., Schlunzen, F., Janell, D., Gluhmann, M., Hansen, H.A., Harms, J., Bashan, A., Bartels, H., Agmon, I., Franceschi, F., et al. (1999). The small ribosomal subunit from Thermus thermophilus at 4.5 A resolution: pattern fittings and the identification of a functional site. Proc Natl Acad Sci U S A *96*, 14252–14257.

Traub, P., and Nomura, M. (1968). Structure and function of E. coli ribosomes. V. Reconstitution of functionally active 30S ribosomal particles from RNA and proteins. Proc Natl Acad Sci U S A *59*, 777–784.

Traub, P., and Nomura, M. (1969a). Studies on the assembly of ribosomes in vitro. Cold Spring Harb Symp Quant Biol *34*, 63–67.

Traub, P., and Nomura, M. (1969b). Structure and function of Escherichia coli ribosomes. VI. Mechanism of assembly of 30 s ribosomes studied in vitro. J Mol Biol *40*, 391–413.

Traub, P., Hosokawa, K., Craven, G.R., and Nomura, M. (1967). Structure and function of E. Coli Ribosomes, IV. Isolation and characterization of functionally active ribosomal proteins. Proc. Natl. Acad. Sci. U. S. A. *58*, 2430–2436.

Treiber, D., and Williamson, J. (1999). Exposing the kinetic traps in RNA folding. Curr. Opin. Struct. Biol. *9*, 339.

Tu, C., Zhou, X., Tropea, J.E., Austin, B.P., Waugh, D.S., Court, D.L., and Ji, X. (2009). Structure of ERA in complex with the 3' end of 16S rRNA: implications for ribosome biogenesis. Proc Natl Acad Sci U S A *106*, 14843–14848.

Tu, C., Zhou, X., Tarasov, S.G., Tropea, J.E., Austin, B.P., Waugh, D.S., Court, D.L., and Ji, X. (2011). The Era GTPase recognizes the GAUCACCUCC sequence and binds helix 45 near the 3' end of 16S rRNA. Proc. Natl. Acad. Sci. U. S. A. *108*, 10156–10161.

Uhlenbeck, O.C. (1995). Keeping RNA happy. RNA *1*, 4–6.

Voet, D., Voet, J., and Pratt, C. (2006). Fundamentals of Biochemistry: Life at the Molecular Level (New Jersey: John Wiley & Sons, Inc.).

Wachi, M., Umitsuki, G., Shimizu, M., Takada, A., and Nagai, K. (1999). Escherichia coli cafA gene encodes a novel RNase, designated as RNase G, involved in processing of the 5' end of 16S rRNA. Biochem Biophys Res Commun *259*, 483–488.

Weitzmann, C.J., Cunningham, P.R., Nurse, K., and Ofengand, J. (1993). Chemical evidence for domain assembly of the Escherichia coli 30S ribosome. FASEB J *7*, 177–180.

Wilson, D.N. (2014). Ribosome-targeting antibiotics and mechanisms of bacterial resistance. Nat Rev Microbiol *12*, 35–48.

Wilson, D.N., and Nierhaus, K.H. (2007). The weird and wonderful world of bacterial ribosome regulation. Crit Rev Biochem Mol Biol *42*, 187–219.

Wimberly, B.T., Brodersen, D.E., Clemons Jr., W.M., Morgan-Warren, R.J., Carter, A.P., Vonrhein, C., Hartsch, T., and Ramakrishnan, V. (2000). Structure of the 30S ribosomal subunit. Nature *407*, 327–339.

Woodson, S.A. (2011). RNA folding pathways and the self-assembly of ribosomes. Acc. Chem. Res. *44*, 1312–1319.

Wu, S., Tutuncuoglu, B., Yan, K., Brown, H., Zhang, Y., Tan, D., Gamalinda, M., Yuan, Y., Li, Z., Jakovljevic, J., et al. (2016). Diverse roles of assembly factors revealed by structures of late nuclear pre-60S ribosomes. Nature *534*, 133–137.

Xia, B., Ke, H., Shinde, U., and Inouye, M. (2003). The role of RbfA in 16S rRNA processing and cell growth at low temperature in Escherichia coli. J Mol Biol *332*, 575–584.

Yang, Z., Guo, Q., Goto, S., Chen, Y., Li, N., Yan, K., Zhang, Y., Muto, A., Deng, H., Himeno, H., et al. (2014). Structural insights into the assembly of the 30S ribosomal subunit in vivo: functional role of S5 and location of the 17S rRNA precursor sequence. Protein Cell *5*, 394–407.

Yoshizawa, S., Fourmy, D., and Puglisi, J.D. (1999). Recognition of the codon-anticodon helix by ribosomal RNA. Science *285*, 1722–1725.

Young, R.A., and Steitz, J.A. (1978). Complementary sequences 1700 nucleotides apart form a ribonuclease III cleavage site in Escherichia coli ribosomal precursor RNA. Proc Natl Acad Sci U S A *75*, 3593–3597.

Yusupov, M.M., Yusupova, G.Z., Baucom, A., Lieberman, K., Earnest, T.N., Cate, J.H., and Noller, H.F. (2001). Crystal structure of the ribosome at 5.5 A resolution. Science *292*, 883–896.

Zengel, J.M., and Lindahl, L. (1994). Diverse mechanisms for regulating ribosomal protein synthesis in Escherichia coli. Prog Nucleic Acid Res Mol Biol *47*, 331–370.

Zillner, K., Jerabek-Willemsen, M., Duhr, S., Braun, D., Längst, G., and Baaske, P. (2012). Microscale thermophoresis as a sensitive method to quantify protein: nucleic acid interactions in solution. Methods Mol. Biol. *815*, 241–252.